BPC-01-300-2
Revision 0
January 1984

HOPE CREEK GENERATING STATION
PLANT UNIQUE ANALYSIS REPORT
VOLUME 2
SUPPRESSION CHAMBER ANALYSIS

Prepared for:
Public Service Electric and Gas Company

Prepared by:
NUTECH Engineers, Inc.
San Jose, California

Prepared by:

Robert S. Quinn

R. D. Quinn, P.E.
Senior Engineer

Reviewed by:

Y. C. Yiu

Y. C. Yiu, P.E.
Group Leader

Approved by:

N. W. Edwards

N. W. Edwards, P.E.
President

Issued by:

Robert A Lehnert

R. A. Lehnert, P.E.
Project Manager

nutech ENGINEERS

REVISION CONTROL SHEET

TITLE: Hope Creek Generating Station Plant Unique Analysis Report, Volume 2

DOCUMENT FILE NUMBER: BPC-01-300-2 Revision 0

Michael C Hsieh — MCH
M. C. Hsieh/Consultant I — INITIALS

Robert A Lehnert — RAL
R. A. Lehnert/Project Manager — INITIALS

Robert S. Quinn — RDQ
R. D. Quinn/Senior Engineer — INITIALS

M. Shamszad — MS
M. Shamszad/Senior Engineer — INITIALS

Y. C. Yiu — YCY
Y. C. Yiu/Group Leader — INITIALS

AFFECTED PAGE(S)	DOC REV	PREPARED BY / DATE	ACCURACY CHECK BY / DATE	CRITERIA CHECK BY / DATE	REMARKS
ii	0	RDQ/1-19-84	YCY/1-19-84	RAL/1-19-84	
iii	0				
iv	0				
v	0				
vi	0				
vii	0				
viii	0				
ix	0				
x	0				
xi	0				
2-1.1	0				
2-1.2	0				
2-1.3	0				
2-1.4	0				
2-2.1	0				
2-2.2	0				
2-2.3	0				
2-2.4	0				
2-2.5	0				
2-2.6	0				
2-2.7	0	RDQ/1-19-84	YCY/1-19-84	RAL/1-19-84	

REVISION CONTROL SHEET
(CONTINUATION)

TITLE: Hope Creek Generating Station Plant Unique Analysis Report, Volume 2

DOCUMENT FILE NUMBER: BPC-01-300-2 Revision 0

AFFECTED PAGE(S)	DOC REV	PREPARED BY / DATE	ACCURACY CHECK BY / DATE	CRITERIA CHECK BY / DATE	REMARKS
2-2.8	0	RDQ/1-19-84	yeg/1-19-84	RAL/1-19-84	
2-2.9	0		MS/1-19-84	yeg/1-19-84	
2-2.10	0				
2-2.11	0				
2-2.12	0				
2-2.13	0				
2-2.14	0				
2-2.15	0				
2-2.16	0				
2-2.17	0				
2-2.18	0				
2-2.19	0				
2-2.20	0				
2-2.21	0		MS/1-19-84	yeg/1-19-84	
2-2.22	0		yeg/1-19-84	RAL/1-19-84	
2-2.23	0				
2-2.24	0				
2-2.25	0				
2-2.26	0				
2-2.27	0				
2-2.28	0				
2-2.29	0				
2-2.30	0				
2-2.31	0				
2-2.32	0				
2-2.33	0				
2-2.34	0				
2-2.35	0				
2-2.36	0				
2-2.37	0				
2-2.38	0				
2-2.39	0				
2-2.40	0	RDQ/1-19-84	yeg/1-19-84	RAL/1-19-84	

REVISION CONTROL SHEET
(CONTINUATION)

TITLE: Hope Creek Generating Station Plant Unique Analysis Report, Volume 2

DOCUMENT FILE NUMBER: BPC-01-300-2 Revision 0

AFFECTED PAGE(S)	DOC REV	PREPARED BY / DATE	ACCURACY CHECK BY / DATE	CRITERIA CHECK BY / DATE	REMARKS
2-2.41	0	RDQ/1-19-84	ycy/1-19-84	RAL/1-19-84	
2-2.42	0				
2-2.43	0				
2-2.44	0		ycy/1-19-84	RAL/1-19-84	
2-2.45	0		MS/1-19-84	ycy/1-19/84	
2-2.46	0	RDQ/1-19-84			
2-2.47	0	MCH/1-19-84			
2-2.48	0				
2-2.49	0	MCH/1-19-84			
2-2.50	0	RDQ/1-19-84			
2-2.51	0				
2-2.52	0				
2-2.53	0	RDQ/1-19-84			
2-2.54	0	MCH/1-19-84			
2-2.55	0	RDQ/1-19-84			
2-2.56	0				
2-2.57	0				
2-2.58	0	RDQ/1-19-84			
2-2.59	0	MCH/1-19-84			
2-2.60	0				
2-2.61	0	MCH/1-19-84	MS/1-19-84	ycy/1-19-84	
2-2.62	0	RDQ/1-19-84	ycy/1-19-84	RAL/1-19-84	
2-2.63	0				
2-2.64	0				
2-2.65	0				
2-2.66	0				
2-2.67	0				
2-2.68	0		ycy/1-19-84	RAL/1-19-84	
2-2.69	0		MS/1-19-84	ycy/1-19-84	
2-2.70	0				
2-2.71	0				
2-2.72	0				
2-2.73	0	RDQ/1-19-84	MS/1-19-84	ycy/1-19-84	

REVISION CONTROL SHEET
(CONTINUATION)

TITLE: Hope Creek Generating Station Plant Unique Analysis Report, Volume 2

DOCUMENT FILE NUMBER: BPC-01-300-2 Revision 0

AFFECTED PAGE(S)	DOC REV	PREPARED BY / DATE	ACCURACY CHECK BY / DATE	CRITERIA CHECK BY / DATE	REMARKS
2-2.74	0	ROQ/1-19-84	MS/1-19-84	ycy/1-19-84	
2-2.75	0		MS/1-19-84	ycy/1-19-84	
2-2.76	0		ycy/1-19-84	RAL/1-19-84	
2-2.77	0				
2-2.78	0				
2-2.79	0	ROQ/1-19-84	ycy/1-19-84	RAL/1-19-84	
2-2.80	0	MCH/1-19-84	MS/1-19-84	ycy/1-19-84	
2-2.81	0	MCH/1-19-84	MS/1-19-84	ycy/1-19-84	
2-2.82	0	ROQ/1-19-84	ycy/1-19-84	RAL/1-19-84	
2-2.83	0				
2-2.84	0				
2-2.85	0				
2-2.86	0				
2-2.87	0				
2-2.88	0				
2-2.89	0				
2-2.90	0				
2-2.91	0				
2-2.92	0				
2-2.93	0				
2-2.94	0				
2-2.95	0				
2-2.96	0				
2-2.97	0	ROQ/1-19-84	ycy/1-19-84	RAL/1-19-84	
2-2.98	0	MCH/1-19-84	MS/1-19-84	ycy/1-19-84	
2-2.99	0				
2-2.100	0				
2-2.101	0	MCH/1-19-84	MS/1-19-84	ycy/1-19-84	
2-2.102	0	ROQ/1-19-84	ycy/1-19-84	RAL/1-19-84	
2-2.103	0	MCH/1-19-84	MS/1-19-84	ycy/1-19-84	
2-2.104	0	MCH/1-19-84	MS/1-19-84	ycy/1-19-84	
2-2.105	0	ROQ/1-19-84	ycy/1-19-84	RAL/1-19-84	
2-2.106	0	ROQ/1-19-84	ycy/1-19-84	RAL/1-19-84	

REVISION CONTROL SHEET
(CONTINUATION)

TITLE: Hope Creek Generating Station Plant Unique Analysis Report, Volume 2

DOCUMENT FILE NUMBER: BPC-01-300-2 Revision 0

AFFECTED PAGE(S)	DOC REV	PREPARED BY / DATE	ACCURACY CHECK BY / DATE	CRITERIA CHECK BY / DATE	REMARKS
2-2.107	0	RDQ/1-19-84	yey/1-19-84	RAL/1-19-84	
2-2.108	0				
2-2.109	0				
2-2.110	0				
2-2.111	0				
2-2.112	0		yey/1-19-84	RAL/1-19-84	
2-2.113	0		MS/1-19-84	yey/1-19-84	
2-2.114	0		yey/1-19-84	RAL/1-19-84	
2-2.115	0	RDQ/1-19-84	yey/1-19-84	RAL/1-19-84	
2-2.116	0	MCH/1-19-84	MS/1-19-84	yey/1-19-84	
2-2.117	0				
2-2.118	0				
2-2.119	0				
2-2.120	0				
2-2.121	0				
2-2.122	0				
2-2.123	0				
2-2.124	0				
2-2.125	0				
2-2.126	0	MCH/1-19-84	MS/1-19-84	yey/1-19-84	
2-2.127	0	RDQ/1-19-84	yey/1-19-84	RAL/1-19-84	
2-2.128	0				
2-2.129	0				
2-2.130	0				
2-3.1	0	RDQ/1-19-84	yey/1-19-84	RAL/1-19-84	

ABSTRACT

The primary containment for the Hope Creek Generating Station was designed, erected, pressure-tested, and N-stamped in accordance with the ASME Boiler and Pressure Vessel Code, Section III, 1974 Edition with addenda up to and including Winter 1974. These activities were performed for the Public Service Electric and Gas Company (PSE&G) by the Pittsburgh-Des Moines Steel Company. Since then, new requirements which affect the design and operation of the primary containment system have been established. These requirements are defined in the Nuclear Regulatory Commission's (NRC) Safety Evaluation Report, NUREG-0661. The NUREG-0661 requirements define revised containment design loads postulated to occur during a loss-of-coolant accident or a safety-relief valve discharge event which are to be evaluated. In addition, NUREG-0661 requires that an assessment of the effects that these postulated events have on the operation of the containment system be performed.

This plant unique analysis report (PUAR) documents the efforts undertaken to address and resolve each of the applicable NUREG-0661 requirements for Hope Creek. It demonstrates, in accordance with NUREG-0661 acceptance criteria, that the design of the primary containment system is adequate and that original design safety margins have been restored. The Hope Creek PUAR is composed of the following six volumes:

- o Volume 1 - GENERAL CRITERIA AND LOADS METHODOLOGY
- o Volume 2 - SUPPRESSION CHAMBER ANALYSIS
- o Volume 3 - VENT SYSTEM ANALYSIS
- o Volume 4 - INTERNAL STRUCTURES ANALYSIS
- o Volume 5 - SAFETY RELIEF VALVE DISCHARGE PIPING ANALYSIS
- o Volume 6 - TORUS ATTACHED PIPING AND SUPPRESSION CHAMBER PENETRATION ANALYSES

Major portions of all volumes of this report have been prepared by NUTECH Engineers, Incorporated (NUTECH), acting as a consultant responsible to the Public Service Electric and Gas Company. Selected sections of Volumes 5 and 6 have been prepared by the Bechtel Power Corporation acting as an agent responsible to the Public Service Electric and Gas Company. This volume, Volume 2, documents the evaluation of the suppression chamber.

NOTE: Identification of the volume number precedes each page, section, subsection, table, and figure number.

TABLE OF CONTENTS

LIST OF ACRONYMS

ACI	American Concrete Institute
ADS	Automatic Depressurization System
AISC	American Institute of Steel Construction
ASME	American Society of Mechanical Engineers
ATWS	Anticipated Transients Without Scram
BDC	Bottom Dead Center
BWR	Boiling Water Reactor
CDF	Cumulative Distribution Function
CO	Condensation Oscillation
DBA	Design Basis Accident
DC	Downcomer
DLF	Dynamic Load Factor
ECCS	Emergency Core Cooling System
FSAR	Final Safety Analysis Report
FSI	Fluid-Structure Interaction
FSTF	Full-Scale Test Facility
HNWL	High Normal Water Level
HPCI	High Pressure Coolant Injection
IBA	Intermediate Break Accident
I&C	Instrumentation and Control
ID	Inside Diameter
IR	Inside Radius
LDR	Load Definition Report
LOCA	Loss-of-Coolant Accident

LIST OF ACRONYMS

(Continued)

LPCI	Low Pressure Coolant Injection
LTP	Long-Term Program
MC	Midcylinder
MCF	Modal Correction Factor
MJ	Mitered Joint
MVA	Multiple Valve Actuation
NEP	Non-Exceedance Probability
NOC	Normal Operating Conditions
NRC	Nuclear Regulatory Commission
NSSS	Nuclear Steam Supply System
NVB	Non-Vent Line Bay
OBE	Operating Basis Earthquake
OD	Outside Diameter
PSD	Power Spectral Density
PSE&G	Public Service Electric and Gas Company
PUA	Plant Unique Analysis
PUAAG	Plant Unique Analysis Application Guide
PUAR	Plant Unique Analysis Report
PULD	Plant Unique Load Definition
QSTF	Quarter-Scale Test Facility
RCIC	Reactor Core Isolation Cooling
RHR	Residual Heat Removal
RPV	Reactor Pressure Vessel
RSEL	Resultant Static-Equivalent Load

LIST OF ACRONYMS
(Concluded)

SBA	Small Break Accident
SBP	Small Bore Piping
SER	Safety Evaluation Report
SORV	Stuck-Open Safety Relief Valve
SRSS	Square Root of the Sum of the Squares
SRV	Safety Relief Valve
SRVDL	Safety Relief Valve Discharge Line
SSE	Safe Shutdown Earthquake
STP	Short-Term Program
SVA	Single Valve Actuation
TAP	Torus Attached Piping
VB	Vent Line Bay
VH	Vent Header
VL	Vent Line
VPP	Vent Pipe Penetration
ZPA	Zero Period Acceleration

LIST OF TABLES

LIST OF TABLES
(Concluded)

LIST OF FIGURES

LIST OF FIGURES
(Continued)

2-1.0 INTRODUCTION

In conjunction with Volume 1 of the Plant Unique Analysis Report (PUAR), this volume documents the efforts undertaken to address the requirements defined in NUREG-0661 which affect the Hope Creek suppression chamber. The suppression chamber PUAR is organized as follows:

- o INTRODUCTION
  - Scope of Analysis
- o SUPPRESSION CHAMBER ANALYSIS
  - Component Description
  - Loads and Load Combinations
  - Analysis Acceptance Criteria
  - Method of Analysis
  - Analysis Results and Conclusion

The INTRODUCTION section contains an overview discussion of the scope of the suppression chamber evaluation. The SUPPRESSION CHAMBER ANALYSIS section contains a comprehensive discussion of the suppression chamber loads and load combinations, and a description of the component parts of the suppression chamber affected by these loads. The section also contains a discussion of the methodology used to evaluate the

effects of these loads, the evaluation results, the acceptance limits to which the results are compared, and a summary of the conclusions derived from the suppression chamber evaluation.

2-1.1 Scope of Analysis

The general criteria presented in Volume 1 are used as the basis for the Hope Creek suppression chamber evaluation. The suppression chamber is evaluated for the effects of LOCA and SRV discharge related loads discussed in Volume 1 and defined by the NRC Safety Evaluation Report NUREG-0661 (Reference 1) and by the Mark I Containment Program Load Definition Report (LDR) (Reference 2).

The LOCA and SRV discharge loads used in this evaluation are developed using the plant unique geometry, operating parameters, and test results contained in the Mark I Containment Program Plant Unique Load Definition (PULD) (Reference 3). The effects of increased suppression pool temperatures which occur during SRV discharge events are also evaluated. These temperatures are taken from the plant's suppression pool temperature response analysis. Other loads and methodology, such as the evaluation for seismic loads, are taken from the plant's original design basis evaluation documented in the Final Safety Analysis Report (FSAR) (Reference 4).

The evaluation includes a structural analysis of the suppression chamber for the effects of LOCA and SRV discharge related loads to confirm that the design of the modified suppression chamber is adequate. Rigorous analytical techniques are used in this evaluation, including use of detailed analytical models for computing the dynamic response of the suppression chamber. Effects such as fluid-structure interaction are considered in the suppression chamber analysis.

The results of the structural evaluation of the suppression chamber for each load are used to evaluate load combinations and fatigue effects in accordance with the Mark I Containment Program Structural Acceptance Criteria Plant Unique Analysis Application Guide (PUAAG) (Reference 5). The analysis results are compared with the acceptance limits specified by the PUAAG and the applicable sections of the American Society of Mechanical Engineers (ASME) Code (Reference 6).

2-2.0 SUPPRESSION CHAMBER ANALYSIS

An evaluation of each of the NUREG-0661 requirements which affect the design adequacy of the Hope Creek suppression chamber is presented in the sections which follow. The criteria used in this evaluation are presented in Volume 1 of this report.

The component parts of the suppression chamber which are examined are described in Section 2-2.1. The loads and load combinations for which the suppression chamber is evaluated are presented in Section 2-2.2. The methodology used to evaluate the effects of these loads and load combinations on the suppression chamber is discussed in Section 2-2.4. The acceptance limits to which the analysis results are compared are described in Section 2-2.3. The analysis results and the corresponding suppression chamber design margins are presented in Section 2-2.5.

2-2.1 Component Description

The Hope Creek suppression chamber is constructed from 16 mitered cylindrical shell segments joined together in the shape of a torus. The configuration of the suppression chamber is illustrated in Figure 2-2.1-1. The proximity of the suppression chamber to other components of the containment is shown in Figures 2-2.1-1 through 2-2.1-6.

The suppression chamber is connected to the drywell by 8 vent lines which, in turn, are connected to a common vent header within the suppression chamber. Attached to the vent header are downcomers which terminate below the surface of the suppression pool. The vent system is supported within the suppression chamber by two vertical support columns at each mitered joint, and one vertical support column at each midcylinder location, as shown in Figures 2-2.1-3 through 2-2.1-5. In addition, the vent system is supported by overhead truss members, as shown in Figure 2-2.1-6. A bellows assembly is provided at the penetration of the vent line to the suppression chamber, as shown in Figure 2-2.1-2, to allow differential movement of the suppression chamber and vent system to occur.

The major radius of the suppression chamber is 56'-4", measured at midcylinder of each mitered cylinder, as shown in Figure 2-2.1-1. The inside diameter of the mitered cylinders which make up the suppression chamber is 30'-8". The suppression chamber shell thickness is typically 1", except at penetrations where it is locally thicker.

The suppression chamber shell is reinforced at each mitered joint location by a T-shaped ring beam, as shown in Figures 2-2.1-4 and 2-2.1-7. A typical mitered joint ring beam is located in a plane 3-1/2" from the mitered joint and on the non-vent line bay side of each mitered joint. As such, the intersection of a ring beam web and the suppression chamber shell is an ellipse. The inner flange of the mitered joint ring beams are rolled to a constant inside radius of 13'-6 1/2". Thus the depth of a mitered joint ring beam web varies from 20" to 23-5/8" and has a constant thickness of 1-1/4". The mitered joint ring beams are attached to the suppression chamber shell by 1/2" partial penetration welds with 1/2" cover fillet welds.

The flanges of the mitered joint ring beams are 12" wide by 1-1/2" thick. The portions of the mitered joint ring beams adjacent to the column connections are

reinforced by 9" wide by 1-1/2" thick cover plates which extend from the horizontal centerline of the suppression chamber to approximately 45° below the centerline, as shown in Figures 2-2.1-4 and 2-2.1-7.

The suppression chamber shell is reinforced at each midcylinder location by a partial T-shaped ring beam which extends above the horizontal centerline of the suppression chamber, as shown in Figures 2-2.1-3, 2-2.1-5, and 2-2.1-9. The midcylinder ring beams have a constant web depth of 30" and a thickness of 1-1/4". The midcylinder ring beams are attached to the suppression chamber shell by 1/2" partial penetration welds with 1/2" cover fillet welds. The flanges of the midcylinder ring beams are 15" wide by 1-1/2" thick.

The ring beams are braced laterally with stiffeners connecting the ring beam webs to the suppression chamber shell, as shown in Figures 2-2.1-3, 2-2.1-4, 2-2.1-5, 2-2.1-7, and 2-2.1-9. The stiffener plates are spaced intermittently around the circumference of the ring beams, concentrated in areas where lateral submerged drag loads and ring beam compressive stresses occur.

The suppression chamber is supported vertically at [illegible] mitered joint and midcylinder location by inside and outside columns, as shown in Figures 2-2.1-3, 2-2.1-4, and 2-2.1-5. The columns and column connection plates are located parallel to the associated mitered joint and midcylinder planes. At each ring beam location the ring beam, columns, and column connections form an integral support system which transfers vertical loads acting on the suppression chamber shell to the reactor building basemat. Since the columns are pinned at both ends, the support system provides full vertical support for the suppression chamber, while allowing lateral movement and thermal expansion to occur.

The suppression chamber support columns consist of built-up members comprised of 2-1/4" thick flange plates and 1" thick web plates. The columns are attached to the suppression chamber shell by 2-1/4" thick pin plates and vertical stiffener plates as shown in Figures 2-2.1-7 and 2-2.1-9. The pin plates are stiffened in the out-of-plane direction as shown in Figures 2-2.1-8 and 2-2.1-10.

The anchorage of the suppression chamber to the basemat is achieved by a system of base plates, stiffeners, and anchor bolts located at each column, as shown in Figure

2-2.1-11. The column base plate assemblies consist of two 3" thick base plates, gusset plates, and two 2-1/4" thick pin plates.

Six 2" diameter anchor bolts are embedded in the basemat at each column base plate location. Twelve anchor bolts at each mitered joint and each midcylinder location provide the principal mechanism for transfer of uplift loads acting on the suppression chamber to the basemat.

The suppression chamber is supported horizontally by a system of restraint members which connect each mitered cylinder at midheight to the adjacent drywell shield wall. The horizontal restraint system is shown schematically in Figure 2-2.1-1. Each suppression chamber mitered cylinder contains a pin plate/pad plate assembly located at midcylinder, and is supported by two W14 x 150 wide flange members as shown in Figure 2-2.1-12. The wide flange members are joined at one end by 2-1/4" tie plates which are bolted to the pin plate/pad plate assembly, and by cover plates at the other end which are bolted to lug plates embedded in the concrete drywell shield wall. The pin plates are slotted radially to permit thermal movement of the suppression chamber. As a result each horizontal

restraint assembly is effective only for tangential loads.

The T-quenchers used for Hope Creek are described in Section 1-4.2. There are a total of 14 T-quenchers arranged as shown in Figures 2-2.1-6 and 2-2.1-13 with ramsheads located at the mitered joints. The associated quencher arms for each T-quencher are located near the plane of the vertical centerline of the suppression chamber.

The T-quencher is supported at the mitered joint by a ramshead support which transfers loads acting on the T-quencher to the mitered joint ring beam, as shown in Figure 2-2.1-4. The T-quencher arms are supported by a support beam which spans between the ring beams directly below the T-quenchers, as shown in Figure 2-2.1-6. Loads which act on the T-quencher arms and the T-quencher support beam are transferred to ring plate supports at midcylinder and the mitered joint, as shown in Figures 2-2.1-3 through 2-2.1-6.

The suppression chamber provides support for many other containment-related structures such as the vent system, catwalk, and monorail. Loads acting on the suppression chamber cause motions at the attachment points of these

structures to the suppression chamber. Loads acting on these structures also cause reaction loads on the suppression chamber. These containment interaction effects are evaluated in the analysis of the suppression chamber.

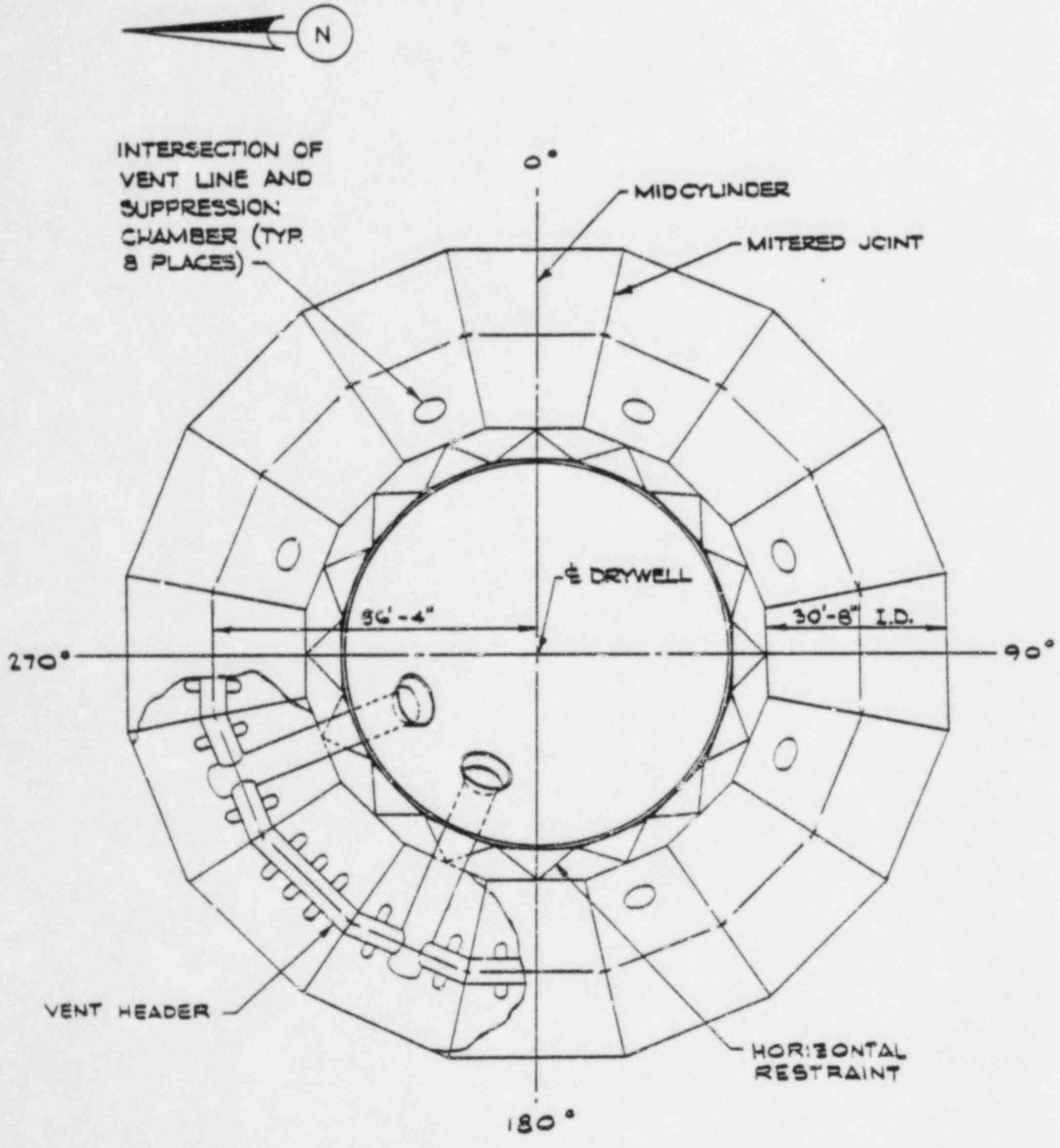

Figure 2-2.1-1

PLAN VIEW OF CONTAINMENT

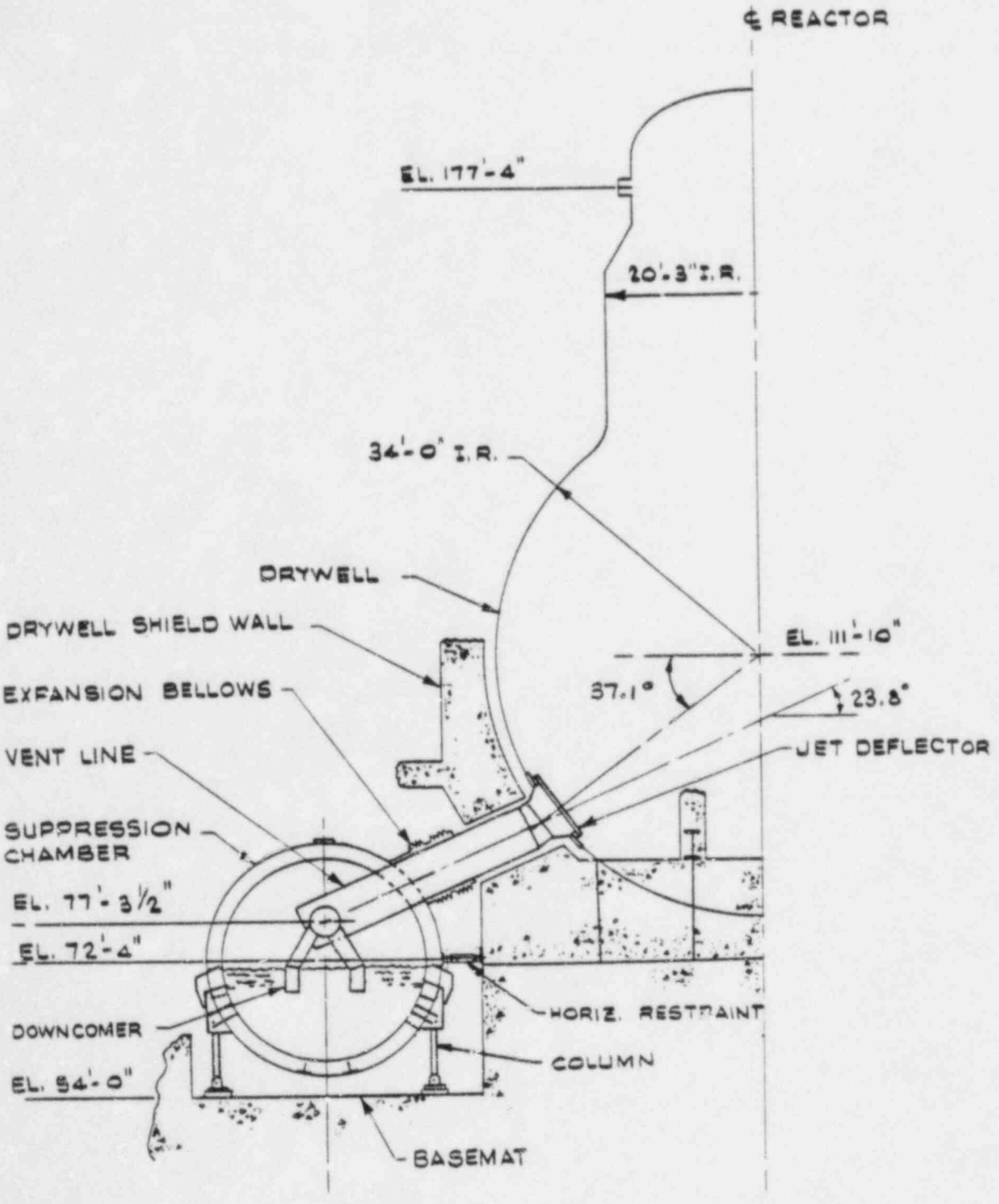

Figure 2-2.1-2

ELEVATION VIEW OF CONTAINMENT

nutech ENGINEERS

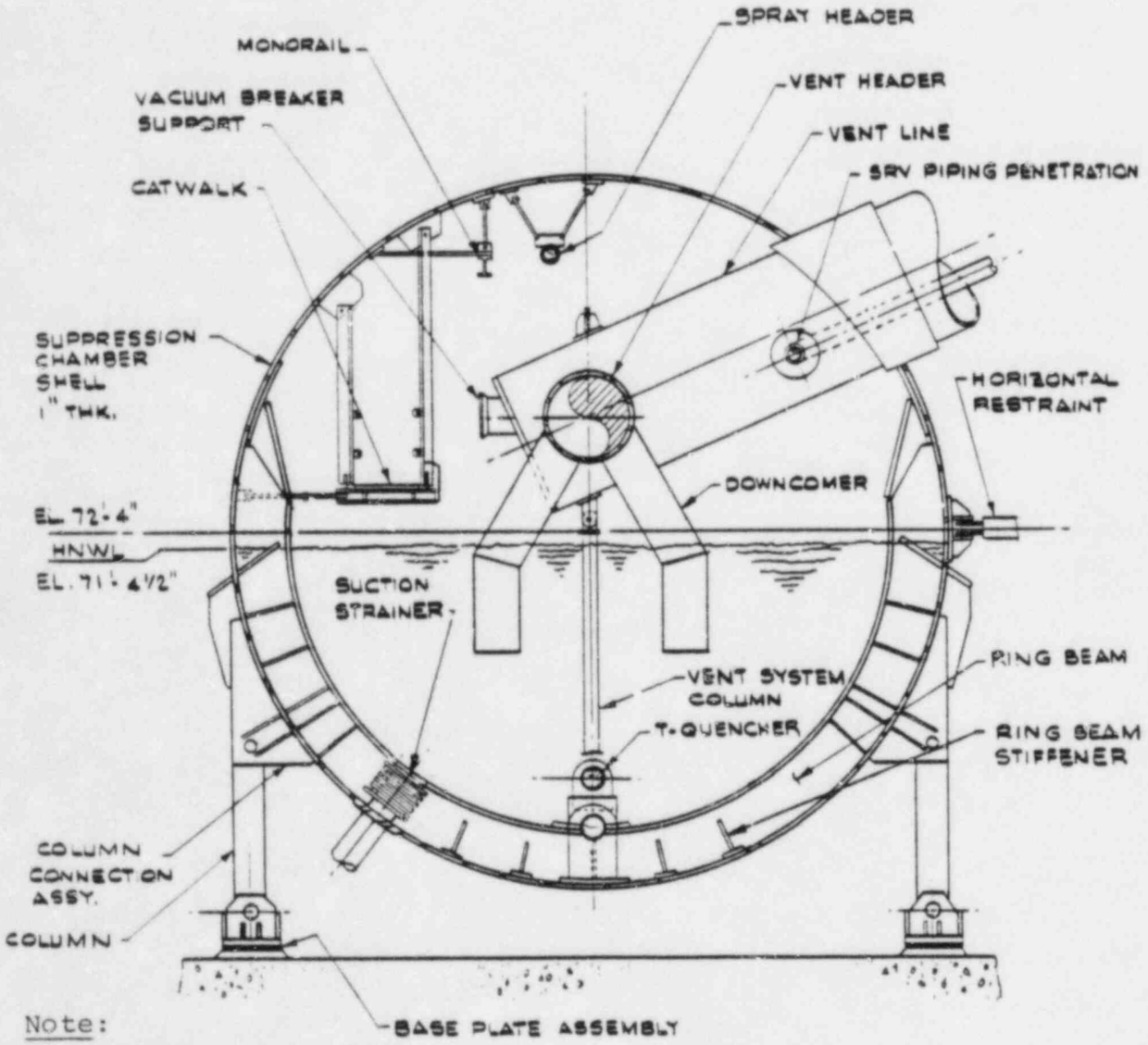

Note:

1. Downcomer stiffener plates not shown for clarity.

Figure 2-2.1-3

SUPPRESSION CHAMBER SECTION - MIDCYLINDER VENT LINE BAY

nutech ENGINEERS

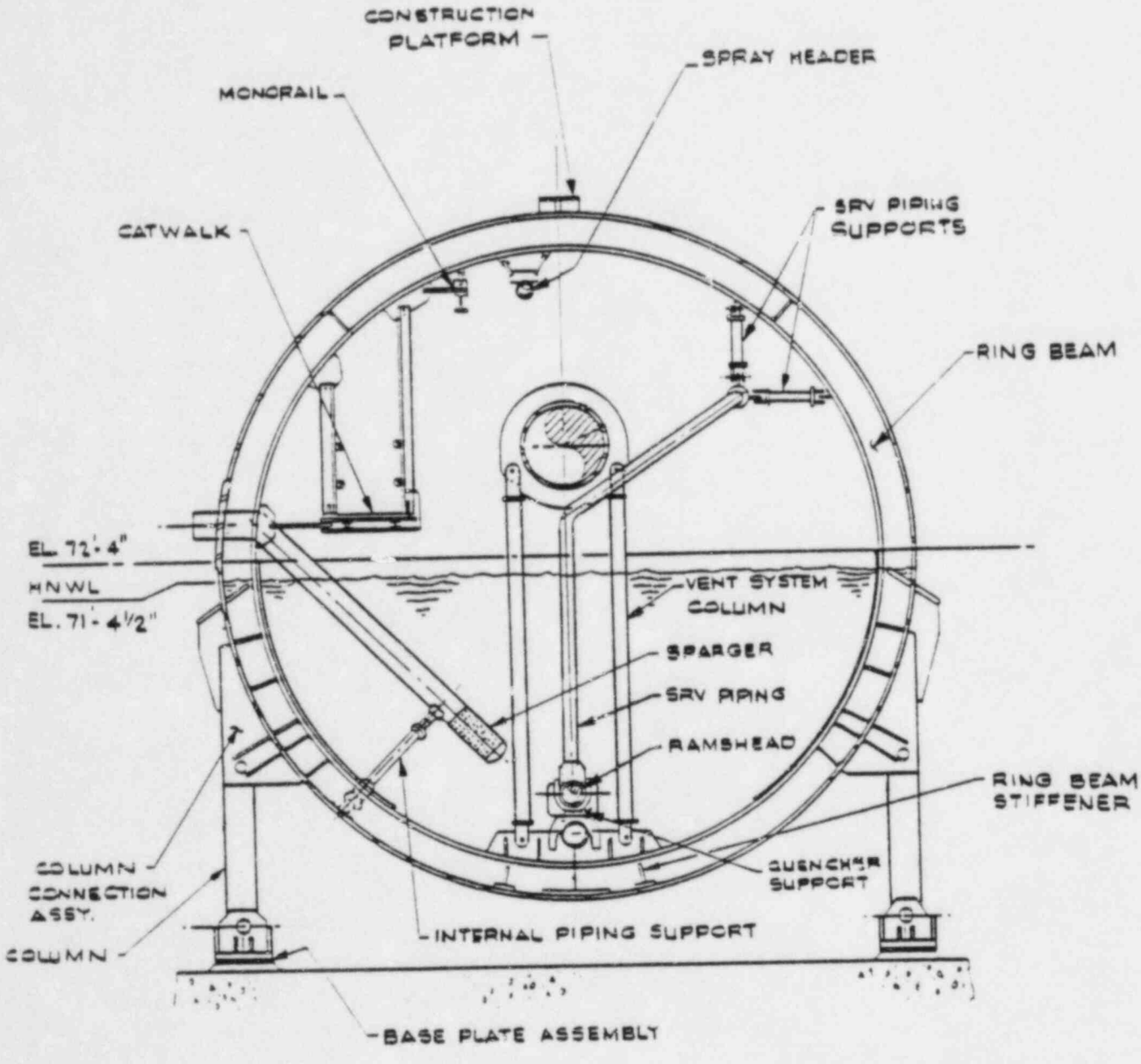

Figure 2-2.1-4

SUPPRESSION CHAMBER SECTION - MITERED JOINT

nutech ENGINEERS

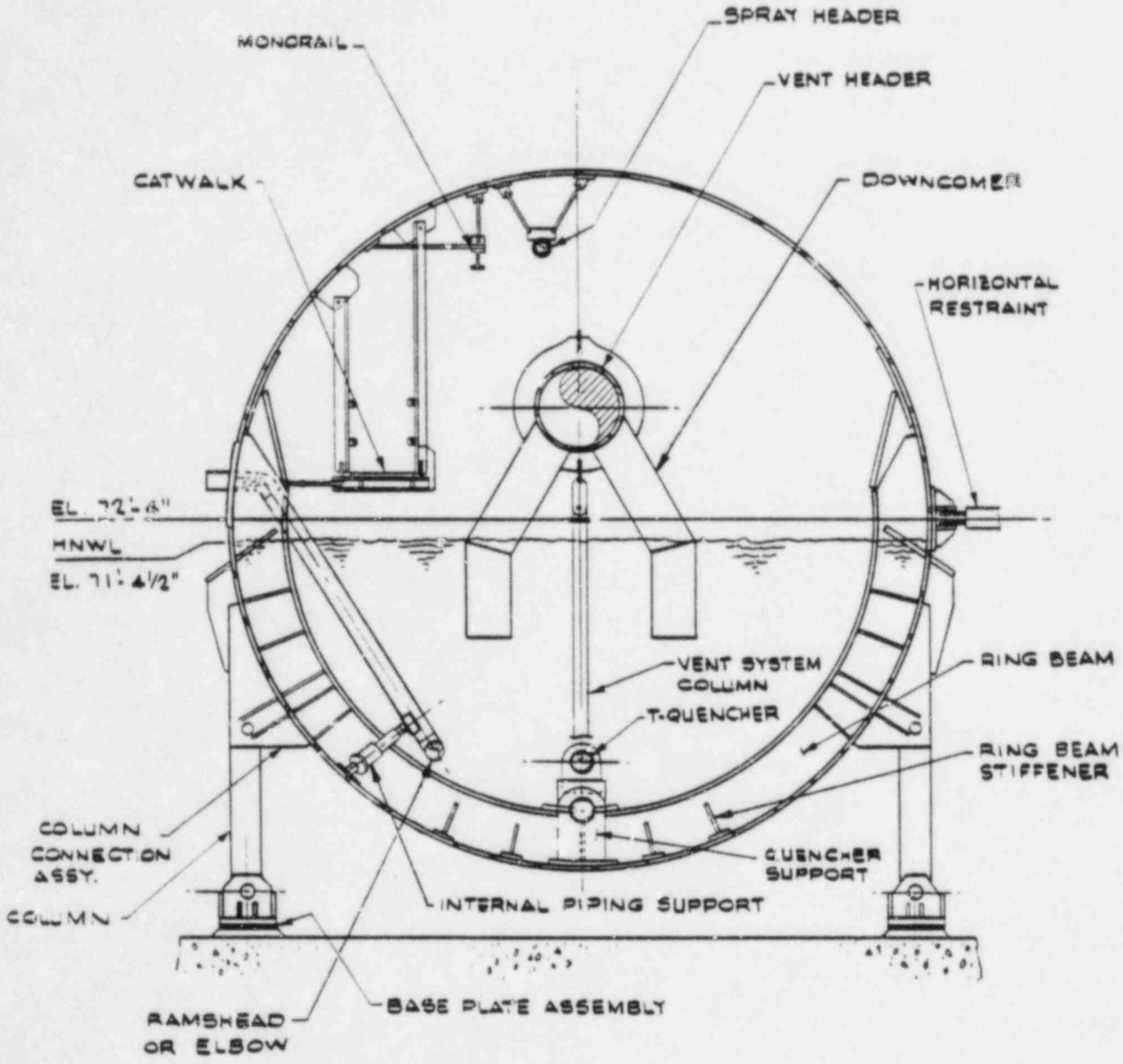

Note:

1. Downcomer stiffener plates not shown for clarity.

Figure 2-2.1-5

SUPPRESSION CHAMBER SECTION - MIDCYLINDER NON-VENT BAY

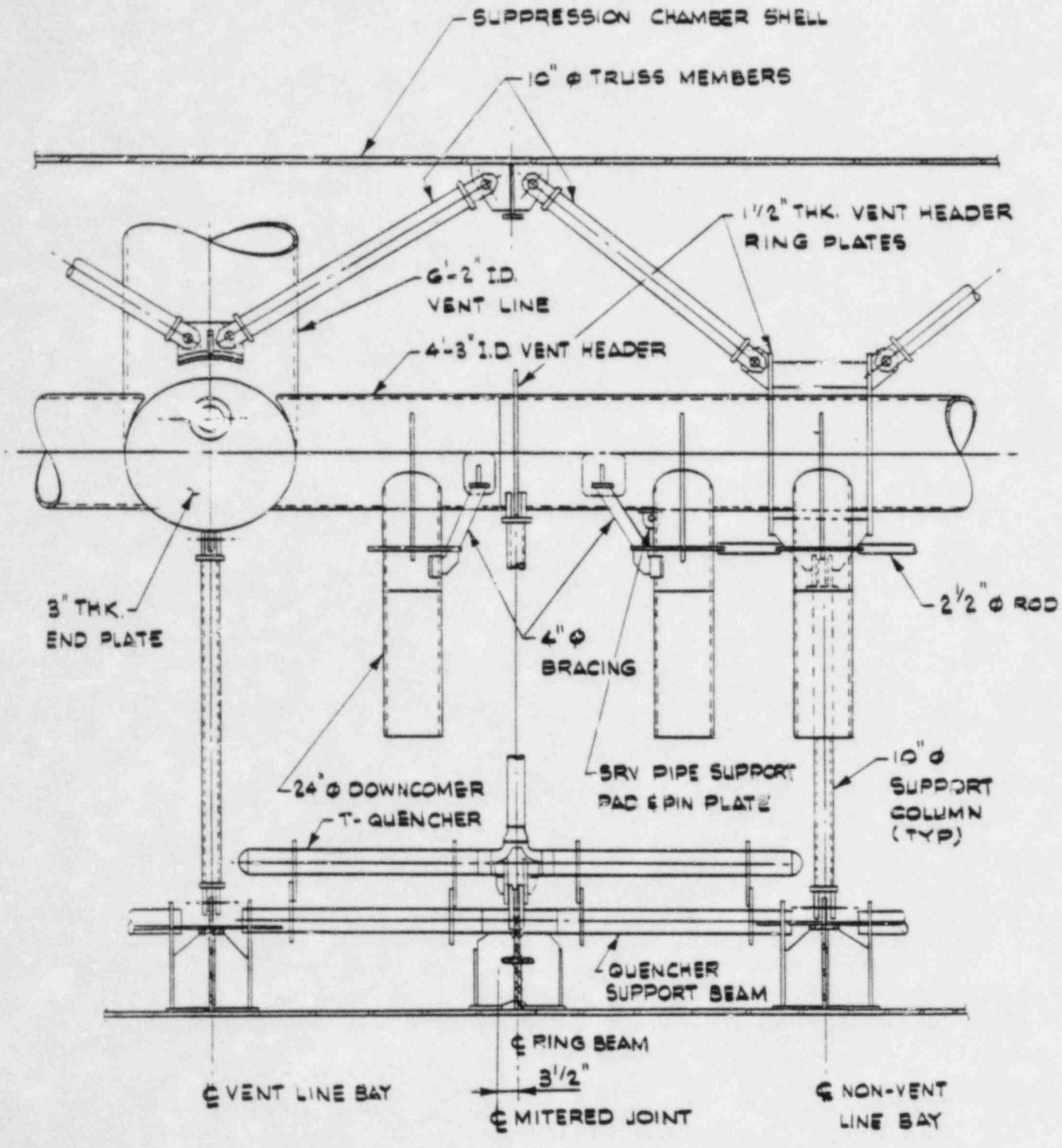

Figure 2-2.1-6

DEVELOPED VIEW OF SUPPRESSION CHAMBER SEGMENT

nutech ENGINEERS

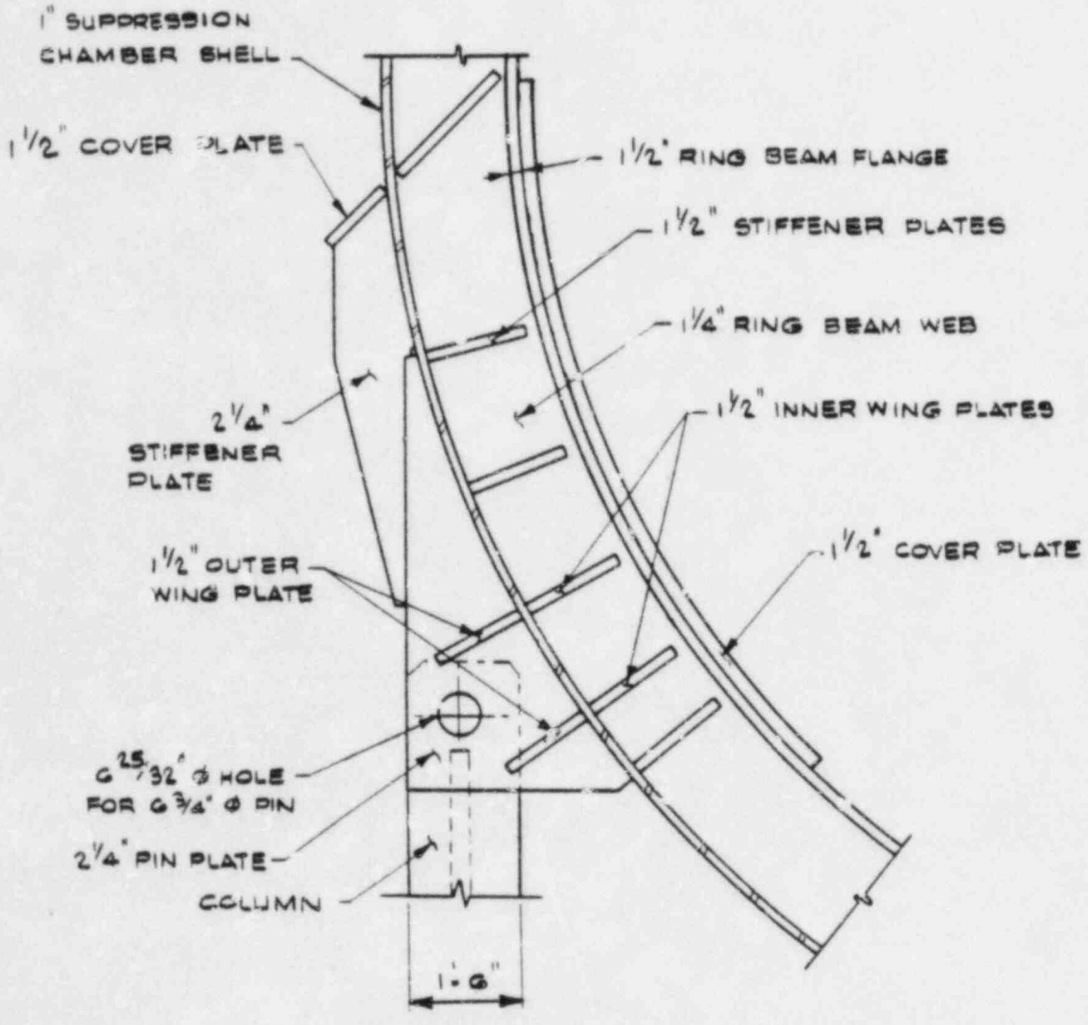

Figure 2-2.1-7

TYPICAL MITERED JOINT COLUMN CONNECTION DETAIL

nutech ENGINEERS

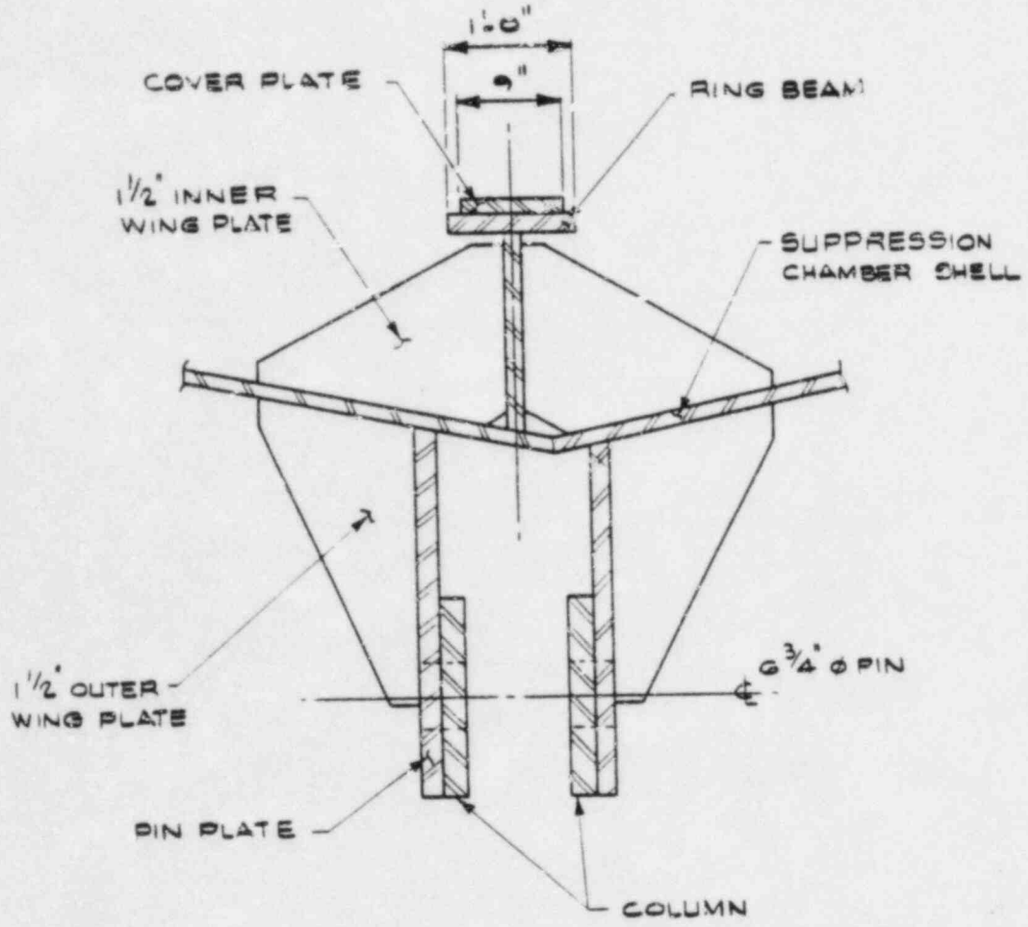

Figure 2-2.1-8

SECTION THROUGH OUTSIDE COLUMN CONNECTION AT MITERED JOINT

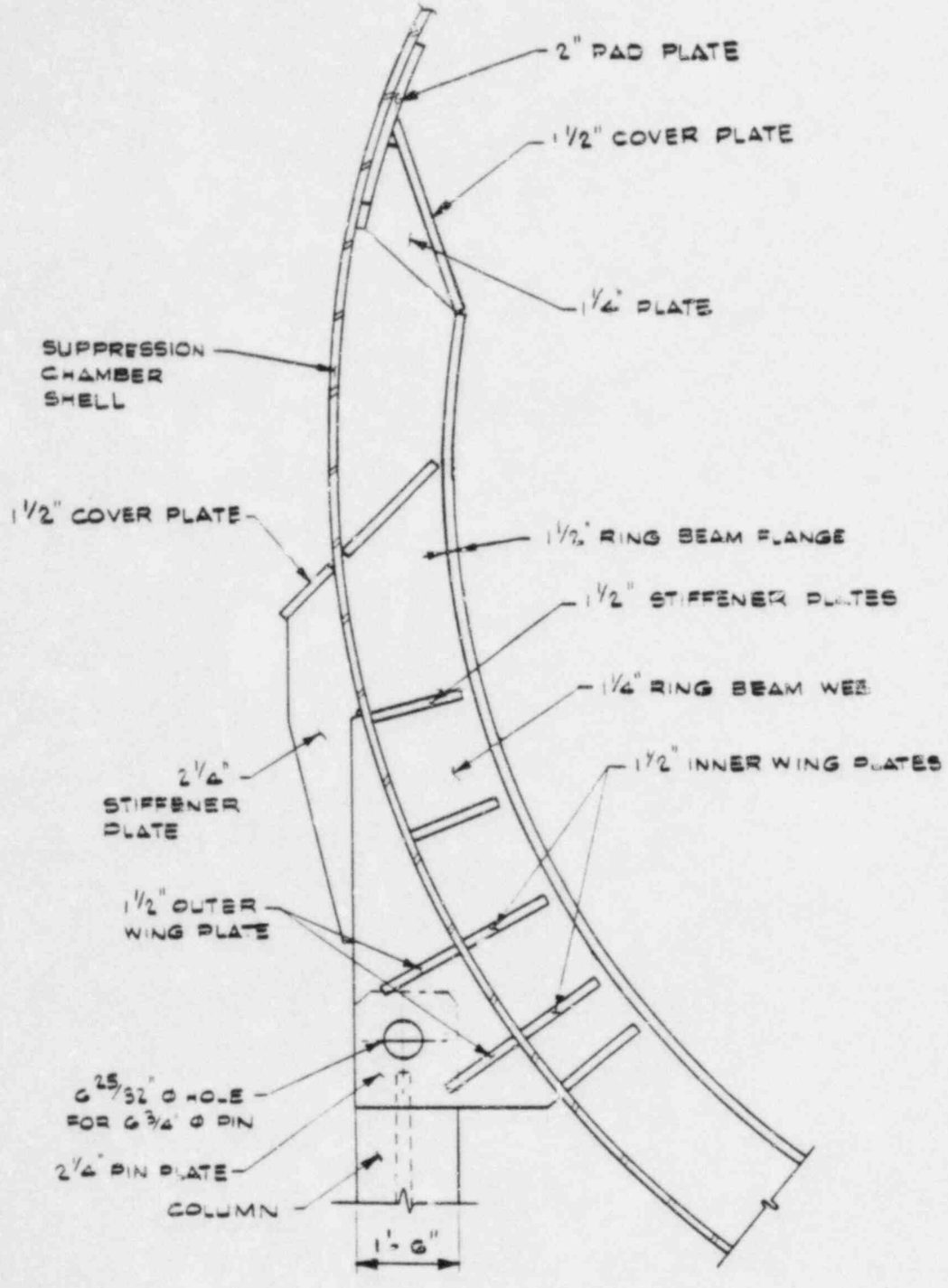

Figure 2-2.1-9

TYPICAL MIDCYLINDER COLUMN CONNECTION DETAIL

nutech ENGINEERS

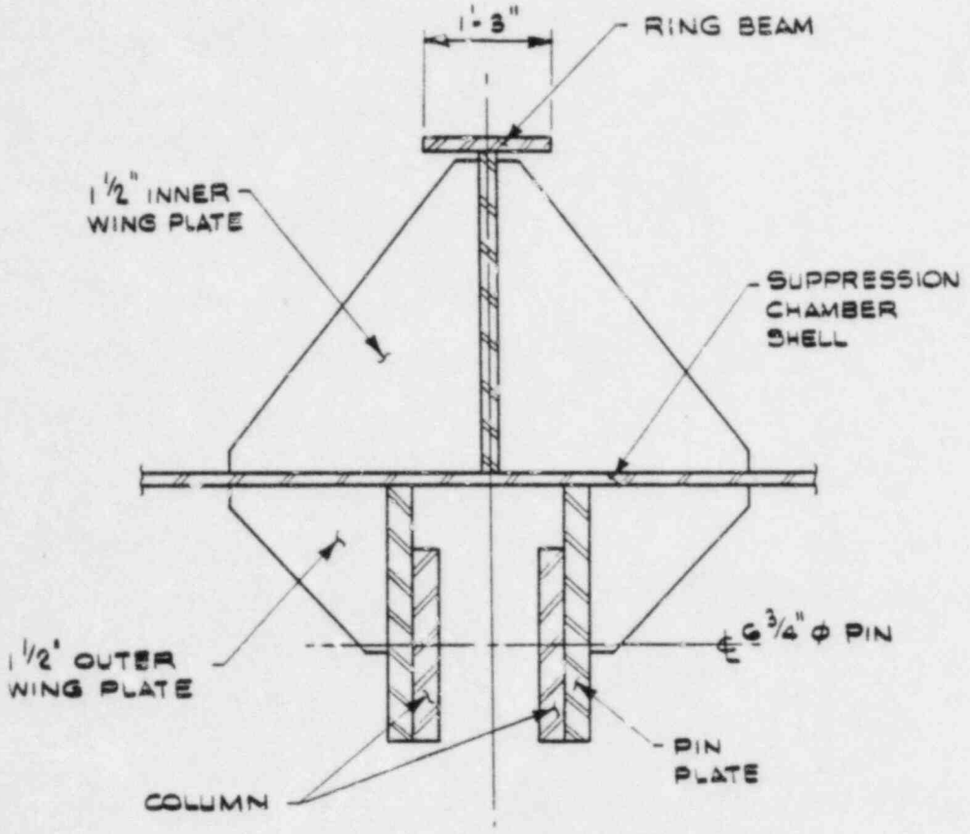

Figure 2-2.1-10

SECTION THROUGH COLUMN CONNECTION AT MIDCYLINDER

nutech ENGINEERS

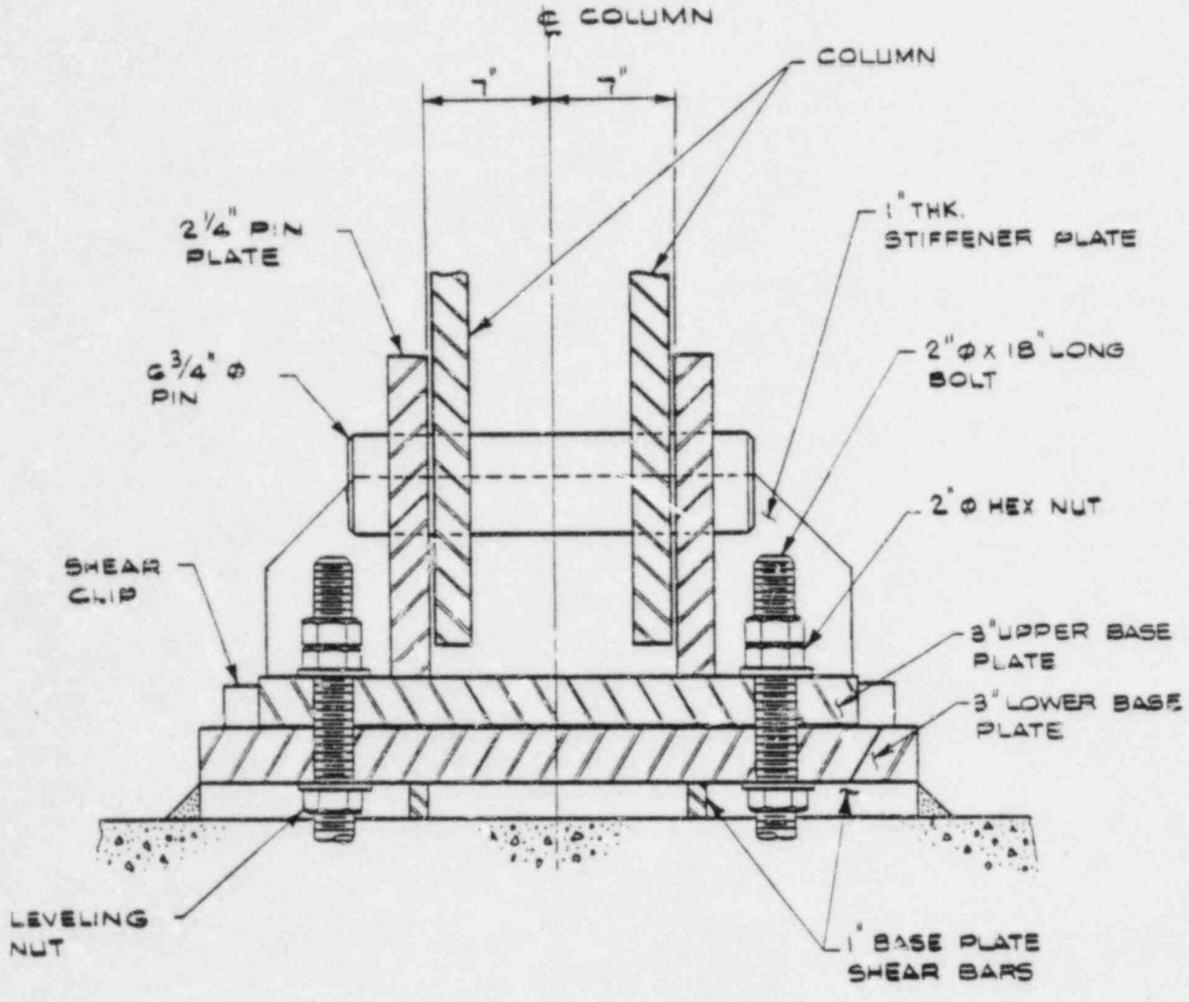

Figure 2-2.1-11

TYPICAL COLUMN BASE PLATE DETAIL

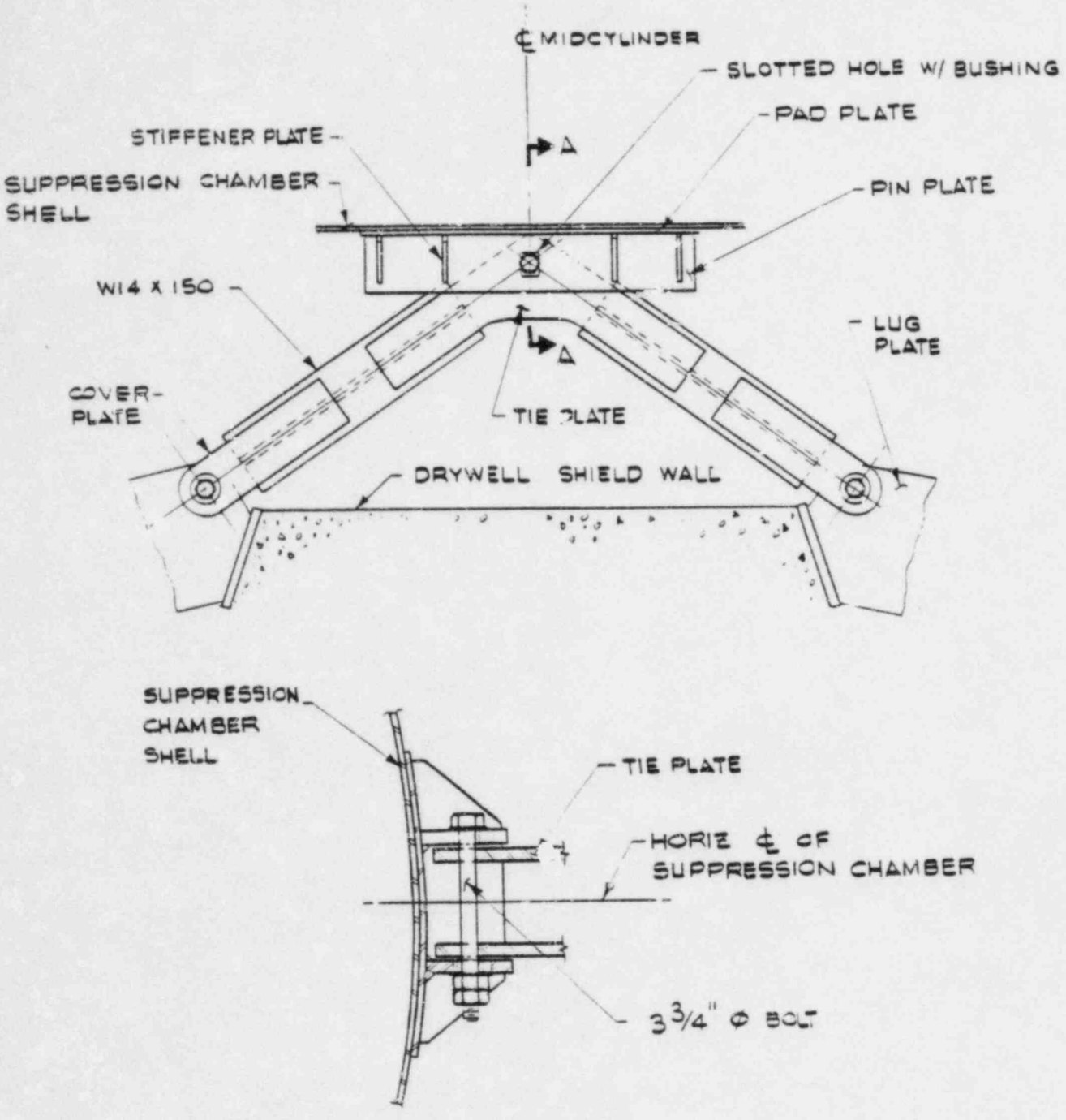

SECTION A-A

Figure 2-2.1-12

SUPPRESSION CHAMBER HORIZONTAL RESTRAINT ASSEMBLY DETAILS

nutech ENGINEERS

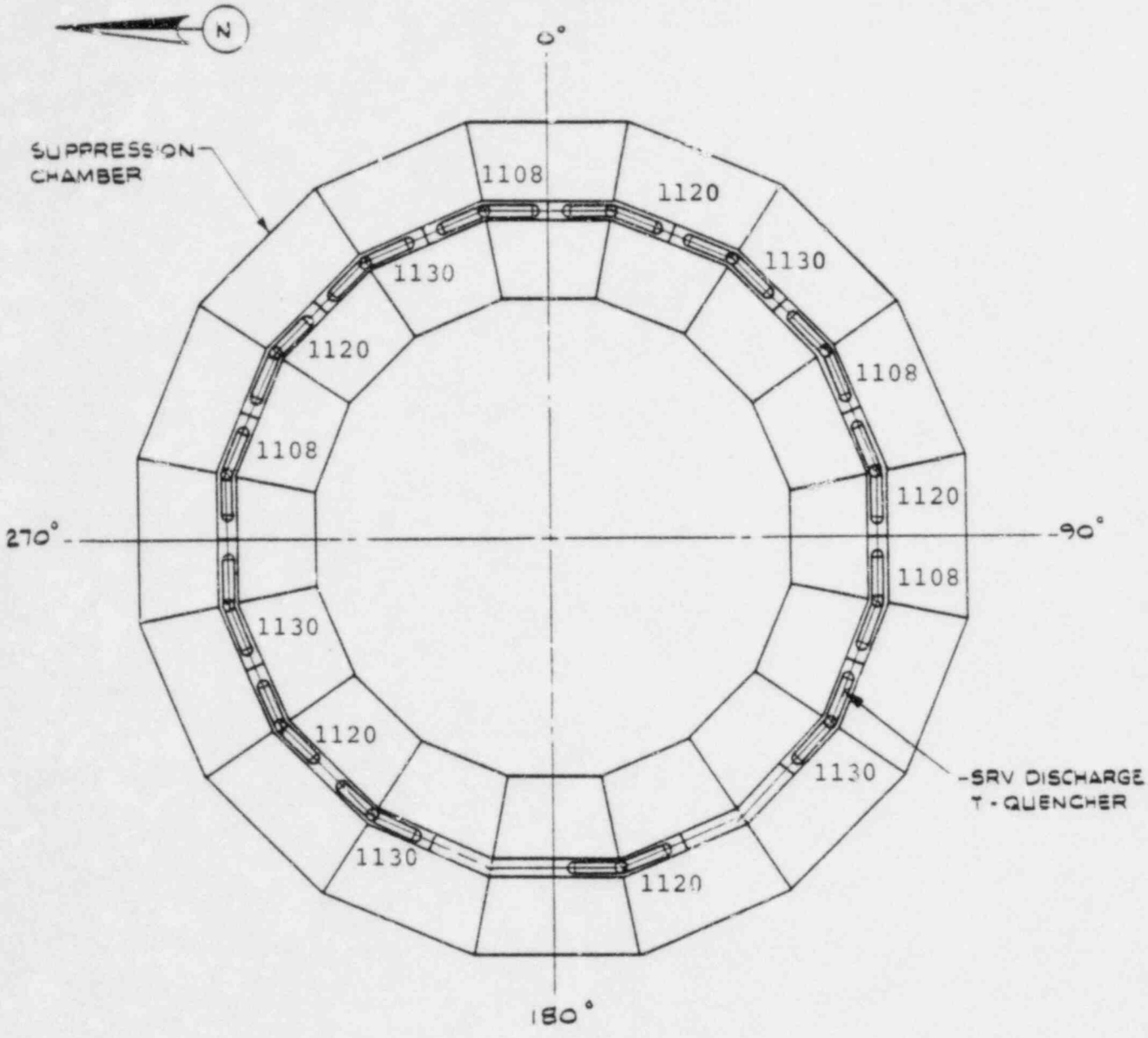

Notes:

1. Set point pressures are shown in psi.
2. The 1130 psi valves are designated ADS valves.

Figure 2-2.1-13

QUENCHER LOCATIONS AND SRV SETPOINT PRESSURES - PLAN VIEW

nutech ENGINEERS

2-2.2 Loads and Load Combinations

The loads for which the Hope Creek suppression chamber is evaluated are defined in NUREG-0661 on a generic basis for all Mark I plants. The methodology used to develop plant unique suppression chamber loads for each load defined in NUREG-0661 is discussed in Section 1-4.0. The results of applying the methodology to develop specific values for each of the governing loads which act on the suppression chamber are discussed in Section 2-2.2.1.

Using the event combinations and event sequencing defined in NUREG-0661 and discussed in Sections 1-3.2 and 1-4.3, the controlling load combinations which affect the suppression chamber are formulated. The controlling suppression chamber load combinations are presented in Section 2-2.2.2.

2-2.2.1 Loads

The loads acting on the suppression chamber are categorized as follows:

1. Dead Weight Loads
2. Seismic Loads
3. Pressure and Temperature Loads
4. Pool Swell Loads
5. Condensation Oscillation Loads
6. Chugging Loads
7. Safety Relief Valve Discharge Loads
8. Containment Interaction Loads

Loads in categories 1 through 3 are defined in the original containment design basis as documented in the plant's FSAR. Revised category 3 pressure and temperature loads result from postulated LOCA and SRV discharge events. Loads in categories 4 through 6 result from postulated LOCA events; loads in category 7 result from SRV discharge events; loads in category 8 are reactions which result from loads acting on other containment structures attached to the suppression chamber.

Not all of the loads defined in NUREG-0661 are evaluated in detail since some are enveloped by others or have a negligible effect on the suppression chamber. Only those loads that maximize the suppression chamber response and lead to controlling stresses are fully evaluated. These loads are referred to as governing loads in subsequent discussions.

Table 2-2.2-1 shows the specific suppression chamber components which are affected by each of the loadings defined in NUREG-0661. The table also lists the section in Volume 1 in which the methodology for developing values for each loading is discussed. The magnitudes and characteristics of each governing suppression chamber load in each load category are discussed in the paragraphs which follow.

1. Dead Weight Loads

   a. Dead Weight of Steel: The weight of steel used to construct the suppression chamber and its supports is considered. The dead weight of steel is determined based on nominal component dimensions and a density of steel of 490 lb/ft^3.

b. Dead Weight of Water: The weight of water contained in the suppression chamber is considered. A volume of water of 122,000 ft^3, corresponding to a water level of 11-1/2" below the suppression chamber horizontal centerline, and a water density of 62.4 lb/ft^3 are used in this calculation. This suppression chamber water volume is the maximum expected during normal operating conditions, as defined in Section 1-2.2.

2. Seismic Loads

a. OBE Loads: The suppression chamber is subjected to horizontal and vertical accelerations during an Operating Basis Earthquake (OBE). This loading is taken from the original design basis for the containment documented in the plant's FSAR.

b. SSE Loads: The suppression chamber is subjected to horizontal and vertical accelerations during a Safe Shutdown Earthquake (SSE). This loading is taken from the original design basis for the containment documented in the plant's FSAR.

3. Pressure and Temperature Loads

a. Normal Operating Internal Pressure Loads: The suppression chamber shell is subjected to internal pressure loads during normal operating conditions. This loading is taken from the original design basis for the containment documented in the plant's FSAR. The range of normal operating internal pressures specified is 0.0 to 2.0 psi. Normal operating internal pressures are enveloped by LOCA internal pressures and are not evaluated further.

b. LOCA Internal Pressure Loads: The suppression chamber shell is subjected to internal pressure during a Small Break Accident (SBA), Intermediate Break Accident (IBA), or Design Basis Accident (DBA) event. The procedure used to develop LOCA internal pressures for the containment is discussed in Section 1-4.1.1. The resulting suppression chamber internal pressure magnitudes at key times during the SBA, IBA, and DBA events are presented in Table 2-2.2-2.

The pressures specified for each event are assumed to act uniformly over the suppression chamber shell surface. The corresponding suppression chamber external or secondary containment pressure for all events is assumed to be 0.0 psig.

c. Normal Operating Temperature Loads: The suppression chamber is subjected to the thermal expansion load associated with normal operating conditions. This loading is taken from the original design basis for the containment documented in the plant's FSAR. The range of normal operating temperatures for the suppression chamber with a concurrent SRV discharge event is 50 to 150°F. Additional suppression chamber normal operating temperatures are taken from the suppression pool temperature response analysis contained in the plant's FSAR. The effects of Normal Operating temperature loads are enveloped by LOCA temperature loads and are not evaluated further except for fatigue evaluation.

d. LOCA Temperature Loads: The suppression chamber is subjected to thermal expansion loads associated with the SBA, IBA, and DBA events. The procedure used to develop LOCA containment temperatures is discussed in Section 1-4.1.1. The resulting suppression chamber temperature magnitudes at key times during the SBA, IBA, and DBA events are presented in Table 2-2.2-2.

Additional suppression chamber temperatures are taken from the suppression pool temperature response analysis contained in the plant's FSAR. These temperatures are enveloped by the maximum LOCA temperatures and are not considered further.

The temperatures specified for each event are assumed to be representative of pool temperatures, air space temperatures, and torus shell metal temperatures throughout the suppression chamber. The ambient temperature for all events is assumed to be 70°F. The column connections and column members are assumed to remain at the ambient temperature throughout the specified events.

4. Pool Swell Loads

a. Pool Swell Torus Shell Loads: During the initial phase of a DBA event, transient pressures are postulated to act on the suppression chamber shell above and below the suppression pool surface. The procedure used to develop local torus shell pressures due to pool swell for the suppression chamber is discussed in Section 1-4.1.3. The maximum pool swell torus shell pressures and key times during the event are shown in Table 2-2.2-3.

These results are based on plant unique QSTF test data contained in the PULD (Reference 3) and include the effects of the generic spatial distribution factors contained in the LDR (Reference 2) and the additional margins on the peak upward and downward loads specified in NUREG-0661 (Reference 1). Pool swell torus shell loads consist of a pseudo-static internal pressure component and a dynamic pressure component and include the effects of the DBA internal pressure dis-

cussed in load case 3a. Pool swell loads do not occur during SBA and IBA events.

b. LOCA Air Clearing Submerged Structure Loads: Transient drag pressures are postulated to act on the submerged components of the suppression chamber during the air clearing phase of a DBA event. The components affected include the mitered joint and midcylinder ring beams. The procedure used to develop the transient forces and spatial distribution of LOCA air clearing drag loads on these components is discussed in Section 1-4.1.6.

The resulting maximum drag pressures acting on the mitered joint and midcylinder ring beams for the controlling LOCA air clearing load case are shown in Table 2-2.2-6. These results include the effects of velocity drag, acceleration drag, interference effects, and wall effects. The LOCA air clearing submerged structure loads which occur during an SBA or IBA event have a negligible effect on the suppression chamber.

As can be seen by examining Table 2-2.2-6, LOCA air clearing submerged structure loads are enveloped by other submerged structure loads. Therefore this loading is not fully evaluated in the suppression chamber analysis.

5. Condensation Oscillation Loads

a. DBA Condensation Oscillation Torus Shell Loads: Harmonic pressures are postulated to act on the submerged portion of the suppression chamber shell during the condensation oscillation phase of a DBA event. The procedure used to develop DBA condensation oscillation torus shell pressures is discussed in Section 1-4.1.7. The resulting normalized spatial distribution of pressures on a typical suppression chamber shell cross-section are shown in Figure 2-2.2-1. The amplitudes for each of the 50 harmonics and 4 DBA condensation oscillation load case alternates are shown in Table 2-2.2-4.

The results of each harmonic in the DBA condensation oscillation loading are combined

using the methodology discussed in Section 1-4.1.7. A 0.874 factor, to account for the difference in the ratio of pool area to the downcomer area between the FSTF and Hope Creek, is also applied to the results.

b. IBA Condensation Oscillation Torus Shell Loads: Harmonic pressures are postulated to act on the submerged portion of the suppression chamber shell during an IBA event. In accordance with NUREG-0661, the torus shell loads specified for pre-chug are used in lieu of IBA condensation oscillation torus shell loads. Pre-chug torus shell loads are discussed in load case 6a. Condensation oscillation loads do not occur during an SBA event.

c. DBA Condensation Oscillation Submerged Structure Loads: Harmonic drag pressures are postulated to act on the submerged components of the suppression chamber during the condensation oscillation phase of a DBA event. The components affected include the mitered joint and midcylinder ring beams. The procedure used to develop the harmonic forces and

spatial distribution of DBA condensation oscillation drag loads on these components is discussed in Section 1-4.1.7.

Loads are developed for the case with the average source strength at all downcomers and the case with twice the average source strength at the nearest downcomer. The results of these two cases are evaluated to determine the controlling loads. The resulting maximum drag pressures acting on the mitered joint and midcylinder ring beams for the controlling DBA condensation oscillation load case are shown in Table 2-2.2-6.

These results include the effects of velocity drag, acceleration drag, torus shell FSI acceleration drag, interference effects, and wall effects. The pool acceleration profile from which the FSI accelerations are derived is shown in Figure 2-2.2-2. The results of each harmonic in the DBA condensation oscillation loading are combined using the methodology discussed in Section 1-4.1.7.

d. IBA Condensation Oscillation Submerged Structure Loads: Harmonic pressures are postulated to act on the submerged components of the suppression chamber during the condensation oscillation phase of an IBA event. In accordance with NUREG-0661, the submerged structure loads specified for pre-chug are used in lieu of IBA condensation oscillation submerged structure loads. Pre-chug submerged structure loads are discussed in load case 6c. Condensation oscillation loads do not occur during an SBA event.

6. Chugging Loads

a. Pre-Chug Torus Shell Loads: During the chugging phase of an SBA, IBA, or DBA event, harmonic pressures associated with the pre-chug portion of a chug cycle are postulated to act on the submerged portion of the suppression chamber shell. The procedure used to develop pre-chug torus shell loads is discussed in Section 1-4.1.8.

The loading consists of a single harmonic with a specified frequency range and can act

either symmetrically or asymmetrically with respect to the vertical centerline of the containment. The circumferential pressure distribution on a typical suppression chamber cross-section for both symmetric and asymmetric pre-chug is shown in Figure 2-2.2-4. The longitudinal pressure distribution for asymmetric pre-chug is shown in Figure 2-2.2-5. The symmetric pre-chug load results in vertical loads on the suppression chamber while the asymmetric pre-chug load results in both vertical and lateral loads on the suppression chamber.

b. Post-Chug Torus Shell Loads: During the chugging phase of an SBA, IBA, or DBA event, harmonic pressures associated with the post-chug portion of a chug cycle are postulated to act on the submerged portion of the suppression chamber shell. The procedure used to develop post-chug torus shell loads is defined in Section 1-4.1.8. The resulting normalized spatial distribution of pressure on a typical suppression chamber cross-section is shown in Figure 2-2.2-1. The pressure amplitudes for each of the 50

harmonics in the post-chug loading are shown in Table 2-2.2-5. The results of each harmonic in the post-chug loading are combined using the methodology discussed in Section 1-4.1.8.

c. Pre-Chug Submerged Structure Loads: During the chugging phase of an SBA, IBA, or DBA event, harmonic drag pressures associated with the pre-chug portion of a chug cycle are postulated to act on the submerged components of the suppression chamber. The components affected include the mitered joint and midcylinder ring beams. The procedure used to develop the harmonic forces and spatial distribution of pre-chug drag loads on these components is discussed in Section 1-4.1.8.

Loads are developed for the case with the average source strength at all downcomers and the case with twice the average source strength at the nearest downcomer. The results of these two cases are evaluated to determine the controlling loads. The resulting maximum drag pressures acting on the mitered joint and midcylinder ring beams for

the controlling pre-chug drag load case are shown in Table 2-2.2-6.

These results include the effects of velocity drag, acceleration drag, torus shell FSI acceleration drag, interference effects, and wall effects. As can be seen by examining Table 2-2.2-6, the ring beam drag pressures due to pre-chug are bounded by post-chug. Therefore post-chug submerged structure loads are used in the analysis in lieu of pre-chug submerged structure loads.

d. Post-Chug Submerged Structure Loads: During the chugging phase of an SBA, IBA, or DBA event, harmonic drag pressures associated with the post-chug portion of a chug cycle are postulated to act on the submerged components of the suppression chamber. The components affected include the mitered joint and midcylinder ring beams. The procedure used to develop the harmonic forces and spatial distribution of post-chug drag loads on these components is discussed in Section 1-4.1.8.

Loads are develcped for the case with the maximum source strength at the nearest two downcomers acting both in phase and out of phase. The results of these cases are evaluated to determine the controlling loads. The resulting maximum post-chug drag pressures acting on the mitered joint and midcylinder ring beams for the controlling post-chug drag load case are shown in Table 2-2.2-6.

These results include the effects of velocity drag, acceleration drag, torus shell FSI acceleration drag, interference effects, and wall effects. The pool acceleration profile from which the FSI accelerations are derived is shown in Figure 2-2.2-3. The results of each harmonic in the post-chug loading are combined using the methodology discussed in Section 1-4.1.8.

7. Safety Relief Valve Discharge Loads

a-c. SRV Discharge Torus Shell Loads: Transient pressures are postulated to act on the submerged portion of the suppression chamber

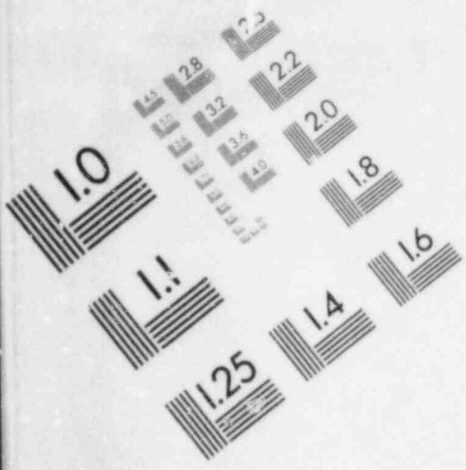

IMAGE EVALUATION TEST TARGET (MT-3)

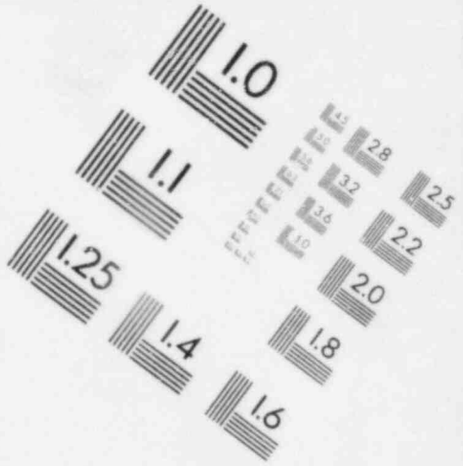

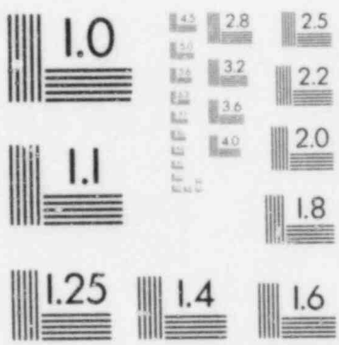

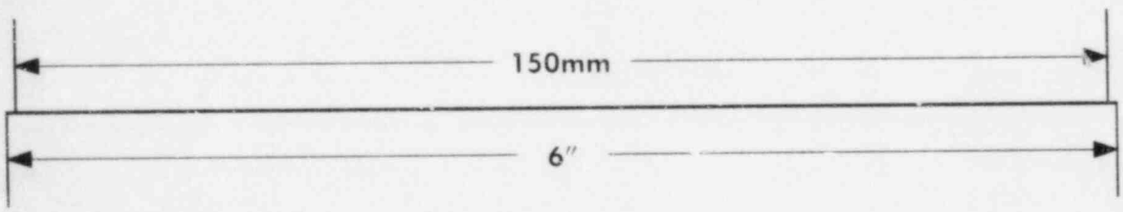

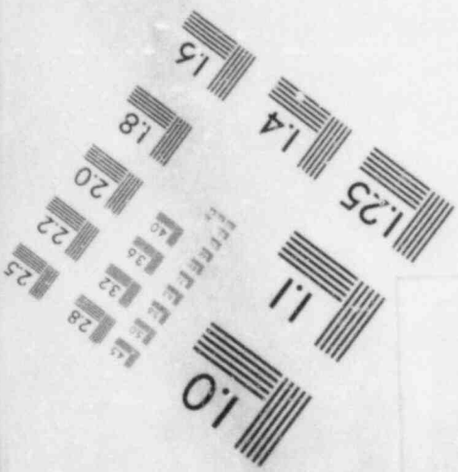

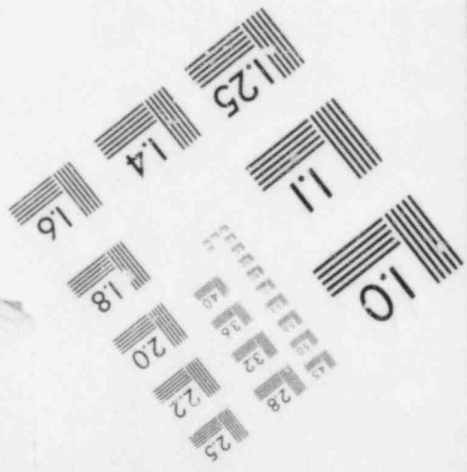

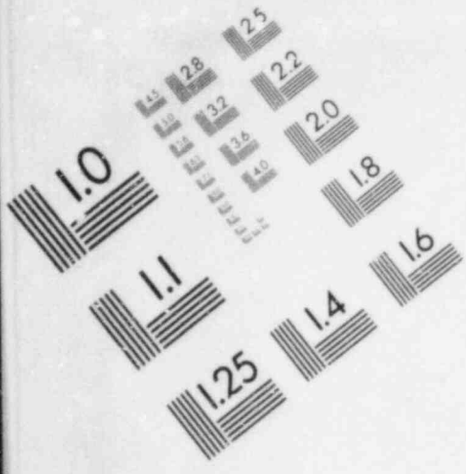

IMAGE EVALUATION TEST TARGET (MT-3)

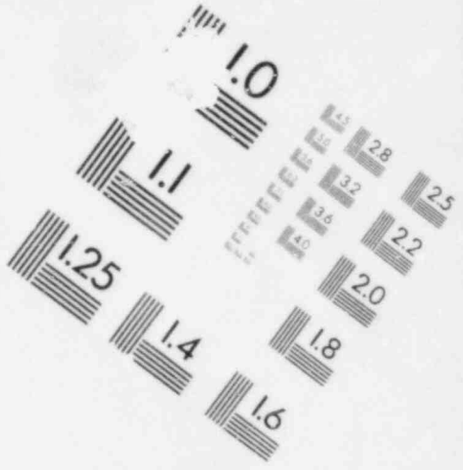

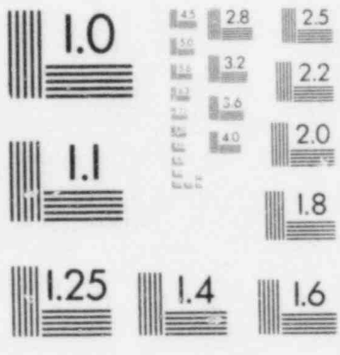

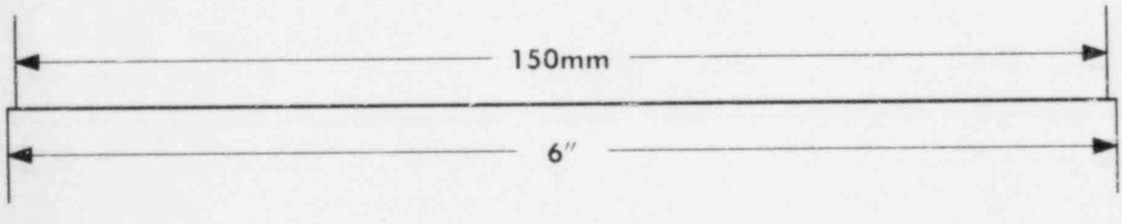

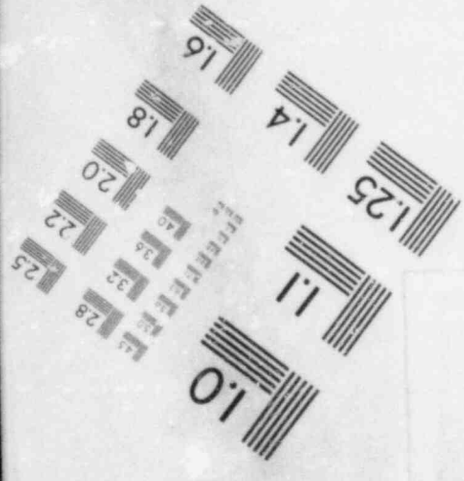

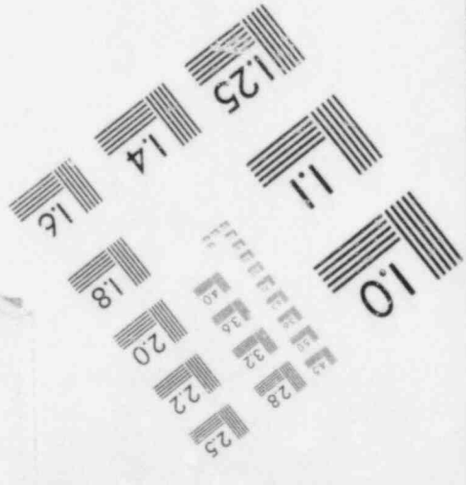

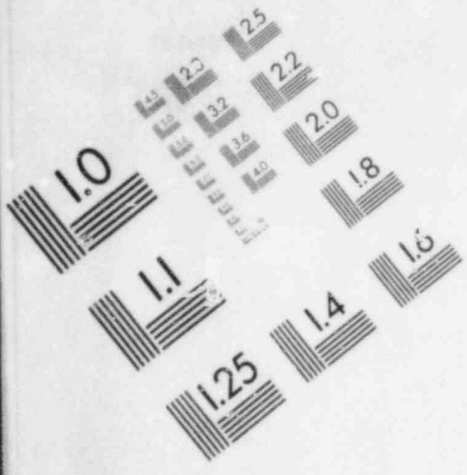

IMAGE EVALUATION TEST TARGET (MT-3)

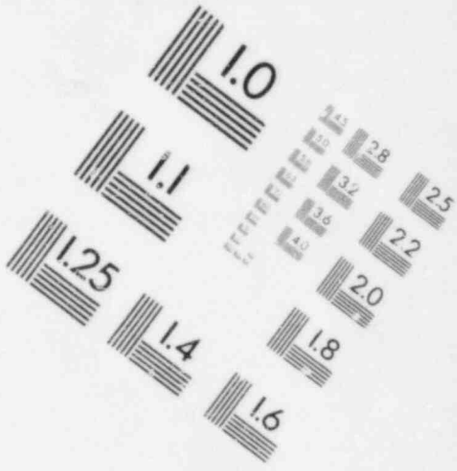

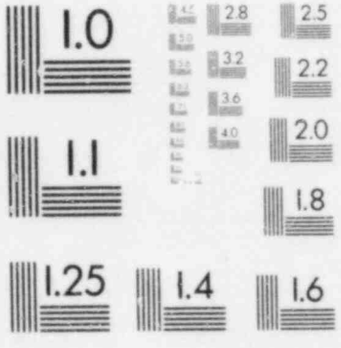

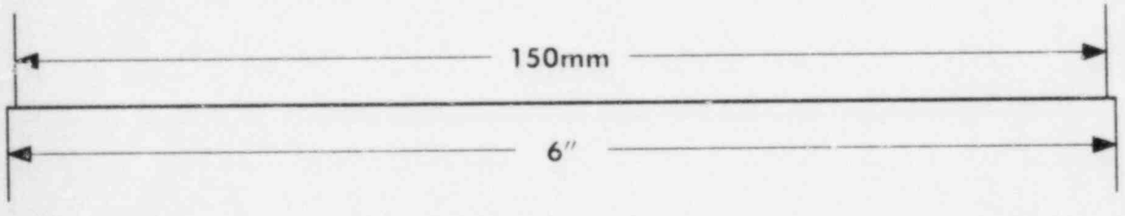

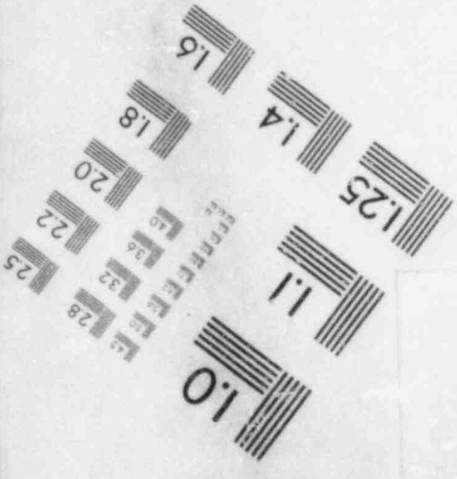

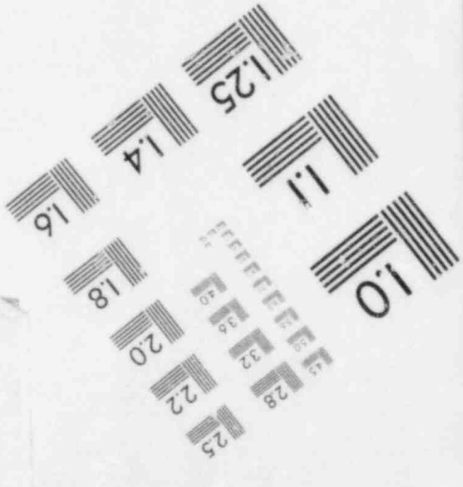

shell during the air clearing phase of an SRV discharge event. The procedure used to develop SRV discharge torus shell loads is discussed in Section 1-4.2.3. The maximum torus shell pressures and characteristics of the SRV discharge pressure transients are developed using an attenuated bubble model.

The SRV actuation cases considered are discussed in Section 1-4.2.1. The location of each quencher and the corresponding SRV set point pressure are shown in Figure 2-2.1-14. The cases which result in controlling load or load combination effects for which torus shell pressures are developed include the single valve actuation case with elevated drywell pressures and temperatures (7a-Case A1.2/C3.2 for the quencher location which results in the highest shell pressures), and the multiple valve actuation case with elevated drywell pressures and temperatures (7b-Case A1.2/C3.2 with pressures from all 14 valves acting in phase).

The single and multiple valve actuation cases with normal operating initial conditions (Case A1.1/C3.1) are enveloped by loading 7a and 7b (Case A1.2/C3.2) and are therefore not evaluated. The ADS valve actuation case with elevated drywell temperatures and pressures (Case A2.2 with pressures from all 5 ADS valves acting in phase) is also enveloped by 7b-Case A1.2/C3.2 and is therefore not evaluated.

The resulting SRV discharge torus shell loads for the single valve Case 7a and multiple valve Case 7b are shown in Figure 2-2.2-8. The results shown include the effects of applying the LDR (Reference 2) pressure attenuation methodology to obtain the spatial distribution of torus shell pressures and the absolute summation of multiple valve effects with application of the bubble pressure cut-off criteria. Also, as specified by the LDR (Reference 2), first actuation pressures are used with subsequent actuation frequencies, and ±25% and ±40% margins are applied to the first and subsequent actuation frequencies, respectively. This methodology is in

accordance with the conservative criteria contained in NUREG-0661.

The distribution of SRV discharge torus shell pressures is either symmetric or asymmetric with respect to the vertical centerline of the containment, depending on the number and location of the valves considered to be actuating. The symmetric pressure distribution which results in the maximum total vertical load on the suppression chamber occurs for the multiple valve Case 7b, as shown in Figure 2-2.2-6. The asymmetric pressure distribution which results in the maximum total horizontal load on the suppression chamber occurs for a multiple valve actuation case with elevated drywell pressures and temperatures (7c - Case A1.2/C3.2 with pressure from three of the four 1108 psi setpoint valves acting in phase to maximize the net lateral load). The longitudinal pressure distribution for the asymmetric multiple valve Case 7c is shown in Figure 2-2.2-7.

As discussed in Section 2-2.4.1, the load combinations which involve pool swell plus single valve SRV loads are bounded by other loading combinations. Since only multiple valve SRV loads are combined with all other LOCA related loads, single valve SRV torus further shell load 7a-Case A1.2/C3.2 is not evaluated further in the suppression chamber analysis.

d. SRV Discharge Air Clearing Submerged Structure Loads: Transient drag pressures are postulated to act on the submerged components of the suppression chamber during the air clearing phase of an SRV discharge event. The components affected include the mitered joint and midcylinder ring beams. The procedure used to develop the transient forces and spatial distribution of the SRV discharge air clearing drag loads on these structures is discussed in Section 1-4.2.4.

Loads are developed for two conditions including the case with four bubbles from each quencher in three consecutive bays acting in phase, and the case with four

bubbles from each quencher in two adjacent bays acting in phase combined with four bubbles from a third adjacent quencher acting out-of-phase. The results are evaluated to determine the controlling loads. The resulting maximum drag pressures acting on the mitered joint and midcylinder ring beams for the controlling SRV discharge drag load case are shown in Table 2-2.2-6. The results include the effects of velocity drag, acceleration drag, interference effects, and wall effects.

8. Containment Interaction Loads

a. Containment Structure Reaction Loads: Loads acting on the suppression chamber, vent system, quencher and quencher supports, catwalk, and monorail cause interaction effects between these structures. These interaction effects result in reaction loads on the suppression chamber shell and ring beams, at the attachment points of these structures to the suppression chamber. The effects of the vent system, quencher, and quencher support reaction loads on the suppression chamber are

considered in the suppression chamber analysis.

The catwalk and monorail reaction loads on the suppression chamber are primarily caused by pool swell loads acting on these structures. As discussed in Section 2-2.4.1, the load combinations which include pool swell loads are enveloped by other loading combinations. Therefore catwalk and monorail reaction loads are not considered in the suppression chamber analysis.

The values of the loads presented in the preceding paragraphs envelop those which could occur during the LOCA or SRV discharge events postulated. An evaluation for the effects of these loads results in conservative estimates of the suppression chamber responses and leads to bounding values of suppression chamber stresses.

Table 2-2.2-1

SUPPRESSION CHAMBER COMPONENT LOADING IDENTIFICATION

Volume 2 Load Designation			PUAR Section Reference	Component Part Loaded		
Category	Load Type	Case Number		Torus Shell	Ring Beams	Column Connections and Support Members
Dead Weight Loads	Dead Weight Steel	1a	1-3.1	X	X	X
	Dead Weight Water	1b	1-3.1	X		
Seismic Loads	OBE Seismic	2a	1-3.1	X	X	X
	SSE Seismic	2b	1-3.1	X	X	X
Pressure and Temperature Loads	NOC Internal Pressure	3a	1-3.1	X		
	LOCA Internal Pressure	3b	1-4.1.1	X		
	NOC Temperature	3c	1-3.1	X	X	
	LOCA Temperature	3d	1-4.1.1	X	X	
Pool Swell Loads	Pool Swell Torus Shell	4a	1-4.1.3	X		
	LOCA Water Clearing (1) Submerged Structure	N/A	1-4.1.5		X	
	LOCA Air Clearing Submerged Structure	4b	1-4.1.6		X	
Condensation Oscillation Loads	DBA C.O. Torus Shell	5a	1-4.1.7.1	X		
	IBA C.O. Torus Shell	5b	1-4.1.7.1	X		
	DBA C.O. Submerged Structure	5c	1-4.1.7.3		X	
	IBA C.O. Submerged Structure	5d	1-4.1.7.3		X	

Table 2-2.2-1
(Concluded)

Volume 2 Load Designation			PUAR Section Reference	Component Part Loaded		
Category	Load Type	Case Number		Torus Shell	Ring Beams	Column Connections and Support Members
Chugging Loads	Pre-Chug Torus Shell	6a	1-4.1.8.1	X		
	Post-Chug Torus Shell	6b	1-4.1.8.1	X		
	Pre-Chug Submerged Structure	6c	1-4.1.8.3		X	
	Post-Chug Submerged Structure	6c	1-4.1.8.3		X	
SRV Discharge Loads	SRV Discharge Torus Shell	7a-7c	1-4.2.3	X		
	SRV Discharge Water Clearing Submerged Structure (1)	N/A	1-4.2.4		X	
	SRV Discharge Air Clearing Submerged Structure	7d	1-4.2.4		X	
Containment Interaction Loads	Containment Structure Reactions	8a	Vol. 3-6	X	X	

Note:

1. The effects of this loading are negligible compared with other submerged structure loadings.

Table 2-2.2-2

SUPPRESSION CHAMBER INTERNAL PRESSURES AND TEMPERATURES FOR LOCA EVENTS (1)

Event Description	Pressure, Temperature Designation	Time (sec)		Pressure (psig) (2)		Temperature (°F) (2)	
		t_{min}	t_{max}	P_{min}	P_{max}	T_{min}	T_{max}
S B A L O C A							
Instant of Break to Onset of Chugging	P_1, T_1	0.	300.	0.75	10.00	95.0	101.0
Onset of Chugging to Initiation of ADS	P_2, T_2	300.	600.	10.00	19.90	101.0	103.0
Initiation of ADS to RPV Depressurization	P_3, T_3	600.	1200.	19.90	22.80	103.0	135.0
I B A L O C A							
Instant of Break to Onset of CO and Chugging	P_1, T_1	0.	5.	0.75	2.00	95.0	95.0
Onset of CO and Chugging to Initiation of ADS	P_2, T_2	5.	300.	2.00	20.70	95.0	112.0
Initiation of ADS to RPV Depressurization	P_3, T_3	300.	500.	20.70	31.70	112.0	167.0
D B A L O C A							
Instant of Break to Termination of Pool Swell	P_1, T_1	0.0	1.5	0.75	7.50	80.0	82.0
Termination of Pool Swell to Onset of CO	P_2, T_2	1.5	5.0	7.75	16.25	82.0	87.0
Onset of CO to Onset of Chugging	P_3, T_3	5.0	35.0	16.20	24.60	87.0	118.0
Onset of Chugging to RPV Depressurization	P_4, T_4	35.0	65.0	24.60	24.60	118.0	118.0

Table 2-2.2-2
(Concluded)

Notes:

1. LOCA pressure and temperature transients are contained in the Hope Creek PULD (Reference 3).

2. Initial pressures and temperatures are assumed to be 0.0 psig and 70°F, respectively.

Table 2-2.2-3

MAXIMUM TORUS SHELL PRESSURES DUE TO POOL SWELL

Location	Torus Shell Pressure (psi) (1,2)	
	Peak Download t=0.260 sec	Peak Upload t=0.520 sec
Submerged Portion	8.36	3.40
Airspace (3)	0.30	7.74

Notes:

1. The values shown are based on the pool swell pressure transients contained in the Hope Creek PULD (Reference 3).
2. Pressures shown include the additional NUREG-0661 pressure margins.
3. The maximum airspace pressure during pool swell is 21.5 psig.
4. Pool swell torus shell pressure transient has a dominant frequency of 2.5 Hz.

Table 2-2.2-4

DBA CONDENSATION OSCILLATION TORUS

SHELL PRESSURE AMPLITUDES

Frequency Interval (Hz)	Maximun Pressure Amplitude (psi) (1)			
	Alternate 1	Alternate 2	Alternate 3	Alternate 4
0 - 1	0.29	0.29	0.29	0.25
1 - 2	0.25	0.25	0.25	0.28
2 - 3	0.32	0.32	0.32	0.33
3 - 4	0.48	0.48	0.48	0.56
4 - 5	1.86	1.20	0.24	2.71
5 - 6	1.05	2.73	0.48	1.17
6 - 7	0.49	0.42	0.99	0.97
7 - 8	0.59	0.38	0.30	0.47
8 - 9	0.59	0.38	0.30	0.34
9 - 10	0.59	0.38	0.30	0.47
10 - 11	0.34	0.79	0.18	0.49
11 - 12	0.15	0.45	0.12	0.38
12 - 13	0.17	0.12	0.11	0.20
13 - 14	0.12	0.08	0.08	0.10
14 - 15	0.06	0.07	0.03	0.11
15 - 16	0.10	0.10	0.02	0.08
16 - 17	0.04	0.04	0.04	0.04
17 - 18	0.04	0.04	0.04	0.05
18 - 19	0.04	0.04	0.04	0.03
19 - 20	0.27	0.27	0.27	0.34
20 - 21	0.20	0.20	0.20	0.23
21 - 22	0.30	0.30	0.30	0.49
22 - 23	0.34	0.34	0.34	0.37
23 - 24	0.33	0.33	0.33	0.31
24 - 25	0.16	0.16	0.16	0.22

Table 2-2.2-4
(Concluded)

Frequency Interval (Hz)	Maximum Pressure Amplitude (psi) (1)			
	Alternate 1	Alternate 2	Alternate 3	Alternate 4
25 - 26	0.25	0.25	0.25	0.50
26 - 27	0.58	0.58	0.58	0.51
27 - 28	0.13	0.13	0.13	0.39
28 - 29	0.19	0.19	0.19	0.27
29 - 30	0.14	0.14	0.14	0.09
30 - 31	0.08	0.08	0.08	0.08
31 - 32	0.03	0.03	0.03	0.07
32 - 33	0.03	0.03	0.03	0.05
33 - 34	0.03	0.03	0.03	0.04
34 - 35	0.05	0.05	0.05	0.04
35 - 36	0.08	0.08	0.08	0.07
36 - 37	0.10	0.10	0.10	0.11
37 - 38	0.07	0.07	0.07	0.06
38 - 39	0.06	0.06	0.06	0.05
39 - 40	0.09	0.09	0.09	0.03
40 - 41	0.33	0.33	0.33	0.08
41 - 42	0.33	0.33	0.33	0.19
42 - 43	0.33	0.33	0.33	0.19
43 - 44	0.33	0.33	0.33	0.13
44 - 45	0.33	0.33	0.33	0.18
45 - 46	0.33	0.33	0.33	0.30
46 - 47	0.33	0.33	0.33	0.18
47 - 48	0.33	0.33	0.33	0.19
48 - 49	0.33	0.33	0.33	0.17
49 - 50	0.33	0.33	0.33	0.21

Note:

1. See Figure 2-2.2-1 for spatial distribution of pressures.

Table 2-2.2-5

POST-CHUG TORUS SHELL PRESSURE AMPLITUDES

Frequency Interval (Hz)	Maximum (1) Pressure Amplitude (psi)
0 - 1	0.04
1 - 2	0.04
2 - 3	0.05
3 - 4	0.05
4 - 5	0.06
5 - 6	0.05
6 - 7	0.10
7 - 8	0.10
8 - 9	0.10
9 - 10	0.10
10 - 11	0.06
11 - 12	0.05
12 - 13	0.03
13 - 14	0.03
14 - 15	0.02
15 - 16	0.02
16 - 17	0.01
17 - 18	0.01
18 - 19	0.01
19 - 20	0.04
20 - 21	0.03
21 - 22	0.05
22 - 23	0.05
23 - 24	0.05
24 - 25	0.04

Table 2-2.2-5

(Concluded)

Frequency Interval (Hz)	Maximum (1) Pressure Amplitude (psi)
25 - 26	0.04
26 - 27	0.28
27 - 28	0.18
28 - 29	0.12
29 - 30	0.09
30 - 31	0.03
31 - 32	0.02
32 - 33	0.02
33 - 34	0.02
34 - 35	0.02
35 - 36	0.03
36 - 37	0.05
37 - 38	0.03
38 - 39	0.04
39 - 40	0.04
40 - 41	0.15
41 - 42	0.15
42 - 43	0.15
43 - 44	0.15
44 - 45	0.15
45 - 46	0.15
46 - 47	0.15
47 - 48	0.15
48 - 49	0.15
49 - 50	0.15

Note:

1. See Figure 2-2.2-1 for spatial distribution of pressures.

Table 2-2.2-6

RING BEAM SUBMERGED

STRUCTURE LOAD SUMMARY

Load Type	Maximum Pressure (psi) (3)	
	Mitered Joint (1)	Midcylinder (2)
LOCA Air Bubble	1.81	2.84
DBA CO	9.97	9.68
Pre-Chug	2.66	3.99
Post-Chug	38.79	14.27
SRV Discharge	14.48	122.35

Notes:

1. The mitered joint ring beam is divided into 14 segments for load determination.

2. The midcylinder ring beam is divided into 11 segments for load determination.

3. The loads shown include dynamic amplification factors.

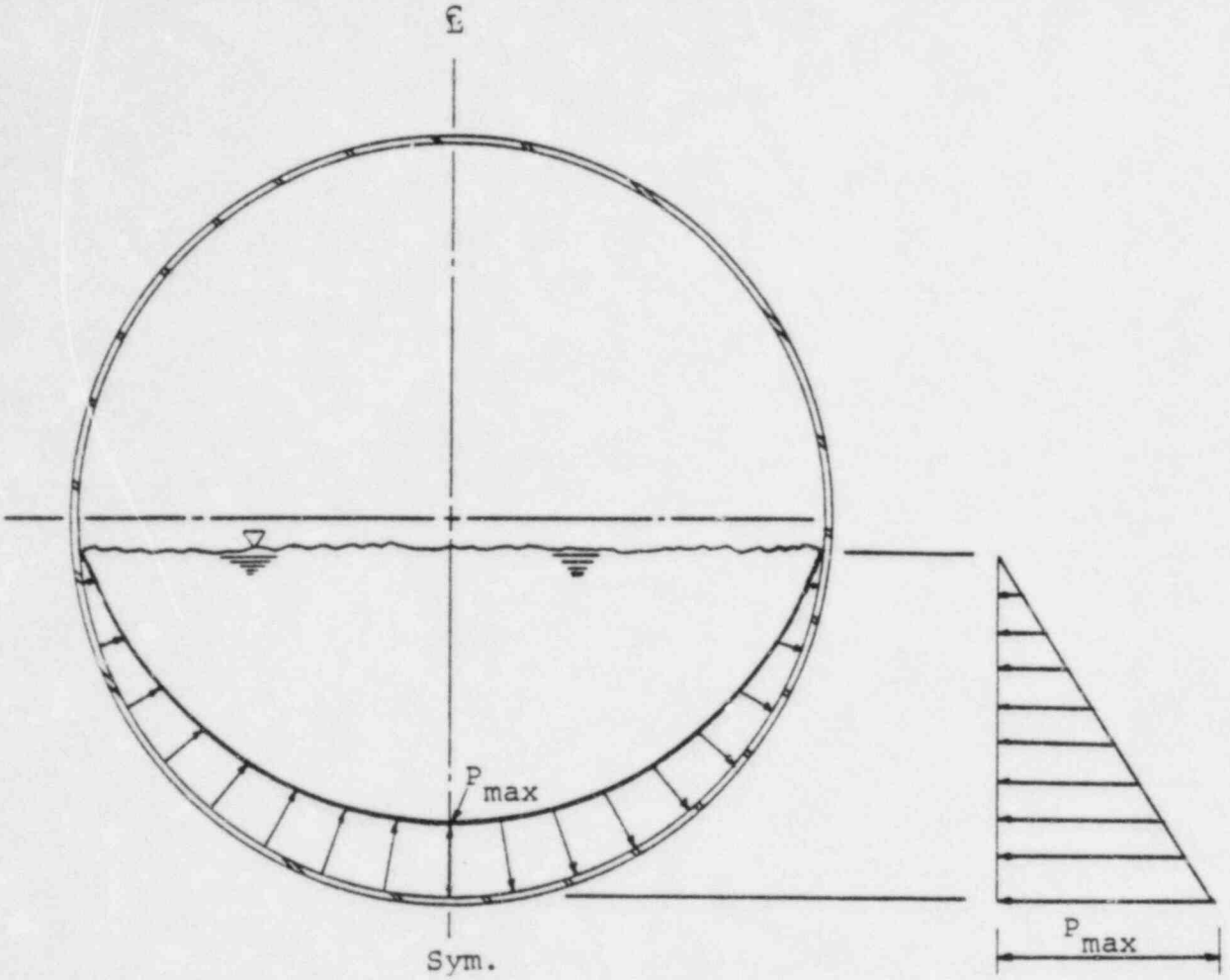

Notes:

1. Pressure amplitudes for DBA condensation oscillation loads shown in Table 2-? 2-4.

2. Pressure amplitudes for post-chug loads shown in Table 2-2.2-5.

Figure 2-2.2-1

NORMALIZED TORUS SHELL PRESSURE DISTRIBUTION FOR DBA CONDENSATION OSCILLATION AND POST-CHUG LOADINGS

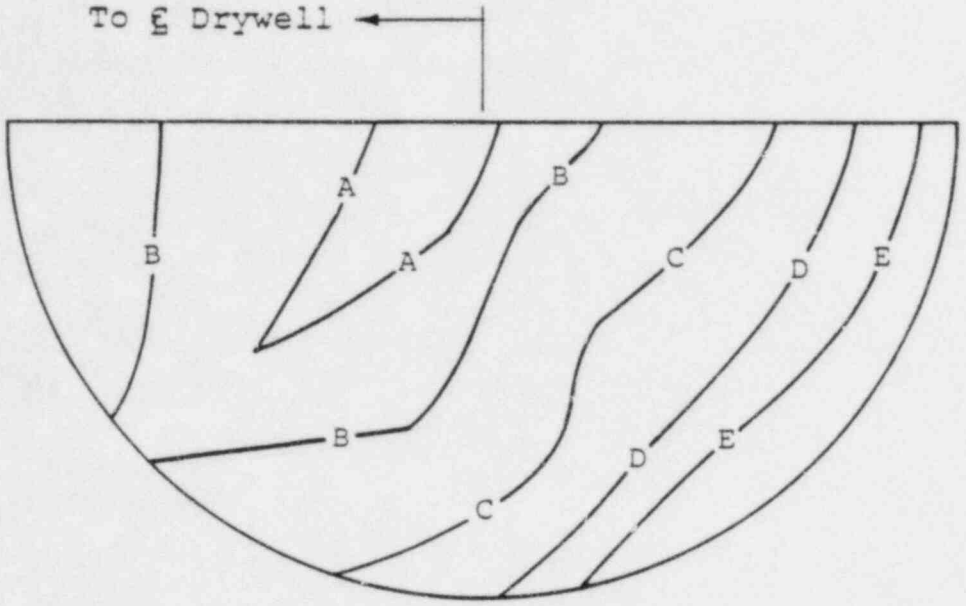

Key Diagram

Normalized Pool Accelerations	
Profile	Pool Acceleration (in/sec^2)
A	50.0
B	200.0
C	500.0
D	1000.0
E	1500.0
Pool accelerations due to harmonic application of torus shell pressures shown in Figure 2-2.2-1 and the Alternate 4 amplitudes shown in Table 2-2.2-4.	

Figure 2-2.2-2

POOL ACCELERATION PROFILE FOR DBA CONDENSATION OSCILLATION TORUS SHELL LOADS AT QUARTER-BAY LOCATION

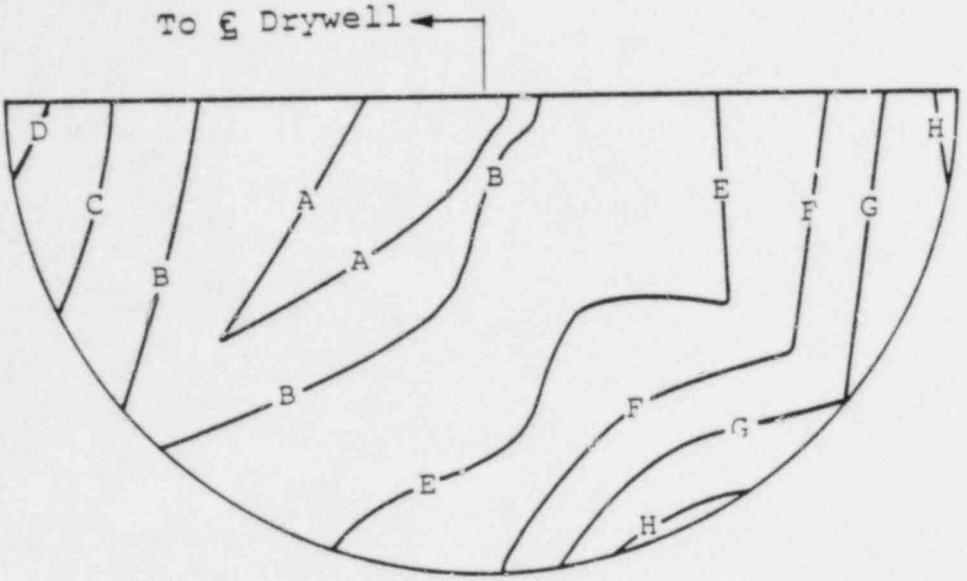

Key Diagram

Normalized Pool Accelerations	
Profile	Pool Acceleration (in/sec^2)
A	20.0
B	50.0
C	100.0
D	150.0
E	200.0
F	400.0
G	600.0
H	800.0
Pool accelerations due to harmonic application of torus shell pressures shown in Figure 2-2.2-1 and the amplitudes shown in Table 2-2.2-5.	

Figure 2-2.2-3

POOL ACCELERATION PROFILE FOR POST-CHUG TORUS SHELL LOADS AT QUARTER-BAY LOCATION

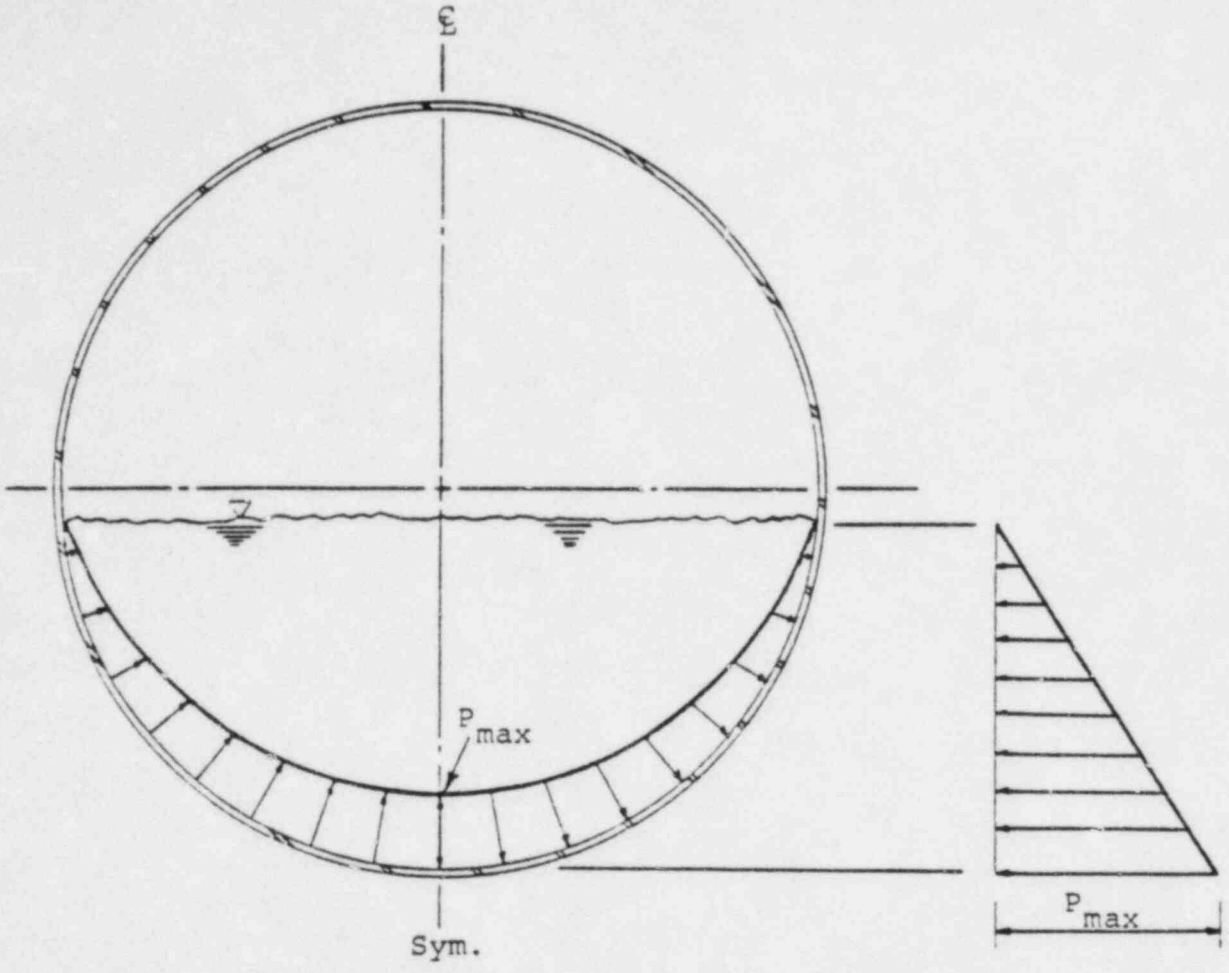

Loading Characteristics
Symmetric Distribution: P_{max} = ± 2.0 psi at all bottom dead center locations Asymmetric Distribution: P_{max} = ± 2.0 psi in one bay with longitudinal attenuation shown in Figure 2-2.2-5 Frequency: Single harmonic in 6.9 to 9.5 Hz range resulting in maximum response Total Integrated Load: Sym Dist: F_{vert} = 152.76 kips per mitered cyl. Asym Dist: F_{horz} = 32.6 kips total horizontal

Figure 2-2.2-4

CIRCUMFERENTIAL TORUS SHELL PRESSURE DISTRIBUTION FOR SYMMETRIC AND ASYMMETRIC PRE-CHUG LOADINGS

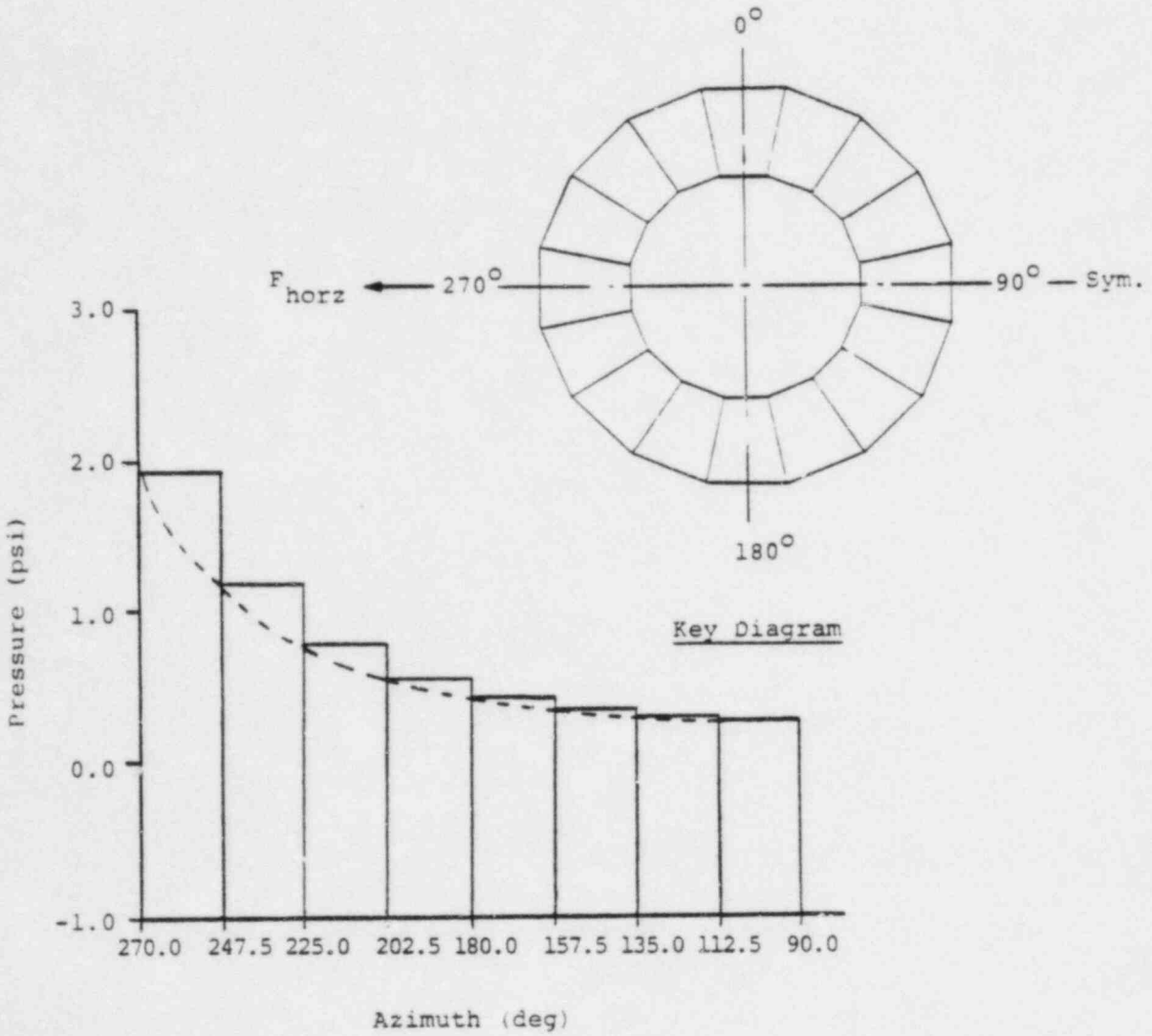

Note:

1. See Figure 2-2.2-4 for circumferential torus shell pressure distribution.

Figure 2-2.2-5

LONGITUDINAL TORUS SHELL PRESSURE DISTRIBUTION FOR ASYMMETRIC PRE-CHUG LOADINGS

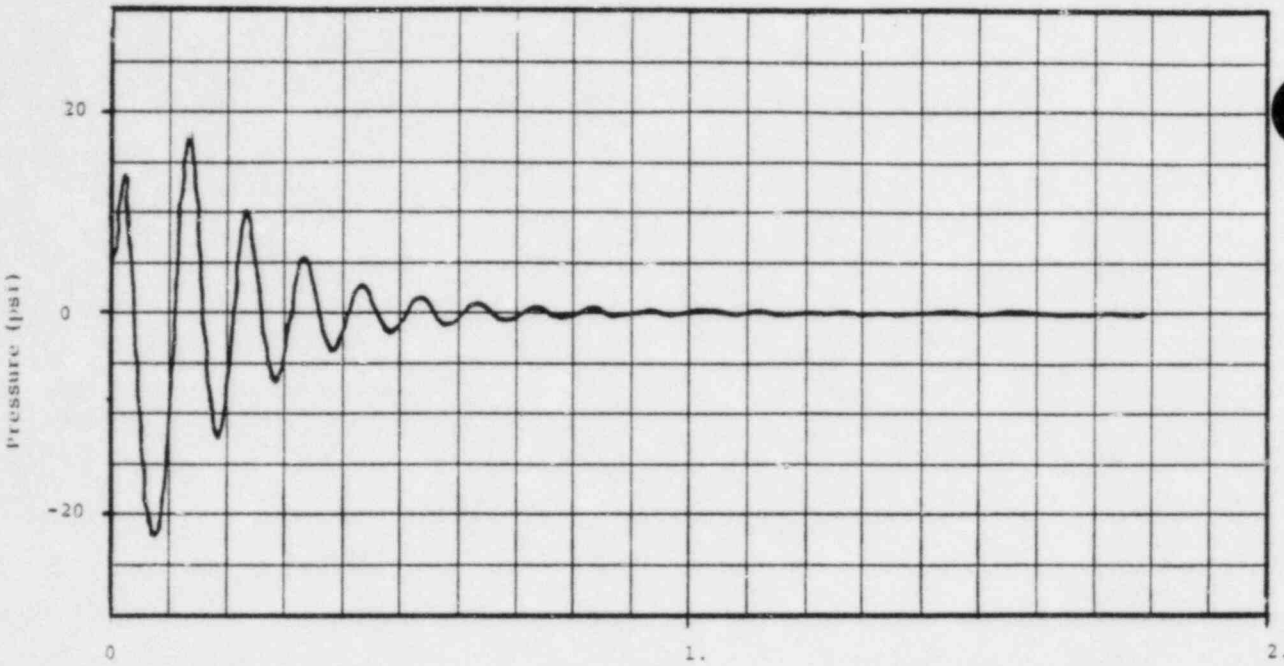

SHELL PRESSURE FORCING FUNCTION (ONE VALVE)

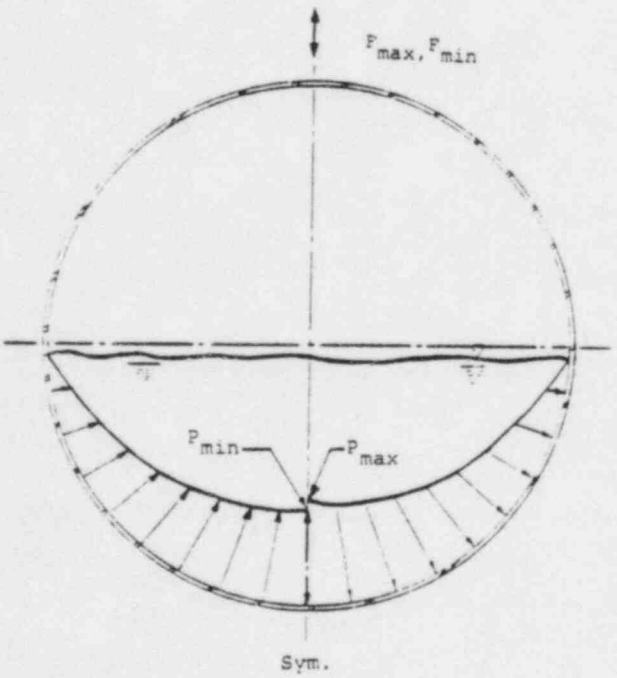

MITERED JOINT SPATIAL DISTRIBUTION

LOADING CHARACTERISTICS
7a and 7b - Case A1.2/C3.2
Pressure (psi): Longest SRVDL
Bubble:
P_{max} = 22.94 P_{min} = -23.50
Shell: One Valve
P_{max} = 17.96 P_{min} = -22.27
Shell: All Valves
P_{max} = 22.94 P_{min} = -23.50
Total Applied Load (kips):
Vertical Per Mitered Cylinder - Multiple Valve Case 7b:
Downward: F_{max} = 1752.0
Upward: F_{min} = 1795.0
Load Frequency (Hz):
Range:
$6.44 \leq f_L \leq 15.02$

Figure 2-2.2-6

SRV DISCHARGE TORUS SHELL LOADS FOR CASE A1.2/C3.2

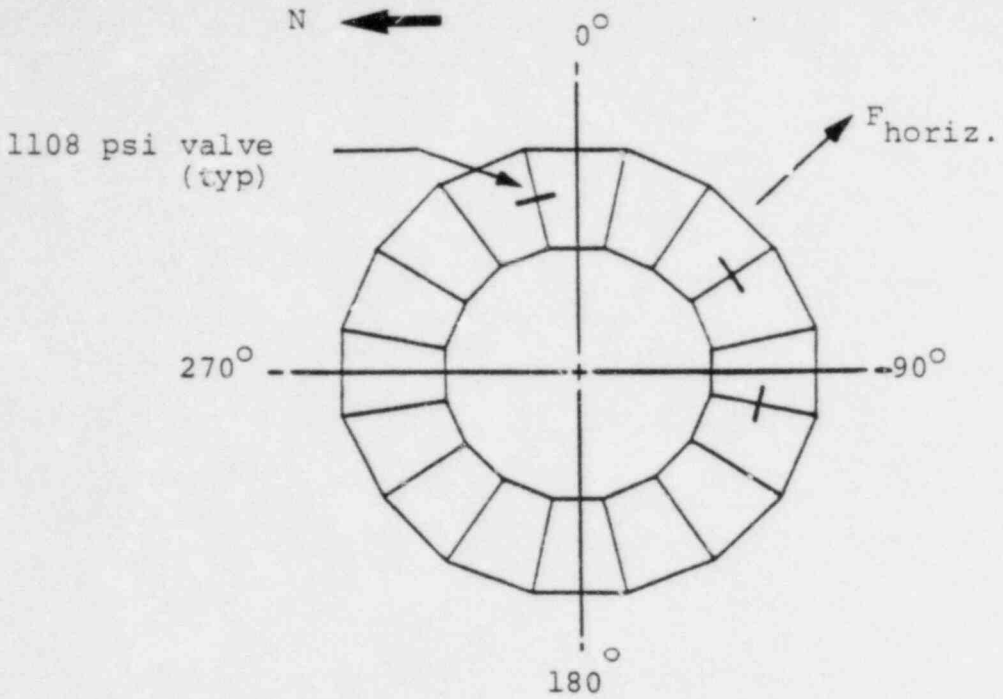

Key Diagram

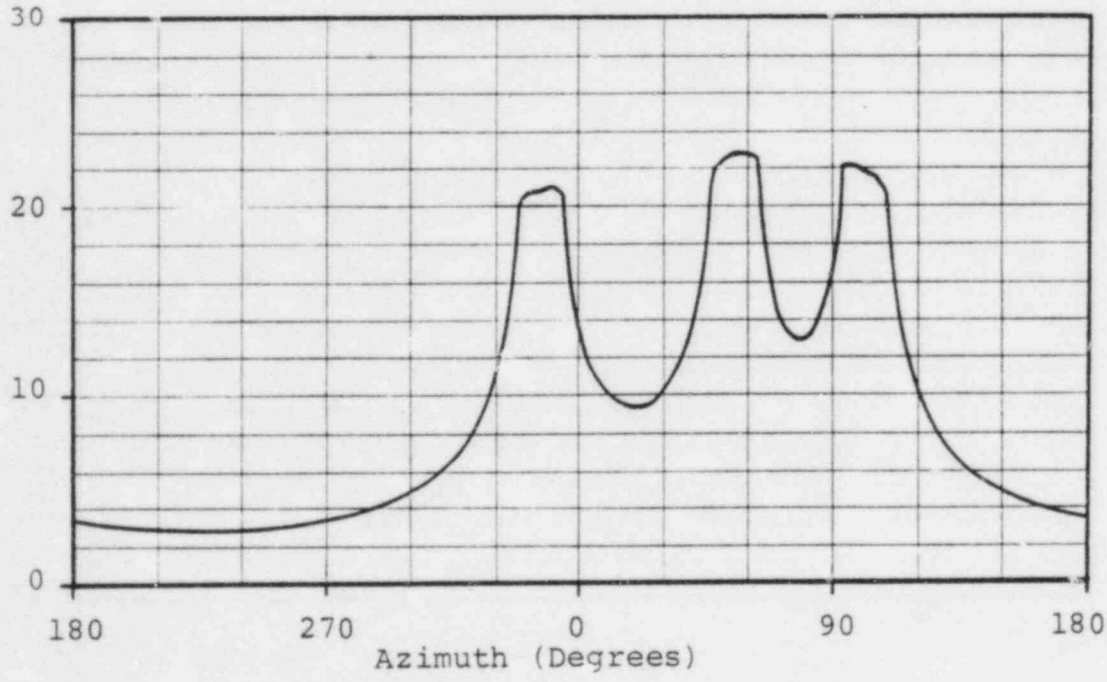

Note:

1. The 1108 psi valve at azimuth 281.25° is assumed not to actuate to maximize the asymmetric load.

Figure 2-2.2-7

LONGITUDINAL TORUS SHELL PRESSURE DISTRIBUTION
FOR ASYMMETRIC SRV DISCHARGE ACTUATION

2-2.2.2 Load Combinations

The load categories and associated load cases for which the suppression chamber is evaluated are presented in Section 2-2.2.1. The NUREG-0661 criteria for grouping the respective loads and load categories into event combinations are presented in Table 2-2.2-7.

The 27 general event combinations shown in Table 2-2.2-7 are expanded to form a total of 107 specific suppression chamber load combinations for the Normal Operating, SBA, IBA, and DBA events. The specific load combinations reflect a greater level of detail than is contained in the general event combinations, including distinctions between SBA and IBA, distinctions between pre-chug and post-chug, distinctions between SRV actuation cases, and consideration of multiple cases of particular loadings. The total number of suppression chamber load combinations consists of 5 for the Normal Operating event, 36 for the SBA event, 42 for the IBA event, and 24 for the DBA event. Several different service level limits and corresponding sets of allowable stresses are associated with these load combinations.

Not all of the possible suppression chamber load combinations are evaluated, since many are enveloped by others and do not lead to controlling suppression chamber stresses. The enveloping load combinations are determined by examining the possible suppression chamber load combinations and comparing the respective load cases and allowable stresses. The results of this examination are shown in Table 2-2.2-8, where each enveloping load combination is assigned a number for ease of identification.

The enveloping load combinations are reduced further by examining relative load magnitudes and individual load characteristics to determine which load combinations lead to controlling suppression chamber stresses. The load combinations which have been found to produce controlling suppression chamber stresses are separated into two groups. The IBA II, IBA III, and DBA II combinations are used to evaluate the suppression chamber vertical supports and shell stresses since these combinations result in the maximum vertical loads and shell pressures on the suppression chamber. The IBA IV combination is used to evaluate the effects of lateral loads on the suppression chamber near the horizontal restraints. The reasoning used to conclude that these are the controlling suppression chamber load

combinations is presented in the paragraphs which follow. Table 2-2.2-9 summarizes the controlling load combinations and identifies which load combinations are enveloped by each of the controlling combinations.

Many of the general event combinations, shown in Table 2-2.2-7, have the same allowable stresses and are enveloped by others which contain the same or additional load cases. No distinction is necessary for load combinations with Service Level A and B conditions for the suppression chamber, since the Service Level A and B allowable stress values are the same.

Many pairs of load combinations contain identical load cases except for seismic loads. One of the load combinations in the pair contains OBE loads and has Service Level A or B allowables, while the other contains SSE loads with Service Level C allowables. At the dominant vertical suppression chamber frequency, both the OBE and SSE vertical accelerations, discussed in Section 2-2.2.1, are small compared to gravity. As a result, suppression chamber stresses and vertical support reactions due to vertical seismic loads are small compared to those caused by other loads in the load combination. The horizontal seismic accelerations

for OBE and SSE at the dominant horizontal suppression chamber frequency are less than 50% of gravity and also result in small suppression chamber stresses compared with those caused by other loads in the load combinations. The Service Level C primary stress allowables for the load combinations containing SSE loads are 33% to 75% higher than the Service Level B allowables for the corresponding load combination containing OBE loads. It is apparent, therefore, that the controlling load combinations for evaluating the suppression chamber are those containing OBE loads and Service Level B allowables.

As shown in Table 2-2.2-2, the pressures and temperatures associated with the times of an ADS type SRV actuations are higher than pressures and temperatures earlier in the SBA and IBA events. Prior to ADS initiation it is postulated that multiple valve SRV actuations will occur, as shown in Figures 2-2.2-8 and 2-2.2-9. As discussed in Section 2-2.2.1, the ADS SRV actuation Case A2.2 is bounded by multiple valve case 7b-Case A1.2/C3.2. Since the multiple valve case 7b is conservatively used in lieu of ADS Case A2.2, combinations which include the higher pressures and temperatures associated with the times of ADS initiation will envelop those combinations with the lower pressures and

temperatures associated with times in the IBA and SBA events prior to ADS initiation.

Applying the above reasoning to the total number of suppression chamber load combinations, a reduced number of enveloping load combinations for each event is obtained. The resulting suppression chamber load combinations for the Normal Operating, SBA, IBA, and DBA events are shown in Table 2-2.2-8, along with the associated service level assignments. For ease of identification, each load combination in each event is assigned a number. The reduced number of enveloping load combinations shown in Table 2-2.2-8 consists of two for Normal Operating Conditions, three for the SBA event, four for the IBA event, and six for the DBA event. The load case designations for the loads which comprise the combinations are the same as those presented in Section 2-2.2.1.

It is evident from an examination of Table 2-2.2-8 that further reductions in the number of suppression chamber load combinations requiring evaluation are possible. Many of the combinations are similar except for variations in LOCA and SRV loads. In addition, load combinations which include pool swell loads are bounded

by other load combinations as discussed in Section 2-2.4. This reasoning is applied to the load combinations shown in Table 2-2.2-8 to determine the governing load combinations.

To ensure that fatigue in the suppression chamber is not a concern over the life of the plant, the combined effects of fatigue due to Normal Operating plus SBA events are evaluated. The relative sequencing and timing of each loading in the SBA, IBA, and DBA events used in this evaluation are shown in Figures 2-2.2-8, 2-2.2-9, and 2-2.2-10. The fatigue effects for Normal Operating plus DBA events are enveloped by the Normal Operating plus SBA events, since combined effects of SRV discharge loads and other loads for the SBA events are more severe than those of DBA. Since IBA combinations are used to envelop the SBA combinations, the Normal Operating plus SBA events are evaluated for fatigue using the stress levels associated with the IBA events. Additional information used in the supression chamber fatigue evaluation is summarized at the bottom of Table 2-2.2-8.

The load combinations and event sequencing described in the preceding paragraphs envelop those postulated to occur during an actual LOCA or SRV discharge event. An

evaluation of the above load combinations results in a conservative estimate of the suppression chamber responses and leads to bounding values of suppression chamber stresses and fatigue effects.

Table 2-2.2-7

MARK I CONTAINMENT EVENT COMBINATIONS

	SRV	SRV + EQ		SBA IBA		SBA + EQ IBA + EQ				SBA+SRV IBA+SRV		SBA+SRV+EQ IBA+SRV+EQ				DBA		DBA + EQ				DBA+SRV		DBA+SRV+EQ			
Earthquake Type		O	S			O	S	O	S			O	S	O	S			O	S	O	S			O	S	O	S
LOADS	1	2	3	4	5	6	7	8	9	10	11	12	13	14	15	16	17	18	19	20	21	22	23	24	25	26	27
Normal	X	X	X	X	X	X	X	X	X	X	X	X	X	X	X	X	X	X	X	X	X	X	X	X	X	X	X
Earthquake		X	X			X	X	X	X			X	X	X	X			X	X	X	X			X	X	X	X
SRV Discharge	X	X	X							X	X	X	X	X	X							X	X	X	X	X	X
LOCA Thermal				X	X	X	X	X	X	X	X	X	X	X	X	X	X	X	X	X	X	X	X	X	X	X	X
LOCA Reactions				X	X	X	X	X	X	X	X	X	X	X	X	X	X	X	X	X	X	X	X	X	X	X	X
LOCA Quasi-Static Pressure				X	X	X	X	X	X	X	X	X	X	X	X	X	X	X	X	X	X	X	X	X	X	X	X
LOCA Pool Swell																X		X	X			X		X	X		
LOCA Condensation Oscillation					X			X	X		X			X	X		X			X	X		X			X	X
LOCA Chugging					X			X	X		X			X	X		X			X	X		X			X	X

Note:

1. See Section 1-3.2 for additional event combination information.

Table 2-2.2-8

CONTROLLING SUPPRESSION CHAMBER LOAD COMBINATIONS

Section 2-2.2.1 Load Designation		Condition/Event	NOC		SBA			IBA				DBA					
		Volume 2 Load Combination Number	I	II	I	II	III	I	II	III	IV	I	II	III	IV	V	VI
		Table 2-2.2-8 Load Combination Number	2	2	14	14	14	14	14	14	14	18	20	25	27	27	27
1) Dead Weight			1a,1b	←												→	1a,1b
2) Seismic	OBE		2a	←								→	2a				
	SSE													2b	←	→	2b
3) Pressure[1]			P[2]	P[2]	P_3	P_3	P_3	P_3	P_3	P_3	P_3	P_2	P_3	P_1	P_3	P_4	P_4
3) Temperature[3]			T[4]	T[4]	T_3	T_3	T_3	T_3	T_3	T_3	T_3	T_1	T_3	T_1	T_3	T_4	T_4
4) Pool Swell												4a,4b		4a,4b			
5) Condensation Oscillation								5b,5d					5a,5c		5a,5c		
6) Chugging	Pre-Chug				6a,6c	6a,6c			6a,6c		6a,6c					6a,6c	
	Post-Chug						6b,6d			6b,6d							6b,6d
7) SRV Discharge	Single		7a,7d											7a,7d	7a,7d[5]	←	7a,7d[5]
	Multiple			7b,7d	7b,7d		7b,7d	7b,7d	7b,7d	7b,7d							
	Multiple Asymmetric					7c,7d					7c,7d						
8) Containment Interaction			8a	←												→	8a
Service Level			B	B	B	B	B	B	B	B	B	B[6]	B	C	C	C	C
Number of Event Occurrences[7]			150	150	1	←										→	1
Number of SRV Actuations[8]			596	370	50	2	50	25	2	2	2	0	0	0	1	1	1

Table 2-2.2-8

(Concluded)

Notes:

1. See Table 2-2.2-2 for SBA, IBA, and DBA internal pressure values.

2. The range of normal operating internal pressures is 0.0 to 2.0 psi as specified by the FSAR.

3. See Table 2-2.2-2 for SBA, IBA, and DBA temperature values.

4. The range of normal operating temperatures is 50.0 to 150.0°F as specified by the FSAR.

5. The SRV discharge loads which occur during this phase of the DBA event have a negligible effect on the suppression chamber.

6. Evaluation of secondary stress range and fatigue not required. When evaluating torus shell stresses, the value of S_{mc} may be increased by the dynamic load factor derived from the analytical model.

7. The number of seismic load cycles used for fatigue is 600.

8. The values shown are conservative estimates of the number of actuations expected for a BWR 4 plant with a reactor vessel diameter of 251 inches equipped with low-low set logic.

Table 2-2.2-9

ENVELOPING LOGIC FOR CONTROLLING
SUPPRESSION CHAMBER LOAD COMBINATIONS

Condition / Event			NOC		SBA			IBA				DBA					
Table 2-2.2-7 Load Combination Number			2	2	14	14	14	14	14	14	14	18	20	25	27	27	27
Table 2-2.2-7 Load Combinations Enveloped			1	1	3-13, 15	3-13, 15	3-13, 15	3-13, 15	3-13, 15	3-13, 15	3-13, 15	16	17	19, 22, 24	21, 23, 26	21, 23, 26	21, 23, 26
Volume 2 Load Combination Designation			I	II	I	II	III	I	II	III	IV	I	II	III	IV	V	VI
Controlling Load Combinations Evaluated	Vertical Support Loads and Torus Shell Pressures	IBA II	X	X	X	X		X			X					X	
		IBA III					X					X		X			X
		DBA II													X		
	Lateral Loads	IBA IV	X	X	X	X	X	X	X	X			X		X	X	X

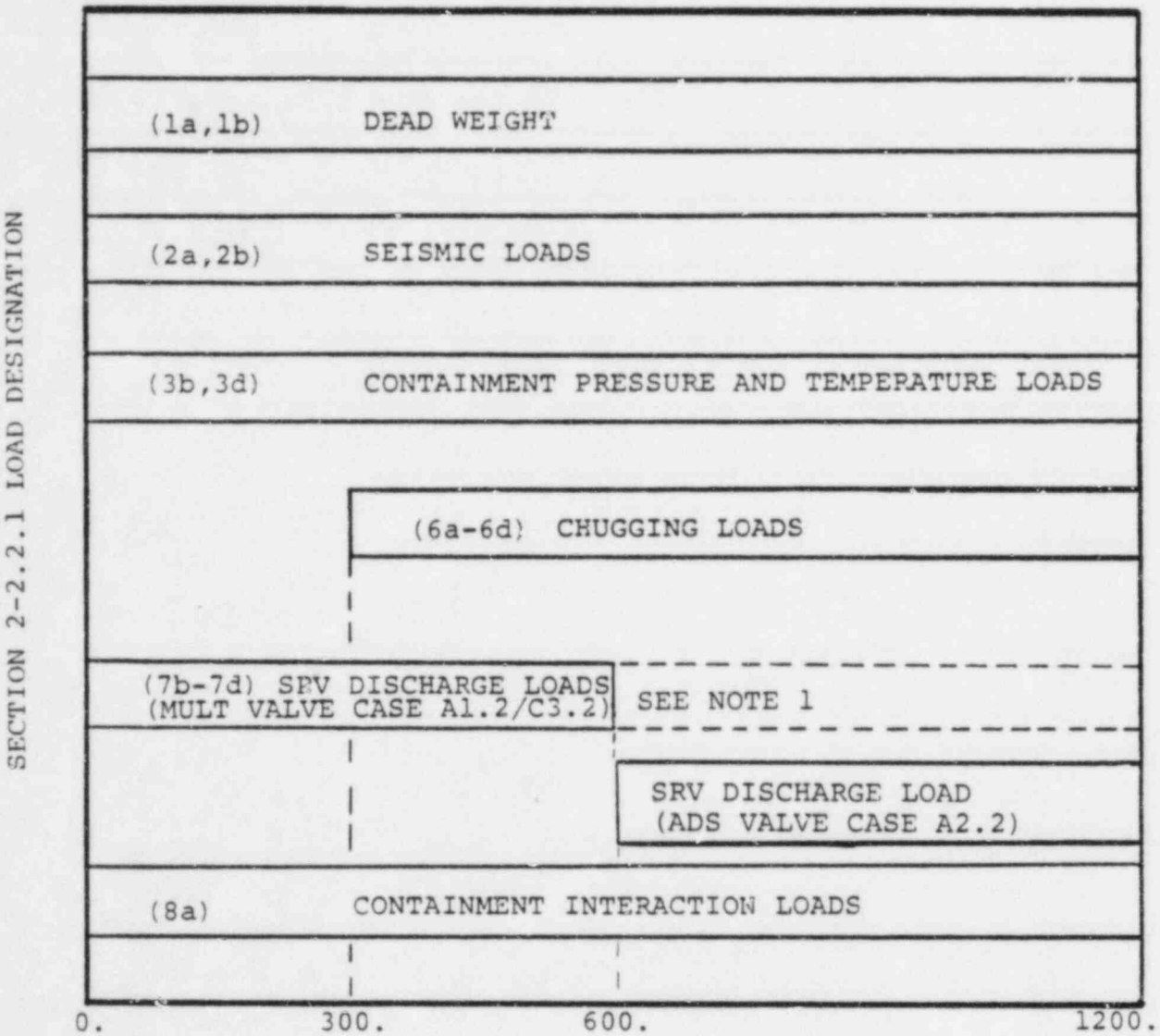

Note:

1. SRV multiple valve case A1.2/C3.2 envelops SRV ADS valve case A2.2.

Figure 2-2.2-8

SUPPRESSION CHAMBER SBA EVENT SEQUENCE

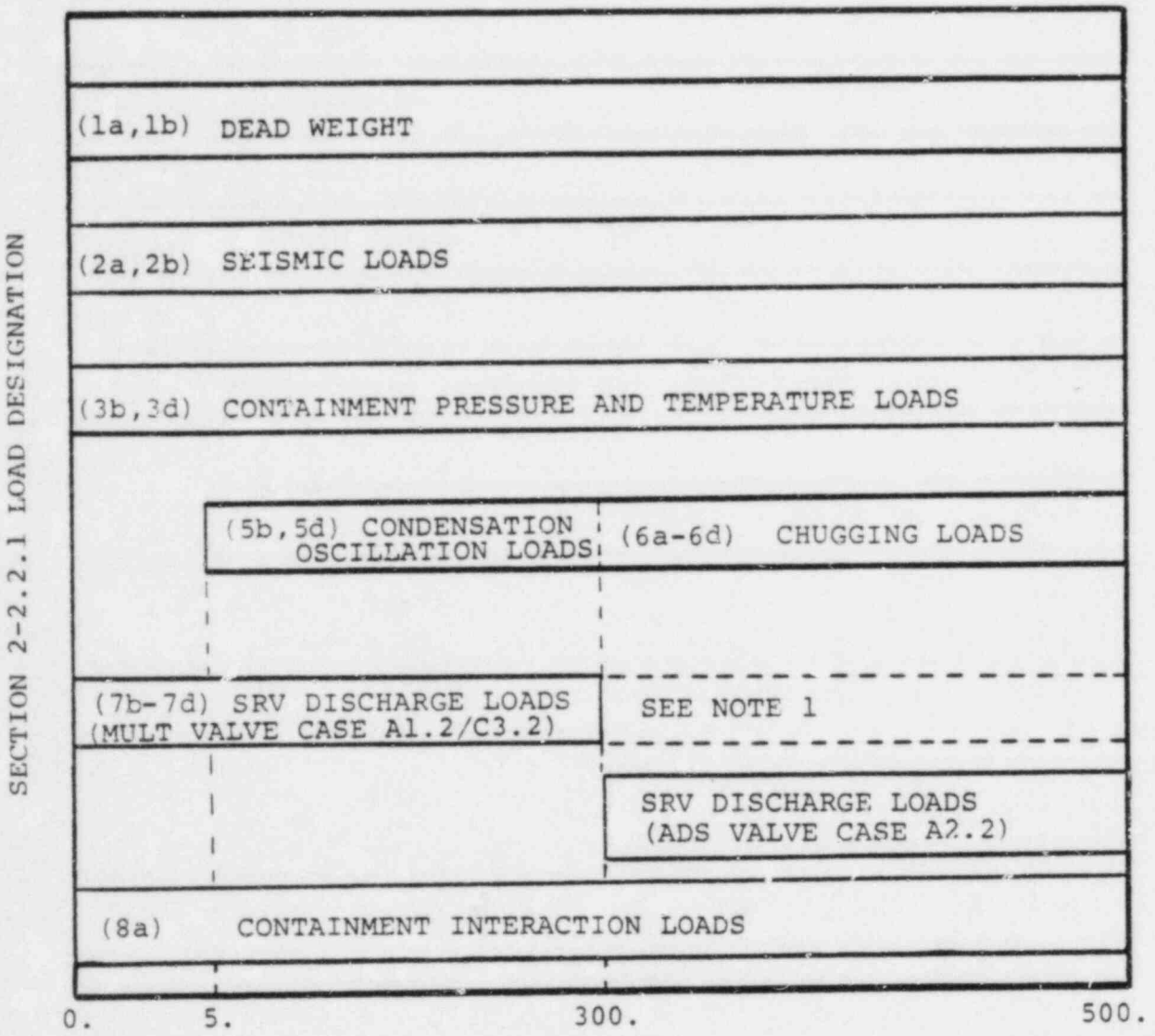

Note:

1. SRV multiple valve case A1.2/C3.2 envelops SRV ADS valve case A2.2.

Figure 2-2.2-9

SUPPRESSION CHAMBER IBA EVENT SEQUENCE

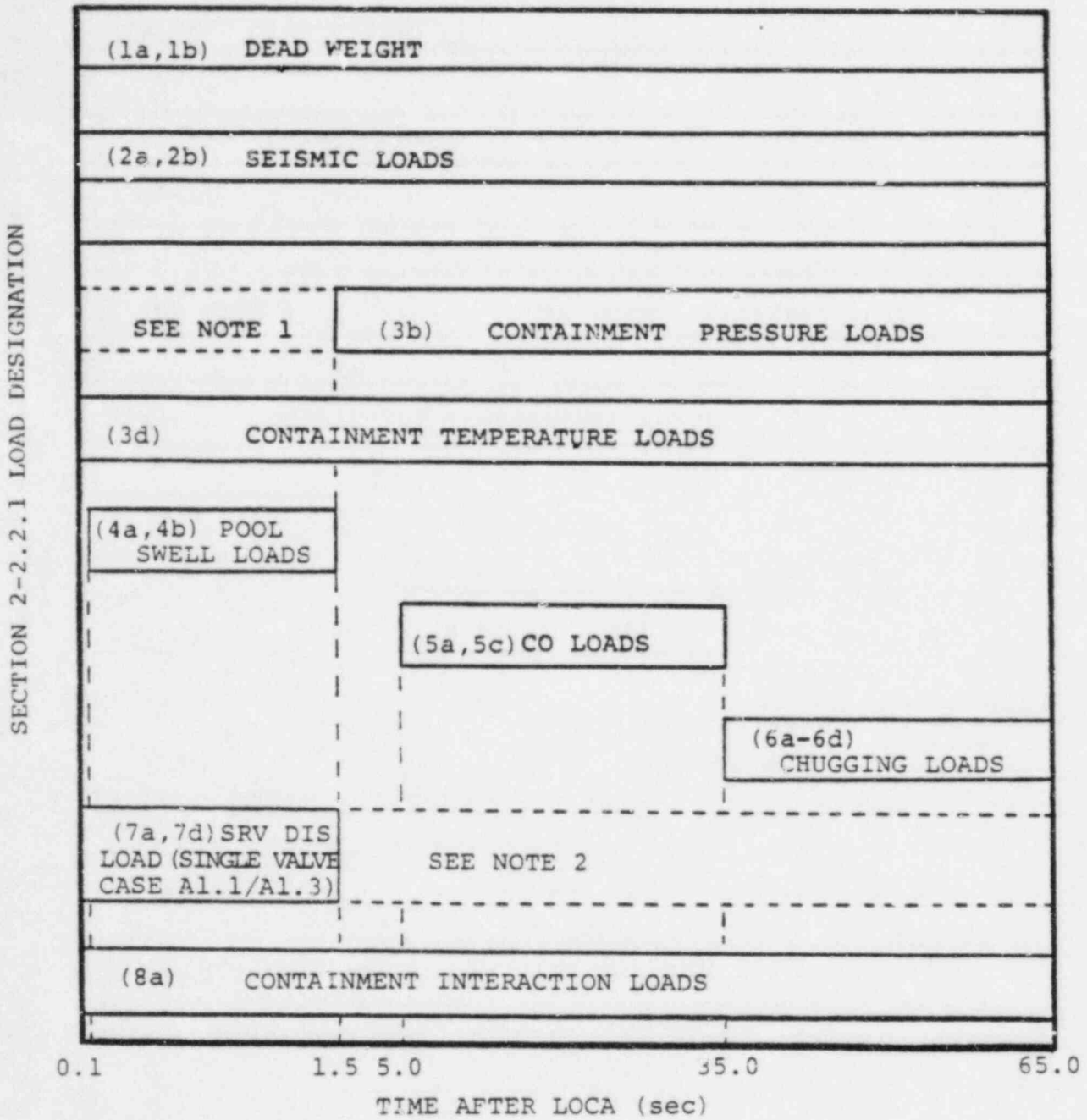

Notes:

1. The effects of internal pressure loads are included in pool swell torus shell loads.

2. The SRV discharge loads which occur during this phase of the DBA event are negligible.

Figure 2-2.2-10

SUPPRESSION CHAMBER DBA EVENT SEQUENCE

2-2.3 Analysis Acceptance Criteria

The acceptance criteria defined in NUREG-0661 on which the Hope Creek suppression chamber analysis is based are discussed in Section 1-3.2. In general, the acceptance criteria follows the rules contained in the ASME Code, Section III, Division 1 including the Summer 1977 Addenda for Class MC components and component supports (Reference 6). The corresponding service limit assignments, jurisdictional boundaries, allowable stresses, and fatigue requirements are consistent with those contained in the applicable subsections of the ASME Code and the Mark I Containment Program Structural Acceptance Criteria Plant Unique Analysis Application Guide (PUAAG) (Reference 5). The acceptance criteria used in the analysis of the suppression chamber are summarized in the paragraphs which follow.

The items examined in the analysis of the suppression chamber include the suppression chamber shell, mitered joint and midcylinder ring beams, and the suppression chamber horizontal and vertical support systems. The specific component parts associated with each of these items are identified in Figures 2-2.1-1 through 2-2.1-13.

The suppression chamber shell and ring beam are evaluated in accordance with the requirements for Class MC components contained in Subsection NE of the ASME Code. Fillet welds and partial penetration welds in which one or both of the joined parts include the suppression chamber shell or ring beams are also evaluated in accordance with the requirements for Class MC component attachment welds contained in Subsection NE of the ASME Code.

The suppression chamber columns, column connections, and associated component parts and welds are evaluated in accordance with the requirements for Class MC component supports contained in Subsection NF of the ASME Code.

As shown in Table 2-2.2-8, the IBA II, IBA III, IBA IV, and DBA II combinations all have Service Level B limits. Since these load combinations have somewhat different maximum temperatures, the allowable stresses are conservatively determined at the highest temperature of the four load combinations. The allowable stresses for each component of the suppression chamber and the vertical support system are determined at the maximum IBA temperature of 167°F. The allowable

stresses for the vertical support column base plate assemblies are also determined at 167°F. The resulting allowable stresses for the load combinations with Service Level B limits are shown in Table 2-2.3-1.

The bearing stresses in the grout and reactor building basemat in the vicinity of the column base plates are evaluated in accordance with the requirements of the ACI Code (Reference 7).

The allowable loads on the suppression chamber horizontal restraints are taken from the FSAR as permitted by NUREG-0661 in cases where the analysis technique used in the evaluation is the same as that contained in the plant's FSAR. The allowable horizontal restraint load for Service Level B conditions is 642 kips per horizontal restraint assembly in a direction parallel to the longitudinal centerline of the mitered cylinder. The suppression chamber shell, in the vicinity of the horizontal restraints, is evaluated in accordance with the requirements for Class MC components previously discussed.

The acceptance criteria described in the preceding paragraphs result in conservative estimates of the existing margins of safety and ensures that the original suppression chamber design margins are restored.

Table 2-2.3-1

ALLOWABLE STRESSES FOR SUPPRESSION CHAMBER COMPONENTS AND SUPPORTS

Item	Material	(1) Material Properties (ksi)	Stress Type	(2) Allowable Stress (ksi)
C O M P O N E N T S				
Shell	SA-516 Gr. 70	S_{mc} = 19.30 S_{ml} = 23.15 S_y = 35.52	Primary Membrane	19.30
			Local Primary Membrane	28.95
			Primary + (3) Secondary Stress Range	69.45
Ring Beam	SA-516 Gr. 70	S_{mc} = 19.30 S_{ml} = 23.15 S_y = 35.52	Primary Membrane	19.30
			Local Primary Membrane	28.95
			Primary + (3) Secondary Stress Range	69.45
S U P P O R T S				
(4) Column Connection	SA-537 Cl. 2	S_y = 56.65	Membrane	34.00
			Extreme Fiber	42.49
Column	SA-537 Cl. 2	S_y = 56.65	Tensile	34.00
			Compressive	32.15
			Net Section Tensile	25.49
			Pullout Shear	22.66
			Bearing	51.00

Table 2-2.3-1
(Concluded)

Item	Material	Material Properties (ksi)	Stress Type	Allowable Stress (ksi) (2)
W E L D S				
Ring Beam to Shell	SA-516 Gr. 70	S_{mc} = 19.30	Primary	15.01
		S_y = 35.52	Secondary	45.03
Column Connection to Shell	SA-516 Gr. 70	S_{mc} = 19.30	Primary	15.01
		S_y = 35.52	Secondary	45.03

Notes:

1. Material properties taken at maximum event temperature of 167°F.
2. Allowables shown correspond to Service Level B stress limits.
3. Thermal bending stresses may be excluded when comparing primary-plus-secondary stress range values to allowables.
4. Stresses due to thermal loads may be excluded when evaluating components supports.

2-2.4 Method of Analysis

The governing loads for which the Hope Creek suppression chamber is evaluated are presented in Section 2-2.2.1. The methodology used to evaluate the suppression chamber for the effects of all loads, except those which result in lateral loads on the suppression chamber, is discussed in Section 2-2.4.1. The methodology used to evaluate the suppression chamber for the effects of lateral loads is discussed in Section 2-2.4.2.

The methodology used to formulate results for the controlling load combinations, examine fatigue effects, and evaluate the analysis results for comparison with the applicable acceptance limits is discussed in Section 2-2.4.3.

2-2.4.1 Analysis for Major Loads

The repetitive nature of the suppression chamber geometry is such that the suppression chamber can be divided into 16 identical segments which extend from midbay of the vent line bay to midbay of the non-vent line bay, as shown in Figure 2-2.1-1. The suppression chamber can be further divided into 32 identical segments extending from the mitered joint to midbay, provided the offset mitered joint ring beam and support columns are assumed to lie in the plane of the mitered joint. The effects of the mitered joint ring beam and support columns offset are considered to have a negligible effect on the suppression chamber response. The analysis of the suppression chamber, therefore, is performed for a typical 1/32nd segment.

A finite element model of a 1/32nd segment of the suppression chamber, as shown in Figure 2-2.4-1, is used to obtain the suppression chamber response to all loads except those resulting in lateral loads on the suppression chamber. The analytical model includes the suppression chamber shell, the mitered joint ring beam with cover plates, the extended midcylinder ring beam,

the column connections and associated column members, and miscellaneous internal and external stiffener plates.

The analytical model is comprised of 962 nodes, 113 beam elements, and 1283 plate bending and stretching elements. The suppression chamber shell has a circumferential node spacing of 9° at quarter-bay with additional mesh refinement near discontinuities to facilitate examination of local stresses. Additional refinement is also included in modeling of the ring beams and column connections at locations where locally higher stresses occur. Small displacement linear-elastic behavior is assumed throughout.

The analytical model used for the suppression chamber stress analysis includes a corrosion allowance of 1/8 inch subtracted from the nominal thicknesses of the torus shell and ring beams, in accordance with the original design requirements contained in the plant's FSAR. The mass densities used in this corroded model are adjusted to account for the weight of the suppression chamber with nominal material thicknesses as shown in Figures 2-2.1-1 through 2-2.1-12.

The boundary conditions used in the analytical model are both physical and mathematical in nature. The physical boundary conditions consist of vertical restraints at each column base plate location. As previously discussed, the vertical support columns are pinned top and bottom to permit movement of the suppression chamber in the horizontal direction. The mathematical boundary conditions consist of either symmetry or anti-symmetry at the mitered joint and mid-cylinder planes, depending on the characteristics of the load being evaluated.

The stiffness effects of the vent system on the suppression chamber are included in the analytical model by means of a coupled stiffness matrix. The matrix mathematically simulates the coupling effects provided by the vent system at the column and upper truss attachment locations. The mass of the vent system is not included in the analytical model as it is small compared to the mass of the suppression chamber and will have a negligible effect on the analysis.

When computing the response of the suppression chamber to dynamic loadings, the fluid-structure interaction effects of the suppression chamber shell and contained fluid (water) are considered. This is accomplished

through use of a finite element model of the fluid shown in Figure 2-2.4-2. The analytical fluid model is used to develop a coupled mass matrix which is added to the submerged nodes of the suppression chamber analytical model to represent the fluid. A water volume corresponding to a water level 11-1/2" below the suppression chamber horizontal centerline is used in this calculation. This is the maximum water volume expected during normal operating conditions. Additional fluid mass is lumped along the length of the ring beams to account for the effective mass of water which acts with these structures during dynamic loadings.

A frequency analysis is performed and all structural modes in the range of 0-35 hertz are extracted. The resulting frequencies and vertical modal weights are shown in Table 2-2.4-1. It is evident from the table that the lowest suppression chamber frequency occurs at about 15.12 hertz, which is above the dominant frequencies of most major hydrodynamic loadings.

Nominal (uncorroded) material thicknesses are used for torus attached piping (TAP) suppression chamber motion generation documented in PUAR Volume 6. The use of nominal material thicknesses to generate TAP motions is

justified since corrosion of the torus shell and ring beams is expected to be highly localized. While this may effect stresses in the torus shell and ring beams, the overall stiffness of the suppression chamber, and therefore displacements, will remain generally unaffected.

A dynamic analysis is performed for each of the hydrodynamic torus shell load cases as specified in Section 2-2.2.1 using the analytical model of the suppression chamber. The analysis consists of either a transient or a harmonic analysis, depending on the characteristics of the torus shell load being considered. The modal superposition technique with 2% damping is utilized in both transient and harmonic analyses.

The remaining suppression chamber load cases specified in Section 2-2.2.1 involve either static loads or dynamic loads which are evaluated using an equivalent static approach. For the latter, conservative dynamic amplification factors are developed and applied to the maximum spatial distributions of the individual dynamic loadings.

The specific treatment of each load in the load categories identified in Section 2-2.2.1 is discussed in the paragraphs which follow:

1. Dead Weight Loads

   a. Dead Weight of Steel: A static analysis is performed for a unit vertical acceleration applied to the weight of suppression chamber steel.

   b. Dead Weight of Water: A static analysis is performed for hydrostatic pressures applied to the submerged portion of the suppression chamber shell.

2. Seismic Loads

   a. OBE Loads: A static analysis is performed for a vertical acceleration applied to the combined weight of suppression chamber steel and water. The vertical acceleration used in the analysis is obtained from the original design basis documented in the plant's FSAR at the lowest suppression chamber vertical frequency of 15.12 hertz. The effects of

horizontal OBE accelerations are evaluated in Section 2-2.4.2.

b. SSE Loads: As discussed in Section 2-2.2.2, load combinations with OBE loads envelop combinations containing SSE loads. Therefore SSE loads are not evaluated for the suppression chamber.

3. Containment Pressure and Temperature

a. Normal Operating Internal Pressure: A static analysis is performed for a 2.0 psi internal pressure, uniformly applied to the suppression chamber shell.

b. LOCA Internal Pressure Loads: A static analysis is performed for the maximum of the SBA, IBA, and DBA internal pressures, shown in Table 2-2.2-2. This pressure is uniformly applied to the suppression chamber shell.

c. Normal Operating Temperature Loads: A static analysis is performed for a 150°F temperature uniformly applied to the suppression chamber shell and ring beams. The column connections

and column members are assumed to remain at the ambient temperature.

d. LOCA Temperature Loads: A static analysis is performed for the maximum of the SBA, IBA, and DBA temperatures, uniformly applied to the suppression chamber shell and ring beams. The SBA, IBA, and DBA event temperatures shown in Table 2-2.2-2 are applied at selected times during each event. The column connections and column members are assumed to remain at the ambient temperature.

4. Pool Swell Loads

a. Pool Swell Torus Shell Loads: The maximum suppression chamber shell pressures due to pool swell are shown in Table 2-2.2-3. Table 2-2.4-2 summarizes results of the analysis of the suppression chamber for major LOCA and SRV loading conditions. These loads are combined into loading combinations and the results are presented in Table 2-2.4-3. As can be seen by examining Table 2-2.4-3, the DBA pool swell combination with Service Level

B allowables is enveloped by other SBA, IBA, and DBA combinations with Service Level B allowables. The DBA pool swell plus single valve SRV case has Service Level C allowables. The Service Level C primary stress allowables are 33% to 75% higher than the Service Level B primary stress allowables. It is apparent by examining Table 2-2.4-3 that the load combinations with Service Level B allowables are more severe than the combinations with pool swell loads and Service Level C allowables. Therefore pool swell loads are not evaluated further in the suppression chamber analysis.

b. LOCA Air Clearing Submerged Structure Loads: As discussed in Section 2-2.2.1, this load is enveloped by other submerged structure loadings and is therefore not evaluated in the suppression chamber analysis.

5. Condensation Oscillation Loads

a. DBA Condensation Oscillation Torus Shell Loads: A dynamic analysis is performed for the four condensation oscillation load alter-

nates shown in Table 2-2.2-4 for frequencies up to 35 hertz. A typical response obtained from the suppression chamber harmonic analysis for the normalized spatial distribution of pressures shown in Figure 2-2.2-1 is provided in Figure 2-2.4-3. During harmonic summation, the amplitudes for each condensation oscillation load frequency interval are conservatively applied to the maximum response amplitudes obtained from the suppression chamber harmonic analysis results in the same frequency interval. For frequencies between 35 and 50 hertz, the pressure amplitudes shown in Table 2-2.2-4 are summed absolutely and analyzed statically using the pressure distribution shown in Figure 2-2.2-1. As can be seen from the harmonic analysis results shown in Figure 2-2.4-3, dynamic amplification is negligible in the 35 to 50 hertz range.

b. IBA Condensation Oscillation Torus Shell Loads: As previously discussed, pre-chug loads described in load case 6a are specified in lieu of IBA condensation oscillation loads.

c. DBA Condensation Oscillation Submerged Structure Loads: An equivalent static analysis is performed for the ring beam DBA condensation oscillation submerged structure loads shown in Table 2-2.2-6. The values of the loads shown include dynamic amplification factors which are computed using first principles and the dominant frequencies of the ring beams. The dominant lateral frequencies are derived from manual calculations using a Rayleigh-Ritz approach. The lateral frequencies used in the response calculations are 39.23 hertz for the mitered joint ring beam and 35.86 hertz for the midcylinder ring beam. The vertical frequency of the ring beams is 15.12 hertz.

d. IBA Condensation Oscillation Submerged Structure Loads: As previously discussed, pre-chug loads described in load case 6c are specified in lieu of IBA condensation oscillation loads.

6. Chugging Loads

a. Pre-Chug Torus Shell Loads: A dynamic analysis is performed for the symmetric pre-chug loads shown in Figure 2-2.2-4. It is evident from the harmonic analysis results shown in Figure 2-2.4-3 that the maximum suppression chamber response in the 6.9 to 9.5 hertz range occurs at the maximum pre-chug load frequency of 9.5 hertz. The effects of lateral loads caused by asymmetric pre-chug are examined in Section 2-2.4.2.

b. Post-Chug Torus Shell Loads: A dynamic analysis is performed for the loads shown in Table 2-2.2-5 for frequencies up to 35 hertz. Typical responses obtained from the suppression chamber harmonic analyses for the normalized spatial distribution of pressures shown in Figure 2-2.2-1 are provided in Figure 2-2.4-3. During harmonic summation, the amplitudes for each post-chug load frequency interval are conservatively applied to the maximum response amplitudes obtained from the suppression chamber harmonic analysis results in the same frequency

interval. For frequencies from 35 to 50 hertz, the pressure amplitudes shown in Table 2-2.2-5 are summed and analyzed statically using the pressure distribution shown in Figure 2-2.2-1. As can be seen from the harmonic analysis results presented in Figure 2-2.4-3, dynamic amplification is negligible in the 35 to 50 hertz range.

c. Pre-Chug Submerged Structure Loads: As discussed in Section 2-2.2.1, post-chug submerged structure loads (6d) are used in lieu of pre-chug submerged structure loads.

d. Post-Chug Submerged Structure Loads: An equivalent static analysis is performed for the ring beam submerged structure loads shown in Table 2-2.2-6. The values of the loads shown include dynamic amplification factors which are computed using first principles and the dominant frequencies of the ring beams as discussed in load case 5c.

7. Safety Relief Valve Discharge Loads

a-c. SRV Discharge Torus Shell Loads: A dynamic analysis is performed for SRV discharge torus shell load 7b-Case A1.2/C3.2 shown in Figure 2-2.2-7. Several frequencies within the range of the SRV discharge load frequencies specified for each case are evaluated to determine the maximum suppression chamber response. The effects of lateral loads on the suppression chamber caused by SRV discharge load 7c-Case A1.2/C3.2 are evaluated in Section 2-2.4.2. As discussed in Section 2-2.2.2, SRV discharge load 7b-Case A1.2/C3.2 envelopes the remaining SRV discharge cases.

The suppression chamber analytical model used in the analysis is calibrated using the methodology discussed in Section 1-4.2.3. The methodology involves use of modal correction factors which are applied to the response associated with each suppression chamber frequency. The resulting correction factors used in evaluating the effects of SRV discharge torus shell loads are shown in Figure 2-2.4-4.

d. SRV Discharge Air Clearing Submerged Structure Loads: An equivalent static analysis is performed for the ring beam SRV discharge drag loads shown in Table 2-2.2-6. The values of the loads shown include dynamic amplification factors derived using the methodology discussed in Section 1-4.2.4.

8. Containment Interaction Loads

a. Containment Structures Reaction Loads: An equivalent static analysis is performed for the vent system support column, vent system upper truss, and T-quencher and T-quencher support reaction loads taken from the evaluation of these components discussed in Volumes 3 and 5 of this report.

The methodology described in the preceding paragraphs results in a conservative evaluation of the suppression chamber response and associated stresses for the governing loads. Use of the analysis results obtained by applying this methodology leads to a conservative evaluation of the suppression chamber design margins.

Table 2-2.4-1

SUPPRESSION CHAMBER FREQUENCY ANALYSIS RESULTS

Mode Number	Frequency (Hz)	Vertical Modal Weight (lb)
1	15.12	64339.4
2	16.94	97320.2
3	21.18	4750.4
4	21.92	2542.2
5	23.87	13872.1
6	24.92	1220.2
7	25.39	7082.2
8	25.82	4087.5
9	27.76	25772.0
10	29.07	17550.2
11	29.44	12230.1
12	30.26	6.9
13	30.88	17465.8
14	31.23	2.8
15	31.89	14743.8
16	33.31	2808.7
17	34.01	1083.6
18	34.71	124.0
19	35.54	2000.9

Table 2-2.4-2

TORUS SHELL LOADS ANALYSIS RESULTS
USED TO ENVELOP POOL SWELL LOADS

Item		Single SRV Discharge	Multiple SRV Discharge	Pre-Chug	Post-Chug	DBA CO	Pool Swell (1)
Torus Shell Membrane Stress at Quarter Bay (ksi)	BDC	5.64	8.33	0.71	1.20	4.12	4.32
	Outside Equator	3.38	4.78	0.37	0.66	2.23	5.18
Total Vertical Reaction Per Mitered Cylinder (kips)	Upward	1989.93	2732.90	214.45	312.58	1181.46	536.72
	Downward	1738.39	2619.17	214.45	312.58	1181.46	1202.27

Note:

1. Results taken from analysis documented in Section 3-2.4.

Table 2-2.4-3

LOAD COMBINATION RESULTS USED TO ENVELOP POOL SWELL TORUS SHELL LOADS (1)

Item		Chugging + Multiple SRV	DBA CO	Poolswell + Single SRV	Poolswell
Torus Shell Membrane Stress at Quarter Bay (ksi)	BDC	9.53	4.12	9.96	4.32
	Outside Equator	5.44	2.23	8.56	5.18
Total Vertical Reaction Per Mitered Cylinder (kips)	Upward	3045.48	1181.46	2526.65	536.72
	Downward	2931.75	1181.46	2940.66	1202.27
Service Limit	Containment	B	B	C	B

Note:

1. Values shown are obtained by combining the individual load results presented in Table 2-2.4-2.

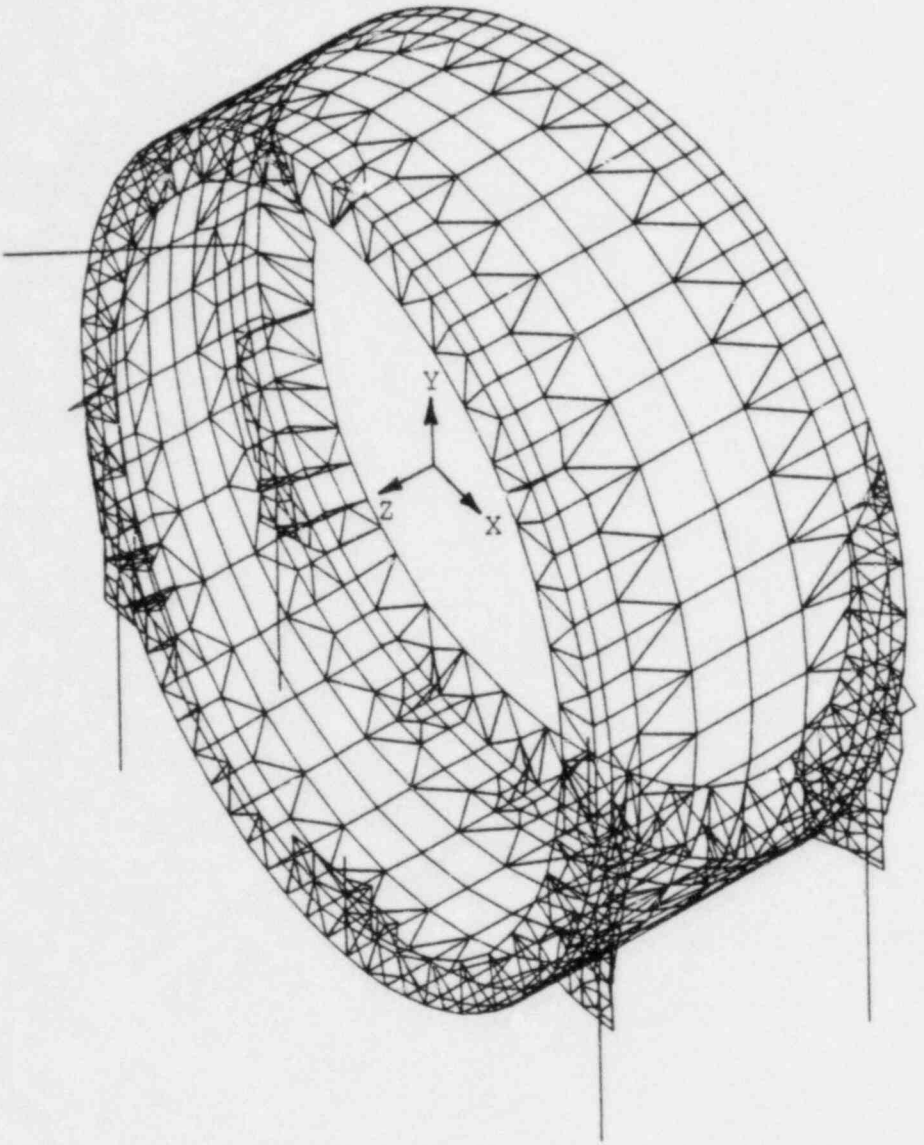

Figure 2-2.4-1

SUPPRESSION CHAMBER 1/32 SEGMENT FINITE ELEMENT MODEL - ISOMETRIC VIEW

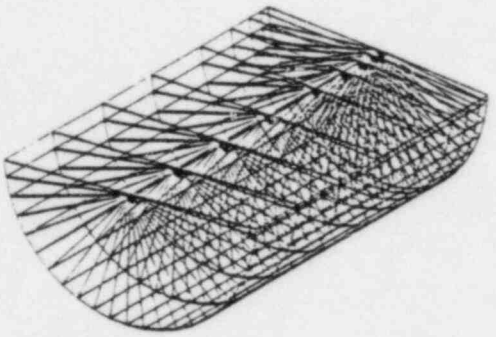

FLUID MODEL CORE

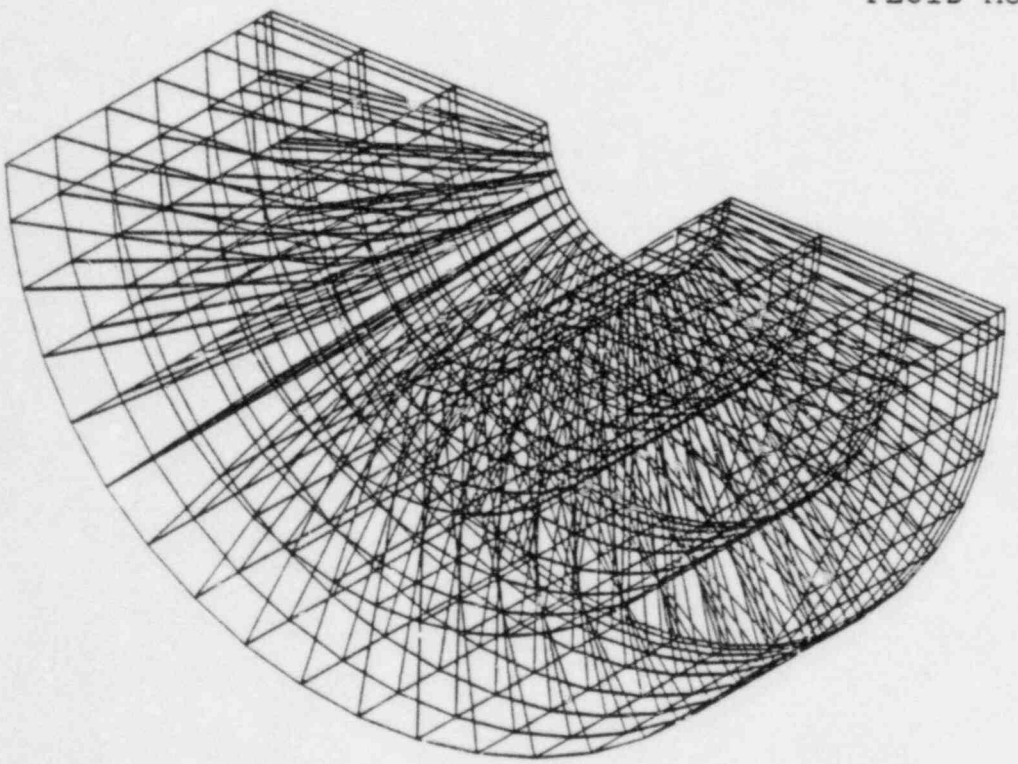

Figure 2-2.4-2

SUPPRESSION CHAMBER FLUID MODEL -
ISOMETRIC VIEW

nutech ENGINEERS

Suppression Chamber Critical Frequencies:

Corroded Thickness: f_{cr} = 15.12 Hz

Nominal Thickness: f_{cr} = 16.00 Hz

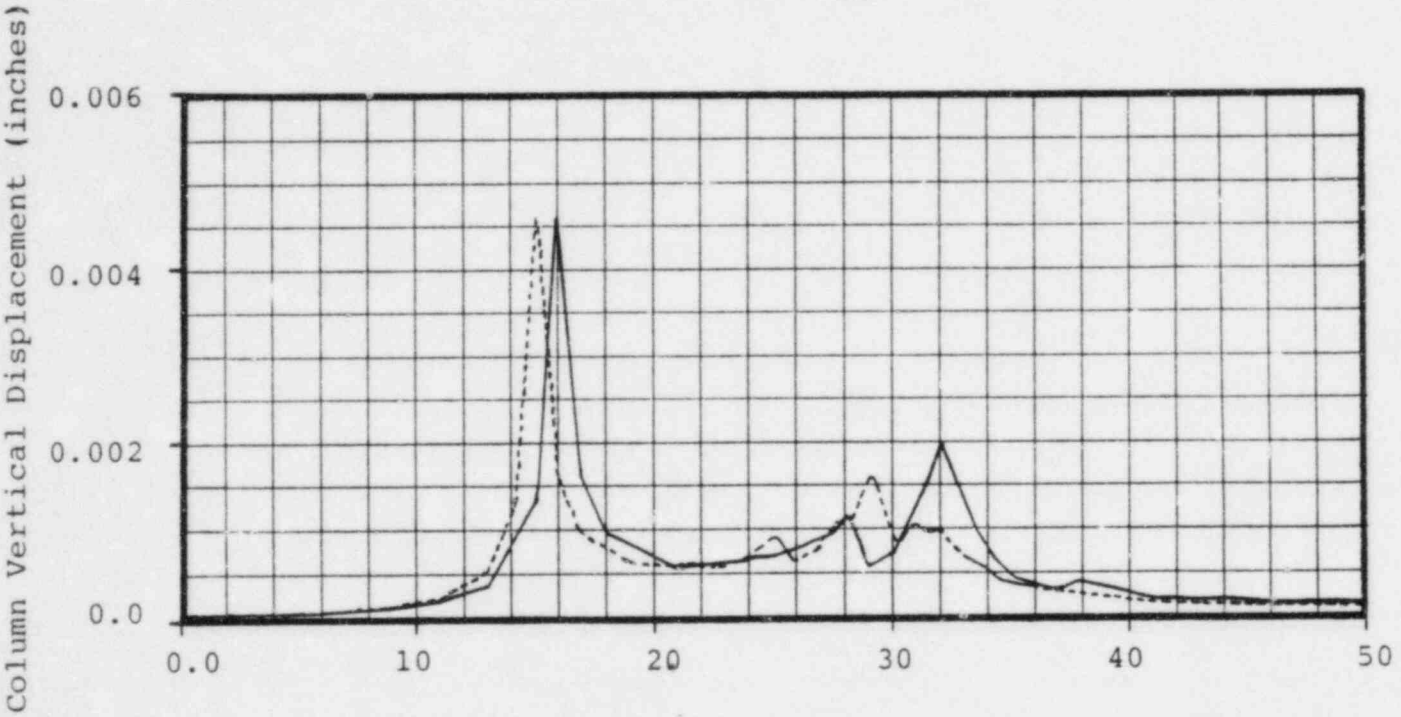

Note:

1. See Figure 2-2.2-1 for spatial distribution of loading.

Figure 2-2.4-3

SUPPRESSION CHAMBER HARMONIC ANALYSIS RESULTS FOR NORMALIZED HYDROSTATIC LOAD

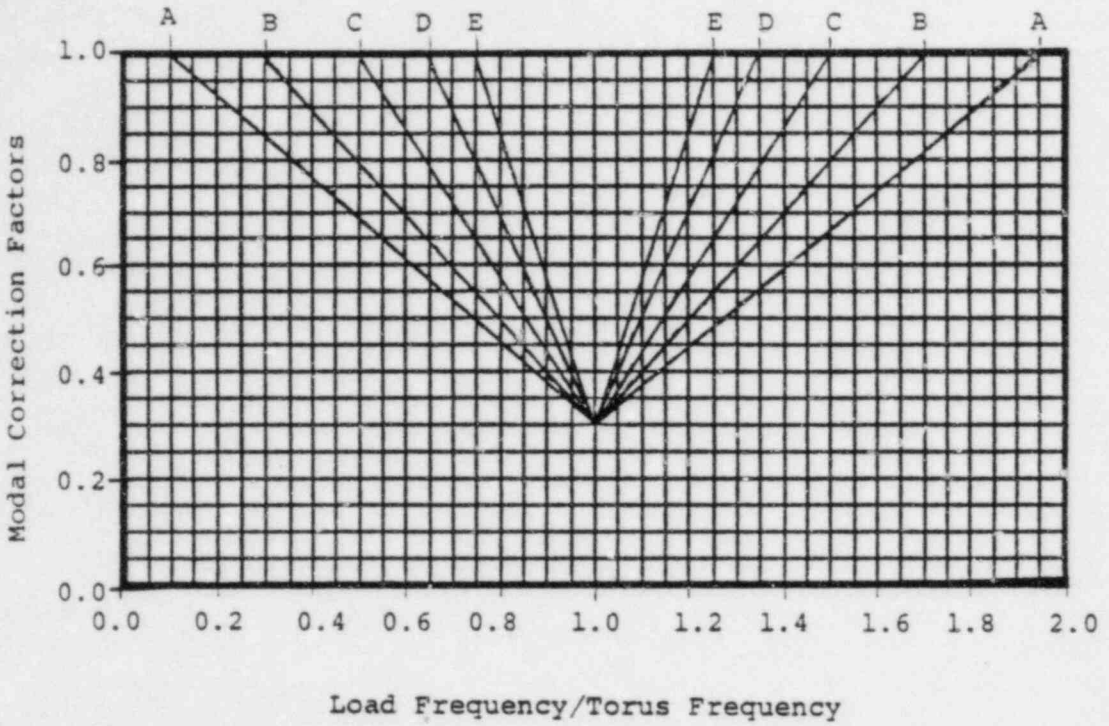

Mode Number	Frequency (Hz)	Correction Factor Case A1.2/C3.2		
		f_ℓ=9.96	f_ℓ=13.95	f_ℓ=15.02
1	15.12	0.78	0.50	0.30
2	16.94	0.88	0.64	0.48
3	21.18	1.00	0.96	0.89
4	21.92	1.00	1.00	0.91
5-19	>23.87	1.00	1.00	1.00

Legend	
Curve	Torus Freq. (Hz)
A	8
B	11
C	14
D	17-23
E	26-32

Figure 2-2.4-4

MODAL CORRECTION FACTORS USED FOR ANALYSIS OF

SRV DISCHARGE TORUS SHELL LOADS

2-2.4.2 Analysis for Lateral Loads

In addition to vertical loads, a few of the governing loads acting on the suppression chamber result in net lateral loads on the suppression chamber, as discussed in Section 2-2.2.1. These lateral loads are transferred to the drywell shield wall by the horizontal restraints described in Section 2-2.1.

The general methodology used to evaluate the effects of lateral loads consists of establishing an upper bound value of the lateral load for each applicable load case. The results for each load case are then grouped in accordance with the controlling load combination described in Section 2-2.2.2, and the maximum total lateral load acting on the suppression chamber is determined.

The maximum total lateral load is conservatively assumed to be aligned about a principal suppression chamber azimuth as shown in Figure 2-2.1-1, and distributed sinusoidally among the 16 horizontal restraint assemblies in a manner similar to the approach documented in the plant's FSAR. Once the maximum seismic restraint load is known, this value is

compared with the allowable horizontal restraint load contained in Section 2-2.3.

Loads on the horizontal restraints result in a shear force and bending moment acting on the suppression chamber shell due to the eccentricity of the seismic restraint pin with respect to the shell middle surface. The effects of these shears and moments on the suppression chamber shell are evaluated by ratioing the shell stress analysis results documented in the plant's FSAR. The resulting shell stresses are then combined with the other loads contained in the controlling load combination being evaluated, and the shell stresses in the vicinity of the seismic restraints are determined.

The magnitudes and characteristics of the governing loads which result in lateral loads on the suppression chamber are presented and discussed in Section 2-2.2.1. The specific treatment of each load which results in lateral loads on the suppression chamber is discussed in the paragraphs which follow:

2. Seismic Loads

a. OBE Loads: The total lateral load due to OBE loads and the corresponding maximum load on a horizontal restraint member pair is obtained using the methodology contained in the original design basis documented in the plant's FSAR. The horizontal acceleration at the dominant suppression chamber horizontal frequency of 12.15 hertz is applied to the combined mass of the suppression chamber and the 20% of the water mass acting with the suppression chamber. The zero-period acceleration (ZPA) is conservatively applied to the remainming 80% of the water mass which is acting in low frequency sloshing. These two effects are combined to determine the total OBE lateral load on the suppression chamber. The resulting loads are shown in Table 2-2.5-6.

b. SSE Loads: As discussed in Section 2-2.2.2, load combinations with OBE loads envelop combinations with SSE loads. Therefore SSE loads are not evaluated for the suppression chamber.

6. Chugging Loads

a. Pre-Chug Torus Shell Loads: The spatial distribution of asymmetric pre-chug pressures, shown in Figures 2-2.2-4 and 2-2.2-5, is integrated and the total lateral load is determined. A dynamic amplification factor is computed using first principles and the maximum pre-chug load frequency of 9.5 hertz. The dynamic amplification factor is based on the dominant horizontal suppression chamber frequency of 12.15 hertz obtained from the original design basis described in the plant's FSAR.

7. Safety Relief Valve Discharge Loads

d. SRV Discharge Torus Shell Loads: The longitudinal distribution of pressures for the SRV discharge 7c-Case A1.2/C3.2, shown in Figure 2-2.2-8, and the appropriate circumferential pressure distribution, similar to the one shown in Figure 2-2.2-6, are integrated and the total lateral load is determined. A dynamic amplification factor

is determined based on the dominant horizontal suppression chamber frequency of 12.15 hertz, obtained from the original design basis described in the plant's FSAR, and the most critical SRV load frequency. A modal correction factor is applied to the response associated with the dominant suppression chamber horizontal frequency and the most critical SRV load frequency. The modal correction factor used is obtained from the graph in Figure 2-2.4-4.

Use of the methodology described in the preceding paragraphs results in a conservative evaluation of suppression chamber shell stresses due to the governing loads which result in lateral loads on the suppression chamber.

2-2.4.3 Methods for Evaluating Analysis Results

The methodology discussed in Sections 2-2.4.1 and 2-2.4.2 is used to determine element forces and stress components in the suppression chamber component parts. The methodology used to evaluate the analysis results, determine the controlling stresses in the suppression chamber components and component supports, and examine fatigue effects is discussed in the paragraphs which follow.

Membrane and extreme fiber stress intensities are computed when the analysis results for the suppression chamber Class MC components are evaluated. The values of the membrane stress intensities away from discontinuities are compared with the primary membrane stress allowables contained in Table 2-2.3-1. The values of membrane stress intensities near discontinuities are compared with local primary membrane stress allowables contained in Table 2-2.3-1. Primary stresses in suppression chamber Class MC component welds are computed using the maximum principal stress or resultant force acting on the associated weld throat. The results are compared to the primary weld stress allowables contained in Table 2-2.3-1. Secondary weld stresses are computed using the same approach, and include the

effects of thermal loads. The results are compared to the secondary weld stress allowables contained in Table 2-2.3-1.

Many of the loads contained in each of the controlling load combinations are dynamic loads resulting in stresses which cycle with time and are partially or fully reversible. The maximum stress intensity range for all suppression chamber Class MC components is calculated using the maximum values of the extreme fiber stress differences which occur near discontinuities. These values are compared with secondary stress range allowables contained in Table 2-2.3-1.

Stresses in suppression chamber Class MC component support welds are computed using the maximum resultant force acting on the associated weld throat. The results are compared to the weld stress limits discussed in Section 2-2.3.

The controlling suppression chamber load combinations which are evaluated are defined in Section 2-2.2.2. During load combination formulation, the maximum stress components in a particular suppression chamber component part at a given location are combined for the

individual loads contained in each combination. The stress components for dynamic loadings are combined so as to obtain the maximum stress intensity.

For evaluating fatigue effects in the suppression chamber Class MC components and associated welds, extreme fiber alternating stress intensity histograms for each load in each event or combination of events are determined. Stress intensity histograms are developed for the suppression chamber components and welds with the highest stress intensity ranges. Fatigue strength reduction factors of 2.0 for major component stresses and 4.0 for component weld stresses are conservatively used. For each combination of events, a load combination stress intensity histogram is formulated and the corresponding fatigue usage factors are determined using the curve shown in Figure 2-2.4-5. The usage factors for each event are then summed to obtain the total fatigue usage.

Use of the methodology described above results in a conservative evaluation of the suppression chamber design margins.

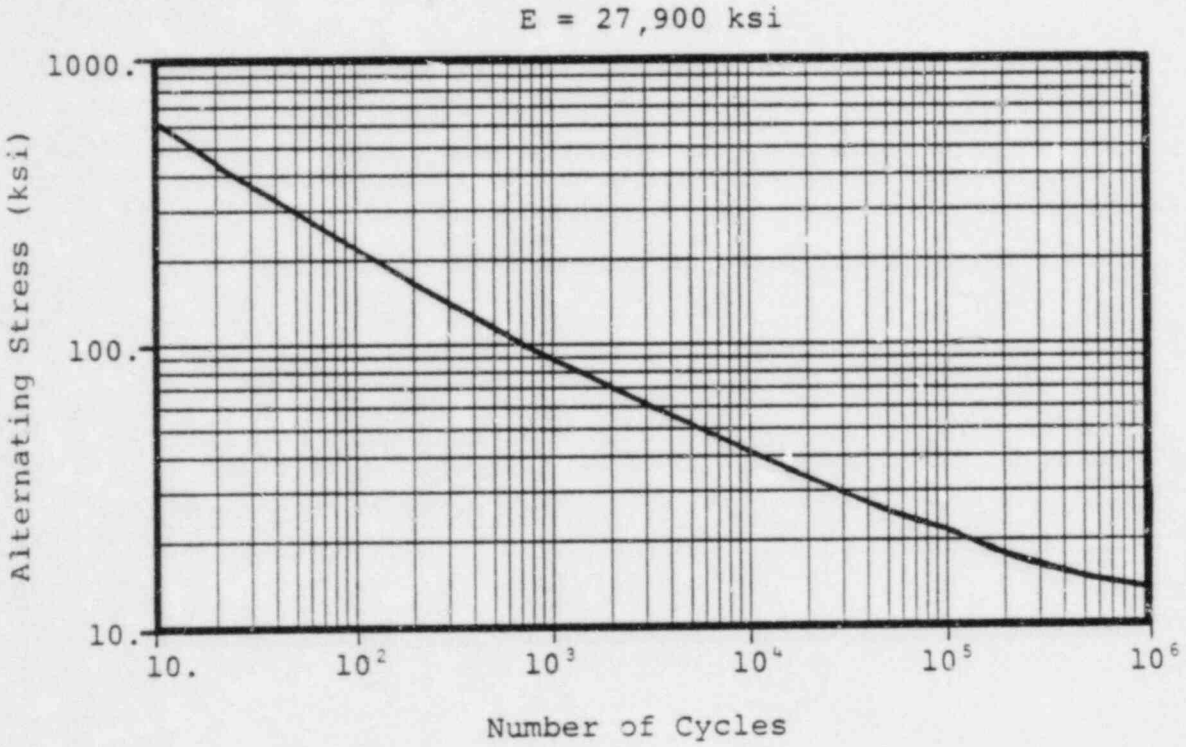

Figure 2-2.4-5

ALLOWABLE NUMBER OF STRESS CYCLES FOR SUPPRESSION CHAMBER FATIGUE EVALUATION

2-2.5 Analysis Results and Conclusions

The geometry, loads and load combinations, acceptance criteria, and analysis methods used in the evaluation of the Hope Creek suppression chamber are presented and discussed in the preceding sections. The results and conclusions derived from the evaluation of the suppression chamber are presented in the paragraphs and sections which follow.

The maximum suppression chamber shell stresses are shown in Table 2-2.5-1 for each of the governing loads. The corresponding loads for the suppression chamber vertical supports are shown in Table 2-2.5-2. The transient responses of the suppression chamber for multiple valve SRV discharge torus shell loads, expressed in terms of total vertical load at the mitered joint and total vertical load at midcylinder, are shown in Figures 2-2.5-1 and 2-2.5-2, respectively.

The maximum suppression chamber shell stresses adjacent to the horizontal restraints are presented in Table 2-2.5-5 for each of the governing loads resulting in lateral loads on the suppression chamber. The corresponding reaction loads on the suppression chamber horizontal restraints are shown in Table 2-2.5-6.

The maximum stresses and associated design margins for the major suppression chamber components and welds are shown in Table 2-2.5-3 for the IBA II, IBA III, and DBA II load combinations. The maximum loads for the suppression chamber vertical support columns for the same load combinations are shown in Table 2-2.5-4. The maximum suppression chamber horizontal restraint reactions and associated shell stresses adjacent to the seismic restraints are shown in Table 2-2.5-7 for the IBA IV combination.

The fatigue usage factors for the controlling suppression chamber component and weld are shown in Table 2-2.5-8. These usage factors are obtained by evaluating the Normal Operating plus SBA event. Since the IBA load combinations are used to envelop the SBA combinations, the stresses from the IBA events are used for the SBA event in the fatigue evaluation.

The suppression chamber evaluation results presented in the preceding paragraphs are discussed in Section 2-2.5.1.

Table 2-2.5-1

MAXIMUM SUPPRESSION CHAMBER SHELL STRESSES FOR GOVERNING LOADS

Section 2-2.2.1 Load Designation		Shell Stress Type (ksi)		
Load Type	Load Case Number	Primary Membrane	Local Primary Membrane	Primary + Secondary Stress Range
Dead Weight	1a + 1b	1.60	2.55	3.78
Seismic	2a	0.43	0.69	2.04
	2b	0.72	1.15	3.40
Pressure and Temperature	3b	7.53	7.33	9.19
	3d	4.85	11.64	12.61
Condensation Oscillation	5a	5.45	6.60	15.70
	5c	0.52	0.63	1.96
Chugging	6a (sym)	0.71	1.02	2.66
	6b	1.42	1.60	3.99
	6d	2.09	2.37	7.67
SRV Discharge	7b	8.70	13.67	29.98
	7d	5.61	6.49	25.29

Note:

1. Values shown are maximums irrespective of time and location.

Table 2-2.5-2

MAXIMUM VERTICAL SUPPORT LOADS FOR
GOVERNING SUPPRESSION CHAMBER LOADINGS

Section 2-2.2.1 Load Designation				Verticle Load (kips)				
Load Type		Load Case No.	Direction	MC Column		MJ Column		Total
				Inside	Outside	Inside	Outside	
Dead Weight		1a + 1b	Upward	N/A	N/A	N/A	N/A	N/A
			Downward	143.51	164.16	147.86	170.05	625.58
Seismic	OBE	2a	Upward	38.75	44.32	39.92	45.91	168.90
			Downward	38.75	44.32	39.92	45.91	168.90
	SSE	2b	Upward	64.58	78.87	66.54	76.52	286.51
			Downward	64.58	78.87	66.54	76.52	286.51
Internal Pressure		3a	Up/Down(2)	-9.38	36.84	9.83	-37.28	0
Thermal		3b	Up/Down(2)	15.52	-32.98	-15.52	32.98	0
Condensation Oscillation		5a	Upward	272.57	308.39	275.88	324.62	1181.46
			Downward	272.57	308.39	275.88	324.62	1181.46
Chugging	Pre-Chug	6a	Upward	49.15	57.81	50.39	57.10	214.45
			Downward	49.15	57.81	50.39	57.10	214.45
	Post-Chug	6b	Upward	71.99	80.83	73.42	86.34	312.58
			Downward	71.99	80.83	73.42	86.34	312.58
SRV Discharge	Multiple Valve	7b	Upward	578.86	812.70	628.98	712.36	2732.90
			Downward	545.86	755.02	597.24	721.50	2619.62

Notes:

1. Values shown are maximums irrespective of time.
2. Negative value indicates tension in column.

Table 2-2.5-3

MAXIMUM SUPPRESSION CHAMBER STRESSES FOR CONTROLLING LOAD COMBINATIONS

Item	Stress Type	Load Combination Stresses (ksi)					
		IBA II (1)		IBA III (1)		DBA II (1)	
		Calc. Stress	Calc. / Allow. (2)	Calc. Stress	Calc. / Allow. (2)	Calc. Stress	Calc. / Allow. (2)
C O M P O N E N T S							
Shell	Primary Membrane	19.24	0.99	18.61	0.96	15.89	0.82
	Local Primary Membrane	24.35	0.84	24.35	0.84	18.98	0.66
	Primary + Secondary Stress Range	60.50	0.87	57.75	0.83	44.66	0.64
Ring Beam	Primary Membrane	15.45	0.80	15.07	0.78	13.44	0.70
	Local Primary Membrane	24.02	0.83	24.19	0.84	17.58	0.61
	Primary + Secondary Stress Range	43.59	0.63	43.76	0.63	33.66	0.48
C O M P O N E N T S U P P O R T S							
Column Connection	Membrane	19.58	0.58	19.29	0.57	11.53	0.34
	Extreme Fiber	22.26	0.52	21.71	0.51	12.08	0.28
Column	Tensile	11.36	0.33	11.65	0.34	3.29	0.10
	Compressive	14.82	0.46	15.11	0.47	7.66	0.24
	Net Section Tensile	18.25	0.72	18.70	0.73	5.29	0.21
	Pullout Shear	10.23	0.45	10.48	0.46	2.96	0.13
	Bearing	39.44	0.77	40.19	0.79	20.38	0.40

Table 2-2.5-3
(Concluded)

Item	Stress Type	Load Combination Stresses (ksi)					
		IBA II (1)		IBA III (1)		DBA II (1)	
		Calc. Stress	(2) Calc. Allow.	Calc. Stress	(2) Calc. Allow.	Calc. Stress	(2) Calc. Allow.
W E L D S							
Ring Beam to Shell	Primary	12.62	0.84	12.45	0.83	8.11	0.54
	Secondary	16.56	0.37	16.39	0.36	10.78	0.24
Column Connection to Shell	Primary	8.10	0.54	7.94	0.53	4.03	0.27
	Secondary	8.64	0.19	8.49	0.19	4.58	0.10

Notes:

1. Reference Table 2-2.2-8 for load combination designation.
2. Reference Table 2-2.3-1 for allowable stresses.

Table 2-2.5-4

MAXIMUM VERTICAL SUPPORT LOADS FOR
CONTROLLING SUPPRESSION CHAMBER LOAD COMBINATIONS

Vertical Support Component		Direction	Maximum Combination Loads (kips)		
			IBA II (1)	IBA III (1)	DBA II (1)
Midcylinder	Inside	Upward	668.45	691.29	236.43
		Downward	934.75	957.59	524.25
	Outside	Upward	921.35	944.37	267.14
		Downward	1199.71	1222.73	620.00
Mitered Joint	Inside	Upward	641.44	664.47	215.85
		Downward	894.04	917.07	511.47
	Outside	Upward	731.92	761.16	254.83
		Downward	1072.11	1101.25	569.71
Total		Upward	2963.16	3061.29	974.25
		Downward	4100.61	4198.64	2225.43

Notes:

1. Reference Table 2-2.2-8 for load combination designation.
2. The allowable upward load is 1160 kips per column.

Table 2-2.5-5

MAXIMUM SUPPRESSION CHAMBER SHELL STRESSES DUE TO LATERAL LOADS

Section 2-2.2.1 Load Designation		Shell Stress Type (1) (ksi)	
Load Type	Load Case Number	Local Primary Membrane	Primary + Secondary Stress Range
OBE Seismic	2a	3.12	22.88
Pre-Chug	6a	0.13	0.97
SRV Discharge	7c	1.40	10.29

Note:

1. Stresses shown are in suppression chamber shell adjacent to horizontal restraint pad plate.

Table 2-2.5-6

MAXIMUM HORIZONTAL RESTRAINT REACTIONS

DUE TO LATERAL LOADS

Section 2-2.2.1 Load Designation		Horizontal Reaction Load (kips)		
Load Type	Load Case Number	Total	Maximum Restraint Load	Dynamic Load Factor
OBE Seismic	2a	1958.12	154.17	N/A
Pre-Chug	6a	83.40	6.57	2.56
SRV Discharge	7c	880.60	69.33	2.50

Table 2-2.5-7

MAXIMUM SUPPRESSION CHAMBER SHELL STRESSES AND HORIZONTAL RESTRAINT REACTIONS FOR CONTROLLING LOAD COMBINATIONS WITH LATERAL LOADS

Item	Stress Reaction Type	Load Combination Stresses/Reactions (ksi, kips)	
		IBA IV (2)	
		Calc. Value	Calc. / Allow. (3)
Shell (1)	Local Primary Membrane	15.60	0.54
	Primary + Secondary Stress Range	55.62	0.80
Horizontal Restraint	Maximum Reaction Load	230.07	0.36

Notes:

1. Stresses shown are in suppression chamber shell adjacent to horizontal restraint pad plate.
2. Reference Table 2-2.2-8 for load combination designation.
3. Reference Section 2-2.3 for allowable stresses and horizontal restraint loads.

Table 2-2.5-8

MAXIMUM FATIGUE USAGE FACTORS FOR SUPPRESSION CHAMBER COMPONENTS AND WELDS

Event Sequence	Load Case Cycles (1)					Event Usage Factor (7)	
	Seismic	Pressure	Temperature	SRV Discharge	Pre + Post Chugging (sec.)	Torus Shell	Weld
NOC W/Single SRV	0	150(2)	150(2)	596	N/A	.347	.308
NOC W/Multiple SRV	0	0	0	370	N/A	.309	.394
SBA 0. to 600. sec.	600(2)	1	1	50(4)	300.(6)	.067	.095
SBA 600. to 1200. sec.	0	0	0	2(5)	600.(6)	.002	.004
Maximum Cumulative Usage Factors				NOC + SBA		.725	.801

Notes:

1. See Table 2-2.2-8 and Figure 2-2.2-8 for load cycles and event sequencing information.
2. Entire number of load cycles conservatively assumed to occur during time of maximum event usage.
3. Total number of SRV actuations shown are conservatively assumed to occur in same suppression chamber bay.
4. Value shown is conservatively assumed to be equal to the number of multiple valve actuations which occurs during the event.
5. Number of ADS actuations assumed to occur during the event.
6. Each chug-cycle has a duration of 1.4 sec.
7. Usage factors are computed for the component and weld which result in the maximum cumulative usage.

Maximum Upward Load = 1339 kips

Maximum Downward Load = 898 kips

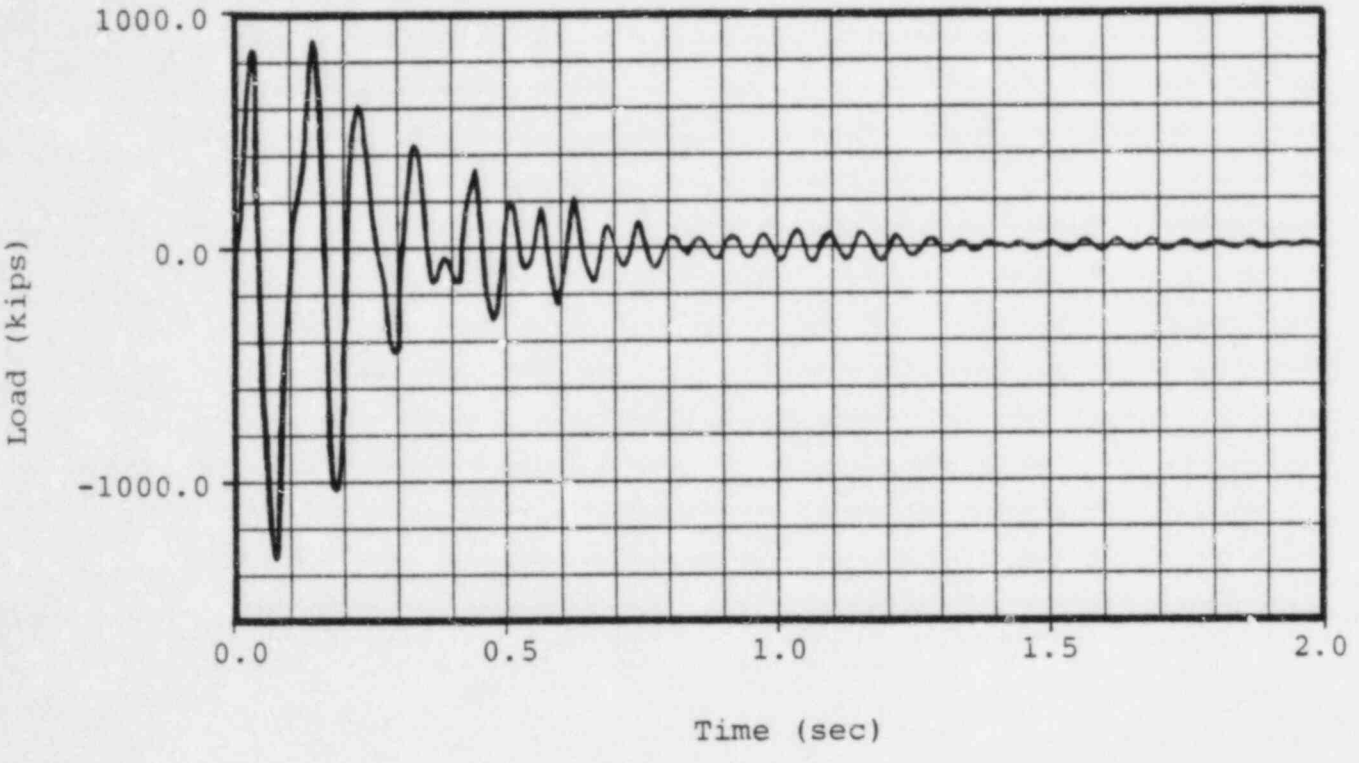

Note:

1. Reference Figure 2-2.2-6 for loading information.

Figure 2-2.5-1

SUPPRESSION CHAMBER RESPONSE DUE TO MULTIPLE VALVE SRV DISCHARGE TORUS SHELL LOADS - TOTAL VERTICAL LOAD AT MITERED JOINT

Maximum Upward Load = 1379 kips

Maximum Downward Load = 904 kips

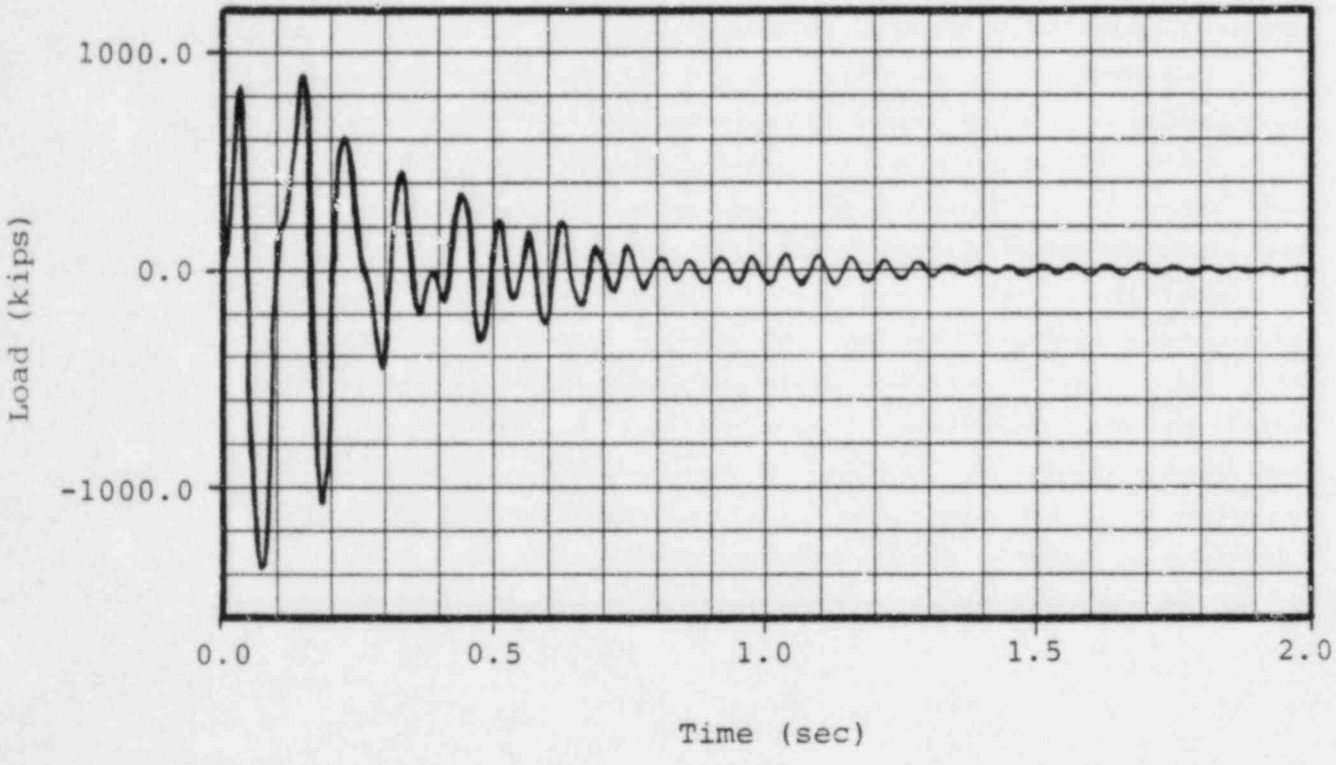

Note:

1. Reference Figure 2-2.2-6 for loading information.

Figure 2-2.5-2

SUPPRESSION CHAMBER RESPONSE DUE TO MULTIPLE VALVE SRV DISCHARGE TORUS SHELL LOADS - TOTAL VERTICAL LOAD AT MIDCYLINDER

2-2.5.1 Discussion of Analysis Results

The results shown in Table 2-2.5-1 indicate that the largest suppression chamber shell stresses occur for IBA internal pressure loads, DBA condensation oscillation torus shell loads, and SRV discharge torus shell loads. The submerged structure loadings, in general, cause only local stresses in the suppression chamber shell adjacent to the ring beams.

Table 2-2.5-2 shows that the largest suppression chamber vertical support loads occur for DBA condensation oscillation loads and SRV discharge torus shell loads.

The results shown in Table 2-2.5-3 indicate that the largest stresses in the suppression chamber components, component supports, and associated welds occur for the IBA II and IBA III load combinations. The suppression chamber shell stresses for the IBA II and IBA III combinations are less than the allowable limits with stresses in other suppression chamber components, component supports, and welds well within the allowable limits. The stresses in the suppression chamber components, component supports, and welds for the DBA II combination are also well within allowable limits.

Table 2-2.5-4 shows that the largest upward and downward vertical support loads occur for the IBA II and IBA III combinations. The vertical support system stresses for all load combinations are less than the allowable limits, as shown in Table 2-2.5-3. The vertical support upward loads are also less than the allowable limit.

The results shown in Tables 2-2.5-5 and 2-2.5-6 indicate that the largest horizontal restraint reactions and associated suppression chamber shell stresses occur for seismic loads and SRV discharge loads. Table 2-2.5-7 shows that the horizontal restraint reactions and suppression chamber shell stresses adjacent to the horizontal restraints for the IBA IV load combination are less than allowable limits.

The results shown in Table 2-2.5-8 indicate that the largest contributor to suppression chamber fatigue effects are SRV discharge loads which occur during Normal Operating conditions. The total fatigue usage factors for the suppression chamber shell and associated welds for the Normal Operating plus SBA events are less than allowable limits.

2-2.5.2 Conclusions

The suppression chamber loads described and presented in Section 2-2.2.1 are conservative estimates of the loads postulated to occur during an actual LOCA or SRV discharge event. Applying the methodology discussed in Section 2-2.4 to evaluate the effects of the governing loads on the suppression chamber results in bounding values of stresses and reactions in suppression chamber components and component supports.

The load combinations and event sequencing defined in Section 2-2.2.2 envelop the actual events postulated to occur during a LOCA or SRV discharge event. Combining the suppression chamber responses to the governing loads and evaluating fatigue effects using this methodology results in conservative values of the maximum suppression chamber stresses, support reactions, and fatigue usage factors for each event or sequence of events postulated to occur throughout the life of the plant.

The acceptance limits defined in Section 2-2.3 are at least as restrictive as those used in the original containment design documented in the plant's FSAR. Comparing the resulting maximum stresses and support

reactions to these acceptance limits results in a conservative evaluation of the design margins present in the suppression chamber and suppression chamber supports. As is demonstrated from the results discussed and presented in the preceding sections, all of the suppression chamber stresses and support reactions are within these acceptance limits.

As a result, the components of the suppression chamber described in Section 2-2.1, which are specifically designed for the loads and load combinations used in this evaluation, exhibit the margins of safety inherent in the original design of the primary containment as documented in the plant's FSAR. The intent of the NUREG-0661 requirements, as they relate to the design adequacy and safe operation of the Hope Creek suppression chamber, are therefore considered to be met.

2-3.0 LIST OF REFERENCES

1. "Mark I Containment Long-Term Program," Safety Evaluation Report, NRC, NUREG-0661, July 1980.

2. "Mark I Containment Program Load Definition Report," General Electric Company, NEDO-21888, Revision 2, December 1981.

3. "Mark I Containment Program Plant Unique Load Definition," Hope Creek Generating Station, General Electric Company, NEDO-24579, Revision 1, January 1982.

4. "Final Safety Analysis Report (FSAR)," Hope Creek Generating Station Unit 1, Public Service Electric and Gas Company, Section 3.8, October 1983.

5. "Mark I Containment Program Structural Acceptance Criteria Plant Unique Analysis Application Guide, Task Number 3.1.3," General Electric Company, NEDO-24583-1, October 1979.

6. ASME Boiler and Pressure Vessel Code, Section III, Division 1, 1977 Edition with Addenda up to and including Summer 1977.

7. American Concrete Institute (ACI) Code, Code Requirements for Nuclear Safety-Related Concrete Structures, ACI-349-80, 1980.